Annual Report 2013 of the Institute for Nuclear and Energy Technologies

Thomas Schulenberg

Thomas Schulenberg

**Annual Report 2013 of the Institute
for Nuclear and Energy Technologies**

Karlsruhe Institute of Technology

KIT SCIENTIFIC REPORTS 7678

Annual Report 2013 of the Institute for Nuclear and Energy Technologies

by
Thomas Schulenberg

Report-Nr. KIT-SR 7678

Content

Structure and Activities of the Institute for Nuclear and Energy Technologies

Thomas Schulenberg

Mission

The Institute for Nuclear and Energy Technologies (Institut für Kern- und Energietechnik, IKET) is situated with its offices and research laboratories on the North Campus of KIT. It is focused on nuclear, fusion and renewable energy technologies for electric power production and on hydrogen technologies as an alternative energy carrier. Its research topics include analyses and tests of thermal-hydraulic phenomena, combustion phenomena and neutron physics which are typical for normal operation or for accidental conditions in nuclear power plants, for future nuclear fusions reactors, for geothermal or solar power plants, but also for mobile systems. Most subjects are application oriented, supported by some basic research projects, if needed.

Organizational structure

IKET is structured into nine working groups as indicated in Fig. 1. Working groups on accident analyses, on accidents management systems and on transmutation as well as the AREVA Nuclear Professional School have been concentrating in 2013 primarily on nuclear applications, whereas the Karlsruhe Liquid metal Laboratory (KALLA) and the Hydrogen group were addressing nuclear as well as other energy technologies, as will be outlined below. The working group on magneto-hydrodynamics is primarily working on nuclear fusion applications, whereas the working group on energy and process engineering is rather concentrating on geothermal energies. Thus, the institute covers a wide field of different energy technologies, and the share of its personnel resources on the different research topics
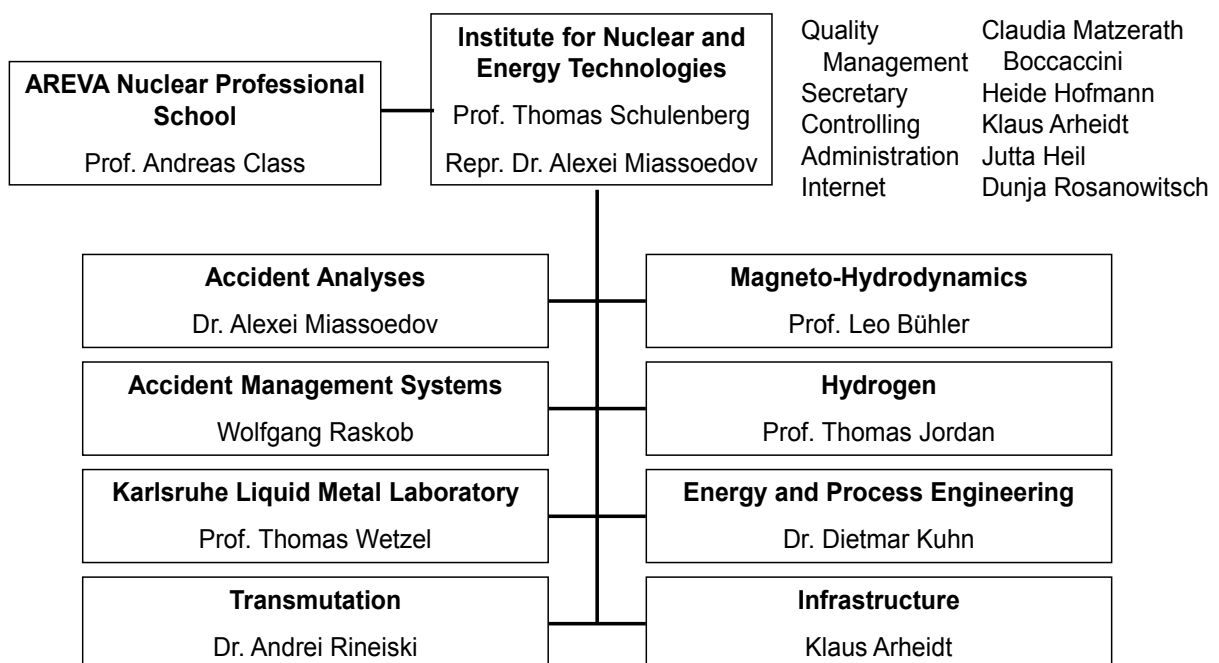
Fig. 1: Organizational structure of the Institute for Nuclear and Energy Technologies (IKET)

is determined each year by the worldwide market request for energy research.

Having a larger share of nuclear and fusion research, IKET has built up a quality management system according to the international standard ISO 9001. Internal audits are performed every year to train the use of its quality guidelines and to improve the quality level further on.

Personnel resources

By the end of 2013, IKET had employed 125 (full time equivalent, FTE) scientists, engineers, technicians and other personnel, as indicated in Fig. 2. An organizational change of the former working group for chemical process technologies, headed by Prof. Olaf Deutschmann, to the new Institute of Catalysis Research and Technology caused a sudden step of personnel resources at the beginning of 2013. Around 46% of the employees were funded in 2013 by the Helmholtz Gemeinschaft (HGF), the others by third party funds of the European Commission, by industry,

by German ministries or by other research funds. Doctoral students as well as students of the Baden-Wuerttemberg Cooperative State University (DHBW) were filling around 20% of these positions at IKET. The active role of the institute in education and training is also expressed by 35 to 40 additional students per year, who perform their bachelor or master theses or who spend an internship in the research laboratories of IKET, as shown in Fig. 3.
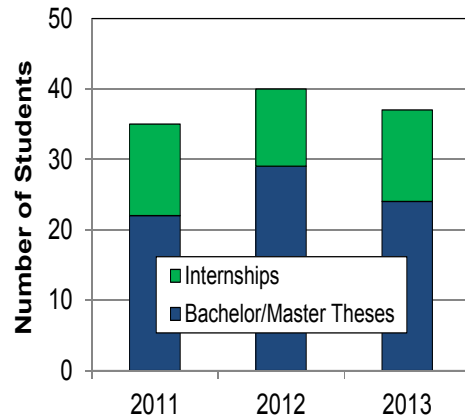
Fig. 3: Additional students performing bachelor theses, master theses or internships.
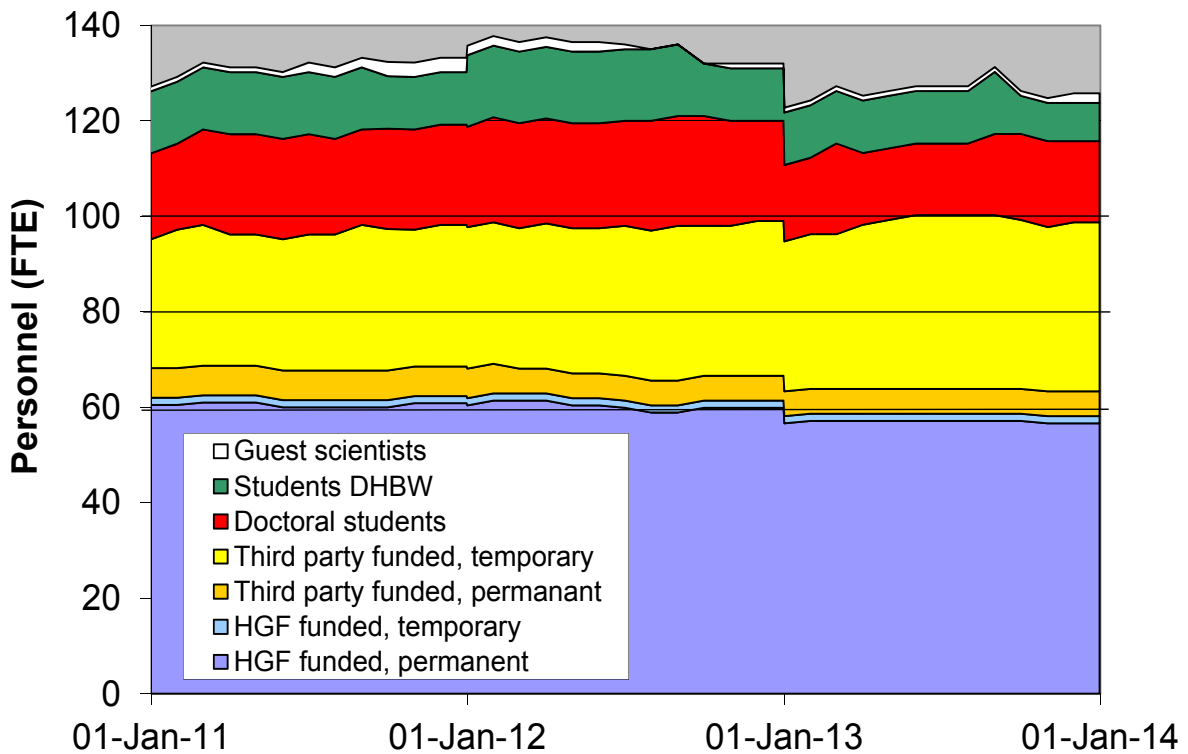
Fig. 2: Personnel resources of the Institute for Nuclear and Energy Technologies

Around 75% of these resources were allocated in 2013 to projects on nuclear energy, which have traditionally a share of around 50% from third party funding at IKET, as shown in Fig. 4. Research on nuclear fusion technologies had to be reduced in 2013, compared with former years, due to budget limitations. The rather increasing trend of research on renewable energies and on hydrogen technologies for mobile applications appears in 2013 overcompensated by the missing group for chemical process technologies, as explained above. The institute had an annual budget in 2013 of around 11 M€, of which around 7 M€ were provided by HGF and around 4 M€ by third parties.

(FH). The increasing trend of teaching activities since the merger of KIT is shown in Fig. 5.

The AREVA Nuclear Professional School is an IKET working group for education and training of young scientist in nuclear engineering, sponsored by AREVA GmbH since 2009. Supported by lecturers of other organizations, this school has been offering compact courses in 2013 on nuclear technologies and methods. Moreover, this group is supervising doctoral students who are financially supported by AREVA, RWE, the European Commission or by other organizations. The contract with AREVA has been extended in 2013 for another 5 years.

Fig. 4: Allocation of personnel resources on research programs.
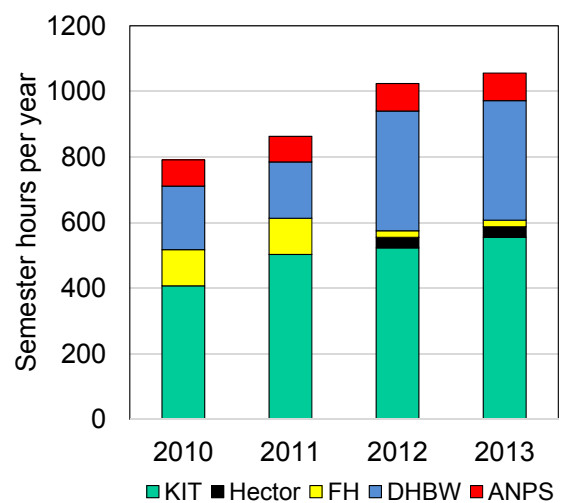
Fig. 5: Teaching activities of employees of IKET, given at different universities.

The number of publications, as usual in research organizations, expresses the productivity of the institute. More than 210 publications, around 3 per scientist and year, were given in 2013 to international journals, to conference proceedings and to KIT Scientific Publishing.

The KIT mission on education and training along with scientific research is impressively demonstrated by more than 1000 semester hours, which employees of IKET were giving in 2013 not only on the university campus of KIT, but also at the Baden-Wuerttemberg Cooperative State University (DHBW), at the Hector School of KIT, in the AREVA Nuclear Professional School of KIT, and in Universities of Applied Sciences

Some Research Highlights of 2013

Research on nuclear energy has been focused in 2013 mainly on analyses, physical modelling and management of severe accidents in nuclear power plants. Since the Fukushima accident in March 2011, the coolability of molten reactor cores, the distribution and combustion of hydrogen, which is produced by oxidizing fuel rods, and the off-site emergency management in the neighborhood of a damaged nuclear power plant have been brought up again as top priority research subjects. As an example, the Accident Analyses group has simulated molten corium interaction with concrete using thermite melt, which is poured over concrete structures. The residual heat, keeping the "corium" hot, has been

simulated by the addition of further thermite in the MOCKA experiments. Fig. 6 shows the simulation of a failing reactor pressure vessel in the DISCO jet experiment, where a liquid corium jet is injected into the reactor cavity.

Fig. 6: DISCO jet experiment: a core melt jet is penetrating the reactor pressure vessel.

Tests with molten salt, simulating the core melt with lower temperatures, have been performed in the LIVE facility to determine how a molten core could be retained in the lower plenum of the reactor pressure vessel and thus avoiding a corium release. New projects on severe accident research have been started in 2013, coordinated by IKET, as a European collaboration (EU project SAFEST), in collaboration with China (EU project ALISA) and in bilateral collaboration with France.

Hydrogen distribution in the containment during a severe accident has been predicted for a Swiss and a Korean nuclear power plant to support the installation of passive, autocatalytic recombiners, which can oxidize such hydrogen without detonations like in Fukushima. Filtered venting systems, removing hydrogen from the containment and thus avoiding a hydrogen accumulation, have been studied for VGB. The dynamic loads of a hydrogen detonation on containment structures were studied experimentally in the HYKA facility of IKET.

The working group for Accident Management Systems has completed the worldwide version of the decision support system RODOS, including the recent ICRP recommendations. Fig. 7 shows, as an example, the prediction of a fictive radioactive release from a fictive reactor in Saudi-Arabia to demonstrate that RODOS is prepared now to support emergency management organizations
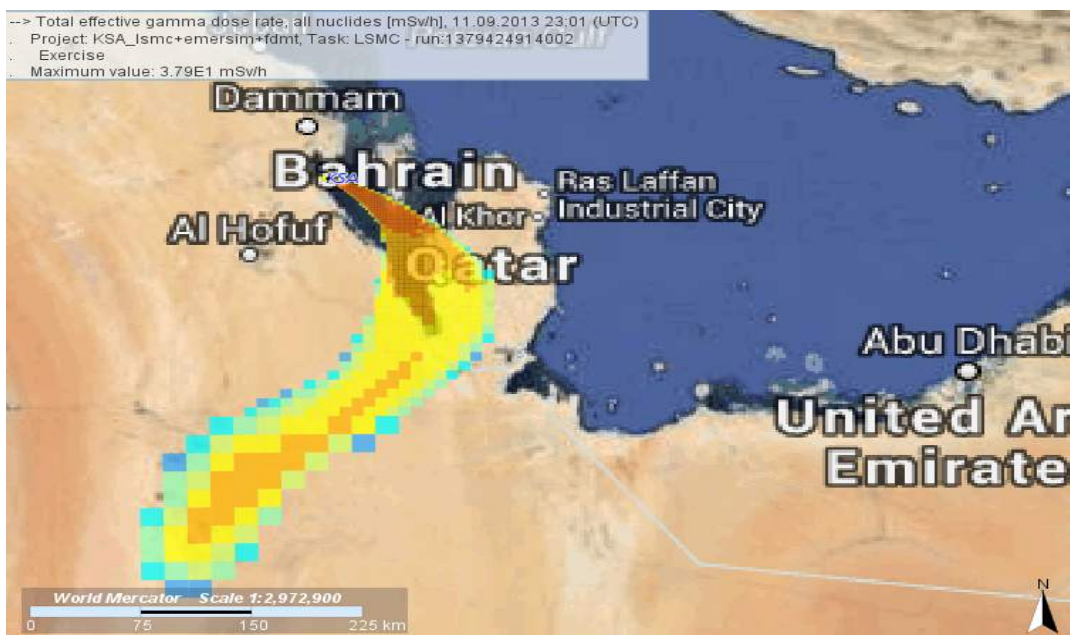
Fig. 7: Total effective gamma dose rate, using the NOMADS weather data for a fictive release from a fictive reactor in Saudi-Arabia (JRodos screen shot).

4

anywhere in the world if a nuclear accident should happen. More than 25 years after the Chernobyl accident, Ukraine has agreed to install this system also in their country, and IKET is actively supporting the RODOS installation there.
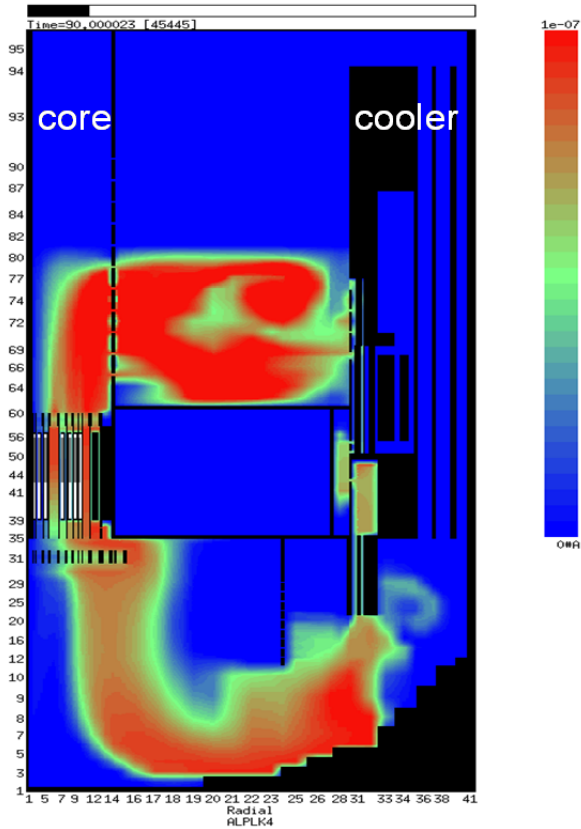
Fig. 8: SIMMER predictions of a fuel particle distribution 90s after a postulated fuel pin failure in the planned MYRRHA facility at SCK/CEN, Belgium.

Studies of the prevention and mitigation of accidents is not only limited at IKET to water cooled reactors. The Transmutation group has been studying nuclear accidents as well for sodium cooled reactor, for lead and gas cooled fast reactors, and even for innovative molten salt reactors. Their usual simulation tool is SIMMER, and a typical result for a postulated failure of a fuel rod in the lead-bismuth cooled transmutation facility MYRRHA is shown exemplarily in Fig. 8. Such studies in the very early design phase of a future nuclear facility can help to avoid later risks significantly. IKET is actively participating in joint national and European projects as well as through OECD and IAEA organizations on the transmutation of spent fuel, both with numerical studies and with experiments with liquid lead bismuth in their KALLA laboratory. An experimental study of

flow and heat transfer of a lead-bismuth cooled fuel assembly has been completed in 2013.

Liquid metal technologies are not only a traditional research field of fast reactors. The new Helmholtz Alliance LIMTECH on liquid metal technologies, founded in 2013, shall cluster various research activities in this field for different energy systems. IKET contributes to these activities e.g. with innovative concepts for a carbon dioxide free production of hydrogen in liquid metals and for high-temperature energy conversion systems of concentrated solar power plants.

Moreover, liquid metals are promising breeding materials for nuclear fusion reactors. Their interaction with the strong magnetic field, however, is a challenge for research on magneto-hydrodynamics. As an example, Fig. 9 shows the complicated flow structure of a flow of heated lead lithium inside a blanket element, predicted by the Magneto-Hydrodynamics group for EU-ROfusion.

Hydrogen is not only a risk for nuclear power plants during severe accidents. It is more and more used today as an alternative energy carrier for carbon free energy systems. As an example, two electric Mercedes shuttle busses, powered by fuel cells using hydrogen as fuel, are operated at KIT since 2013. IKET has been supervising the commissioning of a new hydrogen gas station for these busses, shown in Fig. 10, which was opened officially on June 11, 2013 at KIT.

Research on risks and safety systems for such hydrogen infrastructures is carried out in joint European projects like H2FC (European infrastructure to support hydrogen and fuel cell technologies) and SUSANA (Verification and validation of CFD software for risk analyses), both coordinated by IKET. Moreover, IKET participates in the European project HyIndoor, where passive ventilation strategies in case of hydrogen release in closed compartments are studied experimentally and numerically.

Hydrogen risks could also be an issue of nuclear fusion reactors, e.g. in the tritium processing unit or, even more challenging, in combination with beryllium dust in a Tokamak. In 2013, IKET has been performing combined combustion tests of aluminum dust (simulating Be dust) with hydrogen to assess the risks of detonations.

There are only a few renewable energies, which could be used for base load power production. Among them, the use of geothermal energies is a promising technology especially in countries like Indonesia, where hot water from geothermal reservoirs is easy to access. In 2013, IKET has completed a national project with Indonesia with this objective. A budget for a small modular pilot power plant at KIT with supercritical propane as working fluid has been granted in 2013 and construction works started immediately afterwards.

The following, selected articles shall provide a deeper insight in some of these many research results which were produced in 2013.
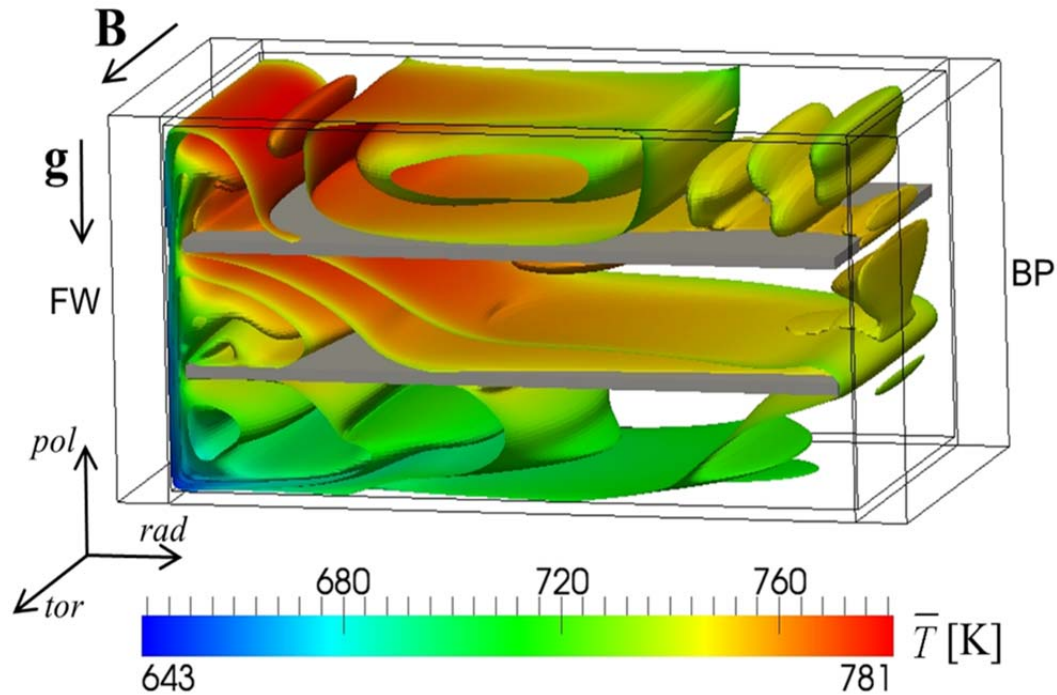
Fig. 9: Magneto-hydrodynamic flow of heated lead lithium inside a blanket module for nuclear fusion.

Fig. 10: The new hydrogen gas station, commissioned under supervision of IKET.

Magnetohydrodynamics for Nuclear Fusion Reactors

Leo Bühler, Thomas Arlt, Hans -Jörg Brinkmann, Victor Chowdhury, Sebastian Ehrhard, Christina Köhly, Chiara Mistrangelo

First numerical simulations concerning liquid metals in tokamak divertor capillary pore systems

The aim of the present study is providing a first description of the behavior of a liquid metal in a capillary porous system (CPS) when an external uniform magnetic field is imposed in order to judge about the feasibility from the magnetohydrodynamic (MHD) point of view of the CPS technology for steady-state divertor applications [Ono, Bell, Hirooka et al. 2012] [Mirnov, 2009]. The final objective is estimating a permeability tensor **K**, which relates the pressure gradient and the fluid velocity (volume flux), to be used for a macroscopic description of the problem. MHD liquid metal flows in a model porous structure have been analyzed for strong imposed magnetic fields [Bühler, Mistrangelo, Najuch, 2014]. The permeability tensor **K** has been determined by means of numerical simulations of liquid metal flows in a microscopic representative fluid volume. Most of the discussed results are obtained for a magnetic field **B** $\simeq$ 4.5 T (*Ha* = 50, where the Hartmann number *Ha* is a non-dimensional measure for the magnetic field strength). The effects of the reciprocal orientation of the forcing pressure gradient and the magnetic field have been studied. Numerical results show that, independently of the orientation of **B**, the permeability
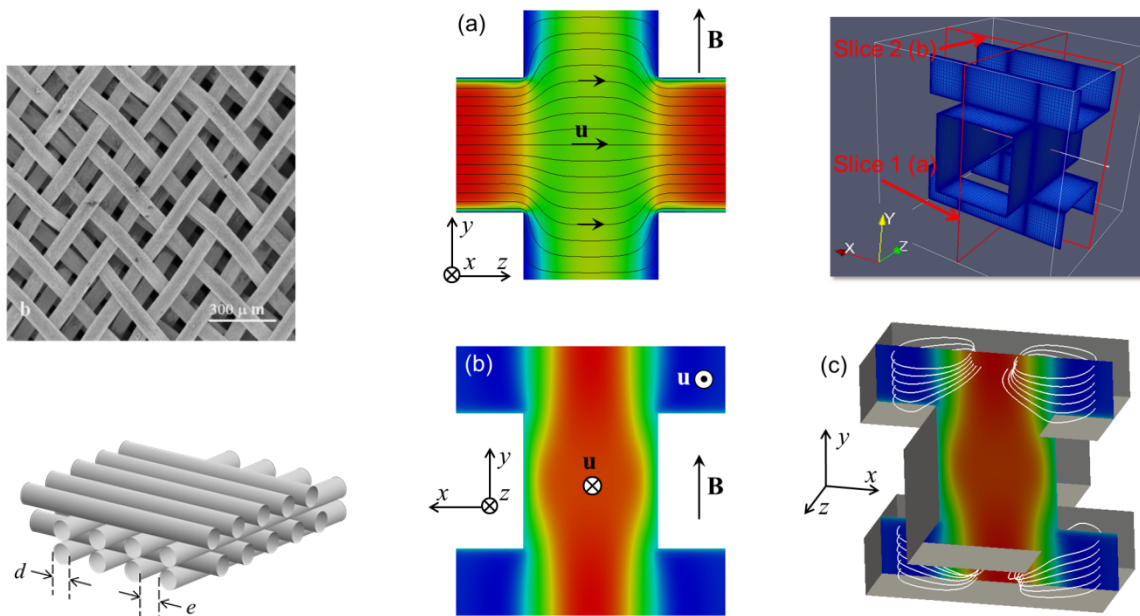
Fig. 1: Mesh used for plasma facing components [Mirnov, Evtikhin 2006] (top) and simplified model geometry (bottom). The latter one has been further simplified by assuming wires of rectangular cross section.

Fig. 2: MHD flow in a representative microscopic volume element of a porous wire mesh. Contours of the *z* - component of velocity on two planes at *x=const* (a) and *z=const* (b) for the flow at *Ha*=50 (*B_y*=4.35T) and applied pressure gradient along *z*. 3D velocity streamlines are visualized in (c). Wires and external domain are electrically insulated.

K strongly reduces in a MHD flow compared to the one in the corresponding hydrodynamic Darcy regime ($Re < 1$). Due to the known fundamental role of the magnitude of the induced current density in determining electromagnetic Lorentz forces and hence the pressure heads that balance those forces, the impact of various electric boundary conditions on the permeability has been carefully investigated.

By progressively increasing the strength of the imposed magnetic field, i.e. the Hartmann number Ha, the dimensionless pressure gradient G_{ij} becomes larger and it varies as $G_{ij} = K_{ij}^{-1} \sim Ha$ for electrically insulating boundary conditions and as $G_{ij} = K_{ij}^{-1} \sim Ha^2$ in the case of a perfectly electrically conducting porous system. The most critical conditions in terms of pressure drop are those where wires and external domain are perfectly conducting. Under these conditions it is found that for a flow at $Ha = 50$ the permeability is 50 times smaller than in the corresponding hydrodynamic flow. Additional studies should be performed to define the range of validity of Darcy's law for MHD flows, i.e. it is necessary to identify the maximum Reynolds number Re for which a linear relation between pressure gradient and velocity can be verified. When Re becomes too large the influence of inertial forces increases and this can cause deviations from Darcy's law.

The present study has been performed by considering lithium as model fluid, but the results are presented in terms of non-dimensional parameters and therefore they become independent of the selected working fluid. A behavior analogous to the one described in the present work is expected when operating with another liquid metal in the same parameter range.

Helium-cooled blanket design development: Investigation of MHD flows in model geometries for liquid metal blankets for fusion reactors

Liquid metal flows in helium cooled lead lithium (HCLL) blankets are expected to be mainly driven by buoyancy forces caused by non-isothermal operating conditions due to neutron volumetric heating and cooling of walls.

Magneto-convective flows in horizontal ducts having electrically and thermally conducting walls have been analyzed numerically for intense magnetic fields [Mistrangelo, Bühler, Aiello, 2014] [Mistrangelo, Bühler, 2014 (6)]. Two configurations are considered. In a first case the flow is studied in slender channels infinitely extended in axial direction, a heat source is distributed uniformly in the fluid and heat is homogeneously extracted from the walls. In a second case, magneto-convective flows in a cavity are investigated, both uniform and spatially varying thermal loads are applied, and the wall cooling depends on the difference between temperatures of wall and helium coolant. A model has been developed that uses an empirical correlation [Gnielinski, 1975] to simulate the heat transfer from the hot structural material into the helium flow. For both cases, isotherms, flow streamlines and electric potential iso-surfaces have been studied for different internal heat sources, i.e. various Grashof numbers Gr in a range between 10^6 and 10^8 corresponding to volumetric heating of about $0.04 \div 5$ MW/m³.

The first simplified case has been selected since it allows getting an overview of the mechanism that determines the onset of convective motions in geometries related to HCLL blankets and the way in which convective instabilities develop from periodic patterns to irregular large time dependent flow structures. When considering a single infinitely long horizontal channel, it is found that if the internal heating is large enough ($Gr > Gr_{cr}$), the stable state, characterized by a parabolic vertical distribution of the temperature, loses its stability and convective motions set in as spatially periodic pairs of counter-rotating rolls with their axes aligned with the horizontal magnetic field. The number of cells depends on the intensity of the magnetic field and on the volumetric thermal load. By increasing the Grashof number instabilities extend towards the lower wall and flow structures become larger. Three main flow regimes have been identified: a 2D stable flow, where a weak convective motion driven by horizontal temperature gradients is present, a first 3D regime characterized by periodic convective rolls aligned with the magnetic field and a second 3D regime in which small structures combine to form larger cells.

In case of three electrically and thermally coupled parallel ducts, the vertical temperature distribution is strongly asymmetric resulting in a significant temperature difference between the two horizontal stiffening plates that depends on the magnitude of the magnetic field (Ha) and the heat source (Gr). Noticeably different flow conditions are present in the three coupled ducts and perturbations in the flow field first occur in the upper duct, then in the middle one and for sufficiently large heat sources in the lower channel. An example is shown in Fig. 3. In the upper duct large irregular structures are present while in the middle channel smaller periodic convective rolls develop. Instabilities start as periodic rolls along the upper stiffening plate where strong temperature gradients are present. The development of convective structures by increasing the volumetric heat source is analogous to the one in a single duct: periodic cells, elongated rolls, larger rotating structures and time dependent instabilities. The numerical results clearly show the importance of the thermal coupling when predicting magneto-convective flows in geometries relevant for liquid metal blanket applications. Fundamental is also the use of realistic electric and thermal conditions of fluid and wall materials.

Three dimensional numerical simulations have been also performed for magneto-convective flows in a breeder unit of a HCLL TBM when a spatially varying power source is present. Realistic thermal and electrical properties of structural material and liquid breeder have been consid-
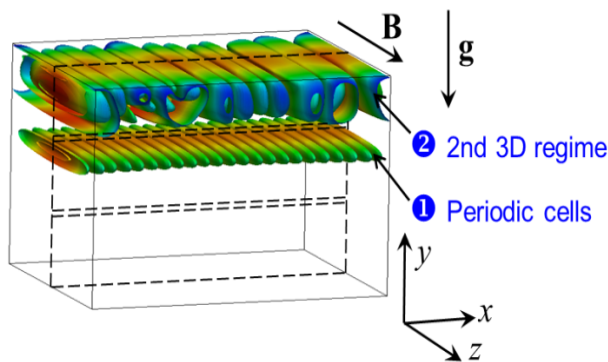
Fig. 3: Iso-surfaces of electric potential for the flow at Ha = 2000 and Gr = 2.2·10^7 in three coupled, infinitely extended ducts.
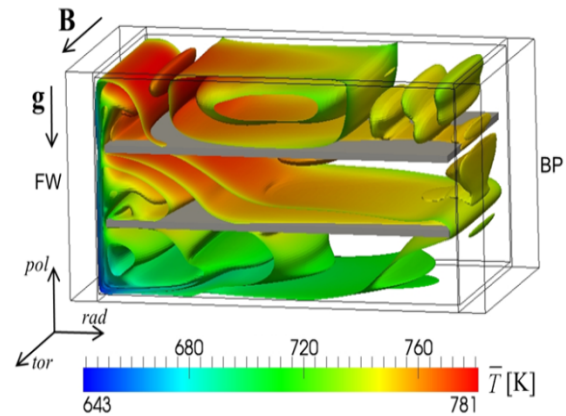
Fig. 4: Iso-surfaces of time averaged electric potential, colored by averaged temperature, for flow at Ha = 2000 and Gr = 1.2 10^8 in a cavity.
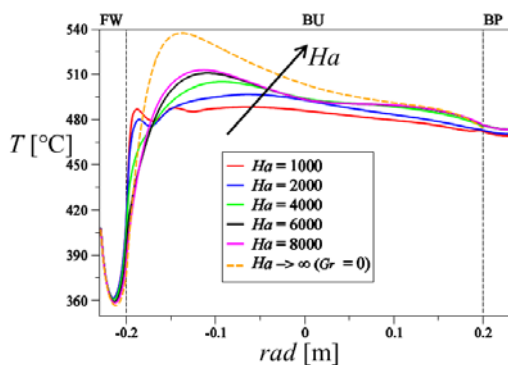
Fig. 5: Radial distribution of time-averaged temperature along the central line of the geometry at y=0, z=0.
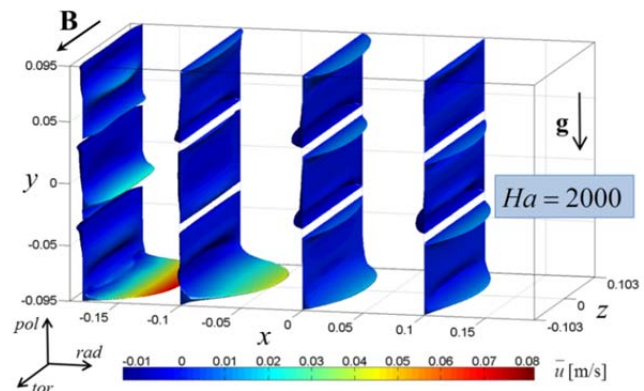
Fig. 6: Time averaged radial velocity distribution in a BU at four x locations for MHD-convective flows at Ha = 2000.

ered, as well as thermal operating conditions as expected in ITER [Villari, Petrizzi, Moro, 2010]. The influence of the radial distribution of the neutron load in the lead lithium has been investigated for increasing strength of the applied magnetic field. The non-uniform thermal conditions, caused by the generated neutron power density and heat extraction through the walls, result in complex convective motions in the form of cells of different size with axes aligned with the toroidal magnetic field (Fig. 4). In all investigated cases a large convective stream is present that moves the fluid from the colder FW to the BP and to the upper stiffening plate.

By increasing the magnitude of the magnetic field, i.e. Ha, the average convective motion and perturbations are significantly damped due to the braking action of the stronger electromagnetic Lorentz forces. As a result, the velocity decreases and the average temperature becomes larger (Fig. 5 and Fig. 6). The increased mean temperature in the BU when increasing Ha indicates the degradation of the convective heat transfer in the liquid metal (Fig. 5). At the FW an intense downward flow is present due to the significant cooling of this wall leading to the formation of a high velocity jet that enters the lower channel (Fig. 6). As a consequence, a stable density stratification establishes between the lower stiffening plate and the first cooling plate. For flows at $H = 2000$, the temperature difference between these two plates can be of the order of 45-55 °C. This strong temperature gradient is most likely reduced if the thermal coupling of adjacent breeder units in a column of a TBM is considered, as it will be analyzed in future work.

Dual coolant lead lithium blanket design: Investigation of MHD flows in model geometries for liquid metal blankets for fusion reactors

Numerical simulations have been performed to investigate MHD flows in model geometries of a liquid metal manifold for dual coolant lead lithium (DCLL) blankets [Mistrangelo, Bühler, 2014 (9)] [Mistrangelo, Bühler, 2014 (10)]. The geometry considered consists of a manifold feeding an array of three parallel poloidal first-wall ducts (Fig. 7). The liquid metal is supplied through an inlet horizontal rectangular channel that expands

in toroidal direction into a larger distribution zone. The transition from radial to poloidal flow is achieved by a 90 degree elbow.

Different design options for the manifold are considered to identify geometric features that can affect flow distribution in parallel ducts. Same flow rate among parallel channels is required to ensure homogeneous heat transfer conditions and to minimize the occurrence of locally overheated ducts where larger thermal stresses could occur. Two possible expanding zones are compared, a sudden expansion and a continuous enlargement (Fig. 7 and Fig. 8). We discuss in the following numerical results for a reference MHD flow at $Ha = 1000$, with an inlet average velocity of about 0.05 m/s. For the description of the results, the coordinate s is introduced, which varies along the central line of the geometry. The sudden expansion is located at $s = 0$ (Fig. 7). In Fig. 7(a), the electric potential distribution is shown on the surface of the manifold. In almost the entire inlet duct, the electric potential does not vary in axial direction and electric current paths are contained in 2D cross-sectional planes (see Fig. 7(b)). Near the expansion, a streamwise potential gradient occurs, which drives electric currents that close inside the fluid (Fig. 7(b)). The poloidal currents interact with the toroidal magnetic field resulting in streamwise Lorentz forces that brake the liquid metal in the middle of the channel. Electromagnetic forces created by radial currents push the PbLi towards the walls that are parallel to the magnetic field. In Fig. 8, the scaled pressure is plotted along the normalized coordinate s for a sudden and a continuous expansion. In both the cases, the pressure profiles in the outlet ducts almost coincide, while in the feeding channel the pressure in the case of a continuous expansion is reduced by a factor two. This is due to the fact that the influence of the viscous internal layer, that forms at the expansion, is less important for longer expansion length. Moreover, in case of continuous expansion, the 3D current loops are longer and the related resistance of the circuit is higher.

The flow partitioning in poloidal ducts is affected by the length of the internal separating walls, by the 3D MHD pressure drop in the expanding zone and by the velocity distribution after the cross-section enlargement. The latter one changes significantly when considering a continuous expansion rather than a sudden one.
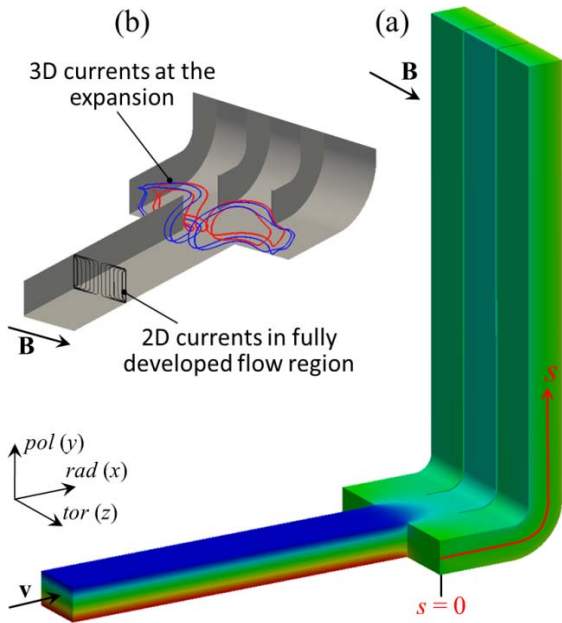
Fig. 7: Surface electric potential distribution: fully developed flow at inlet/outlet and strong 3D effects at the expansion and in the bend
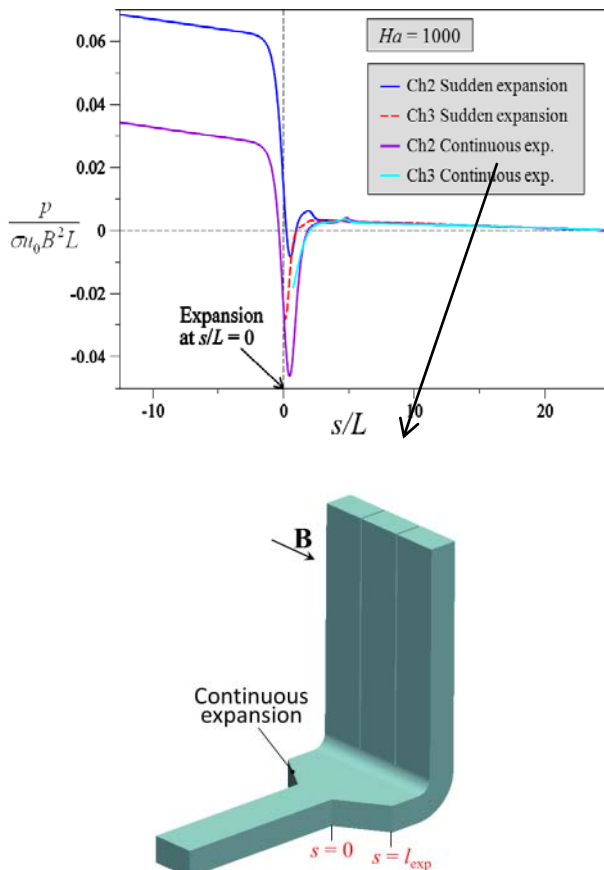
Fig. 8: Axial distribution of scaled pressure in the case of a sudden and a continuous expansion.

References

(1) Ono, M.; Bell, M.; Hirooka, Y.; Kaita, R.; Kugel, H.; Mazzitelli, G.; Menard, J.; Mirnov, S.; Shimada, M.; Skinner C. and Tabares, F.; "Conference Report on the 2nd International Symposium on Lithium Applications for Fusion Devices," *Nuclear Fusion,* vol. 52, p. 037001, 2012.

(2) Mirnov, S.; "Plasma-wall interactions and plasma behaviour in fusion devices with liquid lithium plasma facing components," *Journal of Nuclear Materials*, vol. 390, pp. 876-885, 2009.

(3) Bühler, L.; Mistrangelo C. and Najuch, T.; "Magnetohydrodynamic flows in porous systems," EFDA Final Report, WP13-PEX-03b-T05, 2014.

(4) Mirnov S. und Evtikhin, V.; „The tests of liquid metals (Ga, Li) as plasma facing components in T-3M and T-11M tokamaks," *Fusion Engineering and Design,* Vol. 81, pp. 113-119, 2006.

(5) Mistrangelo, C.; Bühler L. and Aiello, G.; "Buoyant-MHD flows in HCLL blankets caused by spatially varying thermal loads," *IEEE Transactions on Plasma Science,* Vol. 42 (5), pp. 1407 - 1412, 2014.

(6) Mistrangelo C. and Bühler, L.; "Magnetoconvection in HCLL blankets," EFDA Final Report, WP13-DAS-02-T04-D2, 2014.

(7) Gnielinski, V.; "Neue Gleichungen für den Wärme- und den Stoffübergang in turbulent durchströmten Rohren und Kanälen," *Forschung im Ingenieurwesen A,* vol. 41, pp. 8-16, 1975.

(8) Villari, R.; Petrizzi L. and Moro, F.; "Neutronic analysis for HCLL TBM Preliminary design phase," 2010.

(9) Mistrangelo C. and Bühler, L.; "Liquid metal magnetohydrodynamic flows in manifolds of dual coolant lead lithium blankets," *Fusion Engineering and Design,* p. in print, 2014.

(10) Mistrangelo C. and Bühler, L.; "MHD flow in a prototypical manifold of DCLL blankets," EFDA Final Report, WP13-DAS-02-T13-D2, 2014.

(11) Arlt, T.; Chowdhury, V.; Bühler, L.; Mistrangelo, C.; "Influence of contact resistance on MHD liquid metal flows in rectangular ducts", 549th Wilhelm und Else Heraeus-Seminar 'Liquid Metal MHD', Bad Honnef, October 15-18, 2013.

(12) Bühler, C.; Mistrangelo, C.; "Liquid-metal MHD experiments in a scaled mock-up of a fusion test blanket module"; Symposium Simulation von Strömungsprozessen in der Metallurgie (SymSim 2013), Oberhof, 17.-20. Juni 2013.

(13) Bühler, L.; Brinkmann, H.-J.; „MEKKA facility for DCLL blanket MHD experiments"; 1st EU-US DCLL Workshop, Karlsruhe, April 23-24, 2013.

(14) Bühler, L.; Mistrangelo, C.; „Influence of non-insulated gaps between flow channel inserts in ducts of DCLL blankets"; 25th Symposium on Fusion Engineering (SOFE 2013), San Francisco, Calif., June 10-14, 2013, Proceedings on CD-ROM Paper 1351, Piscataway, N.J.: IEEE, 2013, ISBN 978-1-4799-0169-2.

(15) Bühler, L.; "MHD pressure drop at bare welding positions in pipes of DCLL blankets"; KIT Scientific Reports, KIT-SR 7636 (Januar 2013).

(16) Bühler, L.; Mistrangelo, C.; Konys, J.; Bhattacharyay, R.; Huang, Q.; Obukhov, D.; Smolentsev, S.; Utili, M.; "Facilities, testing program and modeling needs for studying liquid metal magnetohydrodynamic flows in fusion blankets"; 11th International Symposium on Fusion Nuclear Technology (ISFNT 2013), Barcelona, E, September 16-20, 2013.

(17) Bühler, L.; "Liquid metal magneto-hydrodynamics in strong magnetic fields". RTG Summer School 'Lorentz Force Velocimetry and Lorentz Force Eddy Current Testing', Karlsruhe, September 30, 2013.

(18) Bühler, L.; Mistrangelo, C.; „Magneto-hydrodynamic flows for fusion applications: modeling and experiments". 549th Wilhelm und Else Heraeus-Seminar 'Liquid Metal MHD', Bad Honnef, October 15-18, 2013.

(19) Bühler, L.; "MHD flows in WCLL blankets: similarities with other designs and concept-specific problems". WCLL Blanket Workshop, Paris, F, October 7-8, 2013.

(20) Bühler, L.; Mistrangelo, C.; "Magnetohydrodynamic flows in breeder units of a HCLL blanket with spatially varying magnetic fields". *Fusion Engineering and Design*, 88 (2013) 2314-2318.

(21) Chowdhury, V.; Bühler, L.; "Experimental investigations of magnetically induced instabilities (Project A3)". LIMTECH Summer School, Dresden, May 27-29, 2013.

(22) Ehrhard, S.; Bühler, L.; "Numerical analysis of magnetohydrodynamic flows in ferromagnetic channels". LIMTECH Summer School, Dresden, May 27-29, 2013.

(23) Ehrhard, S.; "Simulation of MHD flows in ferromagnetic channels". Symposium für Strömungsprozesse (SymSim 2013), Ilmenau, 17.-20. Juni 2013.

(24) Ehrhard, S.; Buehler, L.; "Influence of magnetic field deformation by ferromagnetic wall materials on MHD flows in pipes and ducts of fusion blankets". 11th International Symposium on Fusion Nuclear Technology (ISFNT 2013), Barcelona, E, September 16-20, 2013.

(25) Koehly, C.; Wang, X.R.; Tillack, M.S., Najmabadi, F.; "Alternative design options for a dual-cooled liquid metal blanket for ARIES-ACT2. La Jolla, Calif.: University of California, Center for Energy Research; UCSD-CER-13-02 (August 2013).

(26) Koehly, C.; Tillack, M.S.; Wang, X.R.; Najmabadi, F.; Malang, S.; ARIES Team; "Flow distribution systems for liquid metal cooled blankets". 25th Symposium on Fusion Engineering (SOFE 2013), San Francisco, Calif., June 10-14, 2013, Proceedings on CD-ROM Paper 1173, Piscataway, N.J.: IEEE, 2013, ISBN 978-1-4799-0169-2.

(27) Li-Puma, A.; Boccaccini, L.V.; Bachmann, C.; Norajitra, P.; Mistrangelo, C.; Aiello, G.; Aubert, J.; Carloni, D.; Kecskes, S.; Kang, Q.L.; Morin, A.; Sardain, P.; "Design and development of DEMO blanket concepts in Europe". 11th International Symposium on Fusion Nuclear Technology (ISFNT 2013), Barcelona, E, September 16-20, 2013.

(28) Mistrangelo, C.; Bühler, L.; "Numerical modeling of MHD flows in DCLL blankets, KIT activities". 1st EU-US DCLL Workshop, Karlsruhe, April 23-24, 2013.

(29) Mistrangelo, C.; Bühler, L.; "Buoyancy-driven magnetohydrodynamic (MHD) flows". Symposium Simulation von Strömungsprozessen in der Metallurgie (SymSim 2013), Oberhof, 17.-20. Juni 2013.

(30) Mistrangelo, C.; Bühler, L.; "Influence of variable heat source on magneto-convective flows in HCLL blankets". 25th Symposium on Fusion Engineering (SOFE 2013), San Francisco, Calif., June 10-14, 2013, Proceedings on CD-

ROM Paper 1355, Piscataway, N.J.: IEEE, 2013, ISBN 978-1-4799-0169-2.

(31) Mistrangelo, C.; Bühler, L.; "Liquid metal magnetohydrodynamic flows in manifolds of dual coolant lead lithium blankets". 11th International Symposium on Fusion Nuclear Technology (ISFNT 2013), Barcelona, E, September 16-20, 2013.

(32) Mistrangelo, C.; Bühler, L.; "Numerical and asymptotic modeling of MHD flows for liquid metal blankets". Liquid Breeder Blanket Subtask Collaboration Workshop, Barcelona, E, September 20-21, 2013.

(33) Mistrangelo, C.; Bühler, L.; "Magneto-convective flows in electrically and thermally coupled channels". *Fusion Engineering and Design,* 88 (2013) 2323-2327.

(34) Reimann, J.; Abou-Sena, A.; Nippen, R.; Ferrero, C.; „Pebble bed packing in square cavities". KIT Scientific Reports, KIT-SR 7631 (Januar 2013).

(35) Reimann, J.; Beres, O.; Colle, J.Y.; Dorn, C.; Harsch, H.; Koenigs, R.; Kurinsky, P.; „First measurments of beryllide vapor pressures". Proceedings of the 10th IEA International Workshop on Beryllium Technology, KIT Scientific Reports, KIT-SR 7650, (September 2013) S. 258-262.

(36) Reimann, J.; Abou-Sena, A.; Nippen, R.; Tafforeau, P.; "Pebble bed packing in prismatic containers". *Fusion Engineering and Design*, 88 (2013) 2343-2347.

(37) Reimann, J.; Abou-Sena, A.; Brun, E.; Fretz, B.; „Packing experiments of Beryllium pebble beds for the fusion reactor HCPB blanket". 11th IEA International Workshop on Beryllium Technology (BeWS 2013), Barcelona, E, September 12-13, 2013.

(38) Vladimirov, P.; Reimann, J.; [Hrsg.]; „Proceedings of the 10th IEA international workshop on beryllium technology." KIT Scientific Reports, KIT-SR 7650, (September 2013).

Group: Transmutation

Scenario Analyses for the German study on Partitioning and Transmutation

Andrei Rineiski, Fabrizio Gabrielli, Werner Maschek, Claudia Matzerath Boccaccini, Aleksandra Schwenk-Ferrero, Barbara Vezzoni

Introduction

In 2012-2013, the German Federal Ministry of Economics and Environment (BMWi) supported a study on Partitioning and Transmutation (P&T) for German nuclear waste management options. This P&T study, in which both social and technical issues were addressed, was coordinated by ACATECH, a German national academy of science and engineering. The NUKLEAR project of KIT coordinated the technical part of the study, with the following main topics:

- Nuclear waste characteristics, such as mass, radioactivity, etc. and their evolution with time after the planned ultimate nuclear reactor shutdown in 2022;

- Principal possibilities for transmutation of trans-uranium isotopes (TRUs) into fission products in nuclear reactors and potential transmutation benefits;

- Scenario/system options for transmutation of German TRUs;

- Technology and safety issues.

The Transmutation group (TRANS) of IKET contributed to the above mentioned activities and coordinated studies on scenario/system options.
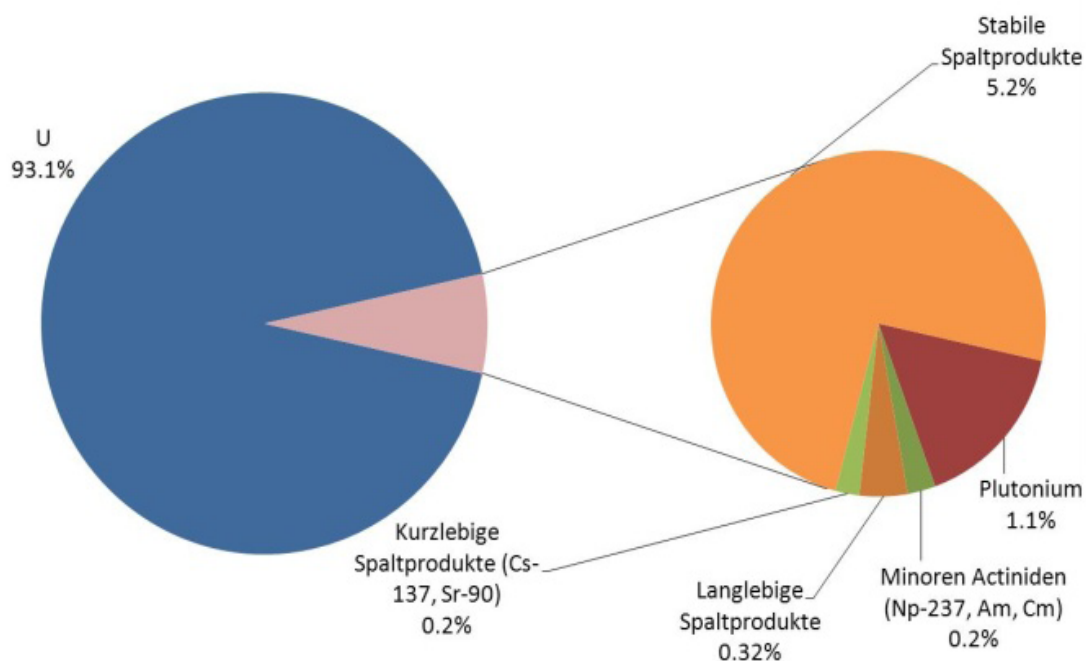
Figure 1: Isotopic composition of spent LWR fuel with a burn-up of about 5% at after 10 years of cooling.

Scenario/system analyses

After the planned shutdown of all German nuclear power plants in 2022, more than 10 thousand tons of the spent nuclear fuel (SNF) will be accumulated in Germany.

SNF contains only a small fraction of trans-uranium elements (TRUs), see Figure 1 (in Figure 1, "Kurzlebige/Langlebige/Stabile Spalt-produkte" stand for Short-lived/Long-lived/Stable Fission products, "Minoren Actiniden" stand for Minor actinides). But their transmutation, i.e. transformation of TRUs into fission products, may facilitate appreciably SNF storage by reducing the storage footprint and lessen long-term risks related to a misuse of the stored nuclear waste, see Figure 2, which shows the radioactivity level evolution of nuclear waste and its components, Fission products and Actinides. Note that the Actinide radioactivity shown at Figure.2 is mainly due to TRUs.

Options for transmutation of German TRUs in the European (several countries cooperate) and German frameworks (Germany incinerated German TRUs) were considered in the P&T study. A European scenario was studied in details in the past in the EU PATEROS project. For this scenario, a small 400 MW_{th} Accelerator Driven System (ADS), the EFIT [Chen, Rineiski, Maschek, 2011], was chosen as the transmutation devise. EFIT was specially designed to burn Minor Actinides (MAs). Note that conventional reactors are not designed to use fuels with a high percentage of MAs. MAs are accumulated in the fuel of conventional reactors during reactor operation, but their fraction there remains low.

It must be limited because of safety reasons. The remaining Pu, the major TRUs component, is stored to be used in future Fast Reactors (FRs) in countries using nuclear energy further.
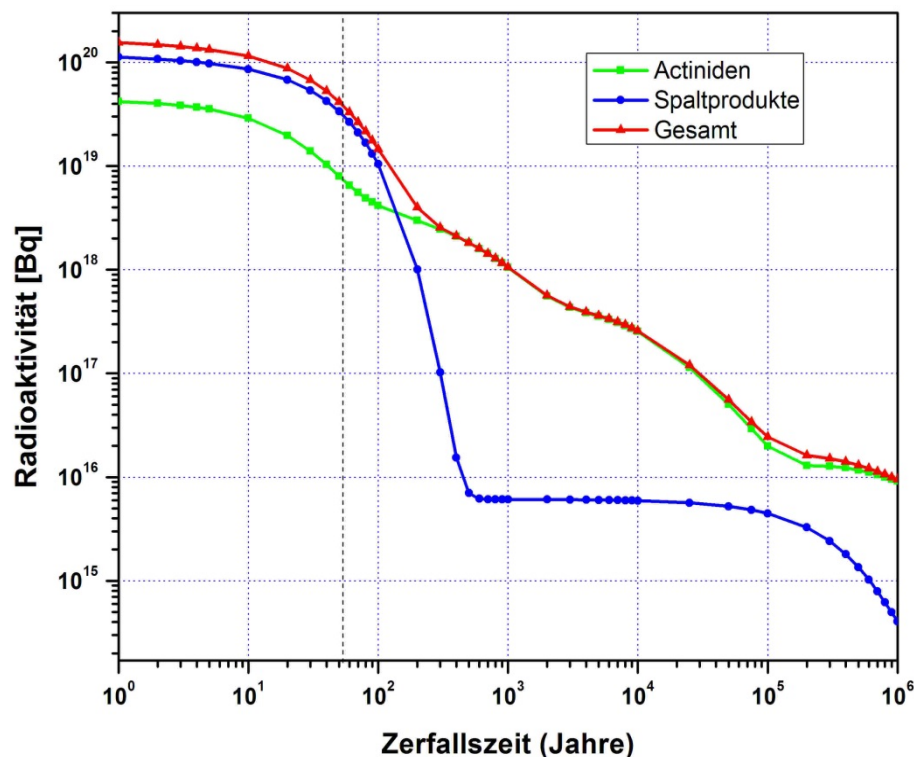
Figure 2: Radioactivity evolution of spent nuclear fuel accumulated in Germany vs decay time in years (Zerfallszeit, Jahre) with its components: Actinides, Fission Products and Total ("Gesamt").
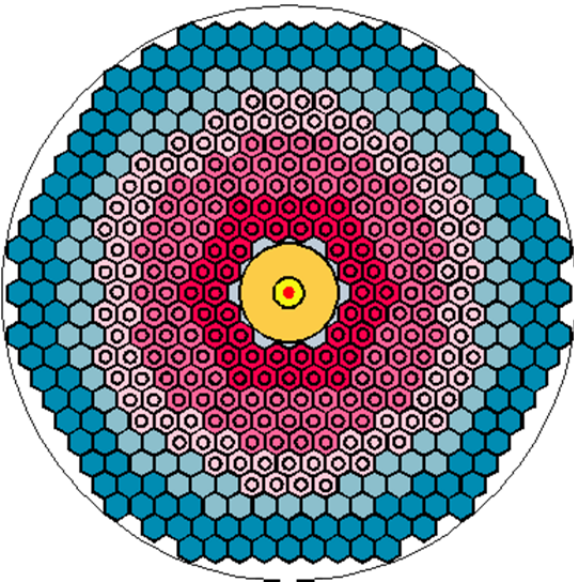
Figure 3: EFIT core layout in plane: the spallation target emitting neutrons (innermost circle) is surrounded by lead "buffer", several rings of hexagonal fuel and reflector/shielding subassemblies.

As Minor Actinines constitute a small fraction of TRUs, the effort on their incineration, i.e. the number of reactors multiplied by time of their operation and by their power is smaller compared to the case of burning all TRUs. After all Minor Actinides of e.g. Germany are burned, the available facilities e.g. in France can be used further to burn MAs during continuous operation of the French reactor fleet. Sharing the development, construction and operation costs by several countries is another advantage of the European scenario. On the other hand, large efforts are still needed to develop the ADS and ADS fuel technology. Note that the ADS fuel does not contain U to reach the maximum possible TRUs incineration rate per power produced.

For a German-only scenario a larger amount of TRUs, both Pu and MAs(not only MAs) should be burned as compared to the German contribution (only MAs) to the European transmutation effort. Unlike the European case, the transmutation should be stopped at the time when the available TRUs amount is not sufficient to fabricate the amount of fuel required for a full core loading. Thus a small amount of TRUs in addition to fuel reprocessing losses remains to be stored. The ADS can be also used for burning all TRUs, but due to a lower MAs content (in view of Pu in the fuel) other systems can be considered, such as fast reactors FRs.
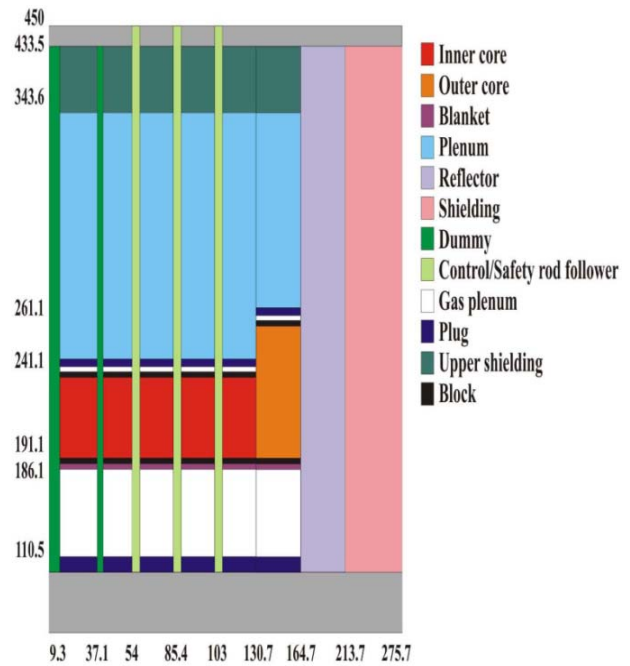
Figure 4: r-Z model of the ASTRID-like core with a lower inner core, higher outer core, MA-bearing fertile lower blanket and upper Na plenum

A large experience has been accumulated at KIT in general and in TRANS in particular on safety analyses of fast reactors and on their optimization for improving their safety and transmutation performance. In the time period 2008-2011 KIT , within the 6th European Framework Programme coordinated safety analyses and optimizations for the European Sodium Fast Reactor, CP-ESFR, a large 3600 MW$_{th}$ industrial scale system, construction and operation of which is considered in France for the time after 2050. More recently the main effort on FR development in Europe has been focused on the French ASTRID project. ASTRID is a smaller, 1500 MW$_{th}$ reactor planned to be built in France after 2020. KIT proposed a modified core design with a ca. 20% lower core (to improve safety parameters) and a ca 20% lower thermal power (to keep the linear power similar after the core height reduction) for the German P&T study.

The preliminary analyses have shown that the safety parameters of the ASTRID-like burner are reasonable. The global coolant void effect is negative. The Doppler constant value is relatively large in magnitude. The transmutation performance per unit is similar to that of EFIT, i.e. only 3 times lower per unit of power in view of using fuel with U matrix.

Analytical calculations have shown that ca. 7 EFIT-like or ca. 7 ASTRID-like reactors operating for 150 years can incinerate all TRUs from the German nuclear waste, except a few percent (contained in the last transmuter and lost due to fuel reprocessing. This conclusion is supported by a preliminary analyses performed with the COSI scenario code.

Conclusions

The German P&T study was supported by KIT to address the main technical issues, including scenarios, systems, fuels, technology and safety. Scenario/system analyses have shown that both ADS and FRs can be used for German nuclear waste management.

In case of a regional (European) scenario, the analyses are based on earlier studies in the EU PATEROS project, for which a small 400 MW_{th} ADS EFIT was considered as MAs transmutation devise. A couple of ADS operating for 150 years may burn all German MAs: to get rid of TRUs in Germany, except a few percent of fuel reprocessing losses, provided that Pu is stored for future use in France. The transmutation may then go further on to deal with the waste produced in France

For the German - only scenario, a 1200 MW_{th} ASTRID-like fast reactor was proposed at KIT, with reasonable safety parameters. It shows a similar TRUs transmutation performance per unit (i.e. ca 3 times lower per unit of power) as compared to EFIT. Ca. 7 ASTRID-like units in average operated for 150 years, may reduce the remaining (due to the last transmuter problem and the reprocessing losses) TRUs amount to a few percent as compared to the inventory accumulated by 2022.

In view of the planned ASTRID construction after 2020 in France and a much larger industrial experience with fast reactors, the ASTRID-like systems will be further studied. One particular objective is to assess their performance in European scenarios.

References

(1) Chen, X-N.; Rineiski, A.; Maschek W.; et al., "Comparative studies of CERCER and CERMET fuels for EFIT from the viewpoint of core performance and safety", *Progress in Nuclear Energy*, vol. 53, no. 7, pp. 855-861, 2011.

(2) Andriolo, L.; Chen, X.N.; Matzerath Boccaccini, C.; Maschek, W.; Rineiski, A.; Delage, F.; "Preliminary safety analysis of mixed oxide sphere-pac driver fuels in the CP-ESFR WH core". 4th International Symposium on Innovative Nuclear Energy Systems (INES 2013), Tokyo, J, November 6-8, 2013.

(3) Chen, X.N.; „On LBE natural convection and its water experimental simulation". 16th International Conference on Emerging Nuclear Energy Systems (ICENES 2013), Madrid, E, May 26-30, 2013.

(4) Chen, X.N.; Li, R.; Rineiski, A.; "Subchannel blockage accident analysis of MYRRHA reactor". 4th Conference on Heavy Liquid Metal Coolants in Nuclear Technologies (HLMC 2013), Obninsk, Russia, September 22-27, 2013.

(5) Chen, X.N.; "Study of one-dimensional ship squat theories". *Chinese Journal of Hydrodynamics*, 28 (2013) 399-407.

(6) Gabrielli, F.; Rineiski, A.; Marchetti, M.; Maschek, W.; „Reactor transient analyses with KIN3D/PARTISN". International Conference on Mathematics and Computational Methods Applied to Nuclear Science & Engineering (M&C 2013), Sun Valley, Idaho, May 5-9, 2013.

(7) Gabrielli, F.; Rineiski, A.; Vezzoni, B.; Maschek, W.; Salvatores, M.; „ASTRID-like reactor cores for burning plutonium and minor actinides". 4th International Symposium on Innovative Nuclear Energy Systems (INES 2013), Tokyo, J, November 6-8, 2013.

(8) Gabrielli, F.; "Fuel for ADS: state-of-the-art, requirements, current and future programs". 2nd International Workshop on Technology and Components of Accelerator-Driven Systems (TCADS 2013), Nantes, F, May 21-23, 2013.

(9) Knebel, J.; Fazio, C.; Maschek, W.; Tromm, W.; „Was tun mit dem nuklearen Abfall?", *Spektrum der Wissenschaft* (2013) Nr.2, S. 34-41.

(10) Kriventsev, V.; "Minimum energy dissipation in modeling of turbulent flow". 13th International Conference 'Nuclear Power Safety and Nuclear Education', Obninsk, Russia, October 1-5, 2013.

(11) Li, R.; Chen, X.N.; Matzerath Boccaccini, C.; Rineiski, A.; Maschek, W.; Forgione, N.; Bandini, G.; "Study on severe accident scenarios: pin failure possibility of MYRRHA-FASTEF critical core". 4th International Symposium on Innovative Nuclear Energy Systems (INES 2013), Tokyo, J, November 6-8, 2013.

(12) Rineiski, A.; Vezzoni, B.; Gabrielli, F.; Maschek, W.; Salvatores, M.; Fazio, C.; „Options for incineration of trans-uranium elements from German spent nuclear fuel". 16th International Conference on Emerging Nuclear Energy Systems (ICENES 2013), Madrid, E, May 26-30, 2013.

(13) Schwenk-Ferrero, A.; "German spent nuclear fuel legacy: Characteristics and high-level waste management issues". *Science and Technology of Nuclear Installations* (2013) Article ID:293792.

(14) Schwenk-Ferrero, A.; Romanello, V.; "Analyses of advanced fuel cycles dedicated to minimization of transuranics mass in german legacy waste using fast critical burners and subcritical transmuters". 16th International Conference on Emerging Nuclear Energy Systems (ICENES 2013), Madrid, E, May 26-30, 2013.

(15) Vezzoni, B.; Rineiski, A.; Gabrielli, F.; „Minor actinides incineration options using an innovative Na-cooled fast reactor". 525th Wilhelm und Else Heraeus-Seminar on Nuclear Physics Data for the Transmutation of Nuclear Waste, Bad Honnef, February 25-27, 2013.

(16) Vezzoni, B.; Gabrielli, F.; Rineiski, A.; Schwenk-Ferrero, A.; Romanello, V.; „Minor actinides incineration options using innovative Na-cooled fast reactors: Impact on phasing-out and on-going fuel cycles". 4th International Symposium on Innovative Nuclear Energy Systems (INES 2013), Tokyo, J, November 6-8, 2013.

(17) Vorobyev, A.; "A smoothed particle hydrodynamics method for the simulation of centralized sloshing experiments". Dissertation, Karlsruher Institut für Technologie 2012, Karlsruhe : KIT Scientific Publishing, 2013, ISBN 978-3-86644-953-4.

(18) Wang, K.; Rineiski, A.; Maschek, W.; Wu, H.; Cao, L.; „Neutron transport model based on the transmission probability method". *Energy Conversion and Management*, 72 (2013) 33-38.

(19) Zhang, D.; Chen, X.-N.; Flad, M.; Rineiski, A.; Maschek, W.; „Theoretical and numerical studies of TWR based on ESFR core design". *Energy Conversion and Management,* 72 (2013), 12-18.

Analysis of Design Basis and Severe Accidents

Alexei Miassoedov, Giancarlo Albrecht, Thomas Cron, Philipp Dietrich, Beatrix Fluhrer, Stephan Gabriel, Xiaoyang Gaus-Liu, Max Kirsthaler, Frank Kretzschmar, Markus Schwall, René Stängle, Tobias Szabó

Introduction

The research activities in the LWR severe accidents domain in the Accident Analysis Group (UNA) are concentrated on the in- and ex-vessel core melt behavior. The overall objective is to investigate the core melt scenarios from the beginning of core degradation to melt formation and relocation in the vessel, possible melt dispersion to the reactor cavity and to the containment, and finally corium concrete interaction and corium coolability in the reactor cavity.

- The experimental platform includes three experimental facilities:

- LIVE to investigate the melt pool behavior in the RPV lower head;

- DISCO to study the melt dispersion to the reactor cavity and direct containment heating;

- MOCKA to study molten corium concrete interaction.

The results of the experiments are being used for the development and validation of codes applied for safety assessment and planning of accident mitigation concepts, such as MELCOR and AS-TEC. The strong coupling between the experiments and analytical activities contribute to a better under-standing of the core melt sequences and thus improve safety of existing reactors by severe accident mitigation measures and by safety installations where required.

The understanding of major processes for the assessment of the plant response/behaviour under design basis or beyond design basis situations still have to be further developed. For this purpose, experimental investigations are carried out in the WENKA and COSMOS facilities that allow to answer the remaining open issues of thermal-hydraulics and physico-chemical phenomena during postulated design and beyond design transients/accidents, including their interaction to further improve the simulation tools and for the derivation of appropriate science-based countermeasures.

LIVE experiments

The main objective of the LIVE program is to study the late in-vessel core melt behavior and core debris coolability both experimentally in large scale 2D and 3D geometry and in supporting separate-effects tests [Meyer et al. 2009], and analytically using CFD codes in order to provide a reasonable estimate of the remaining uncertainty band under the aspect of safety assessment. The LIVE-3D test facility allows the investigation of a melt pool in the lower plenum of a RPV in 3D geometry with simulated internal heat generation. Other test facilities had only a 2D geometry or were performed without heating of the melt. The main part of the LIVE-3D test facility is a 1:5 scaled semi-spherical lower head of the typical pressurized water reactor, as shown in Fig. 1.
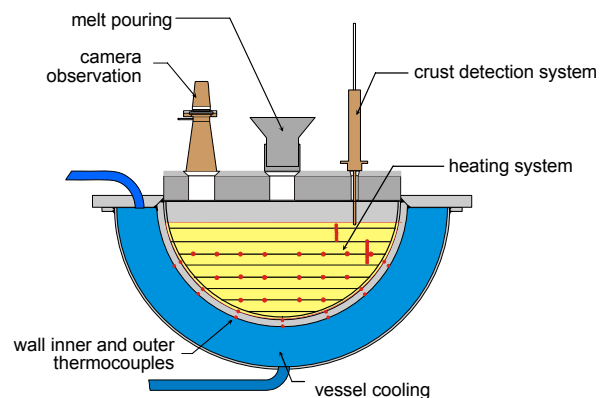
Fig. 1: Scheme of the LIVE-3D test vessel

The diameter of the test vessel is 1 meter. The top area of the test vessel is covered with an insulated lid. The test vessel is enclosed in a cooling vessel to simulate the external cooling. The melt is prepared in an external heating furnace designed to generate 220 l of the simulant melt. The volumetric decay heat is simulated by means of 6 heating planes providing a maximum power of about 28 kW.

To investigate both the transient and the steady state behavior of the simulated corium melt, an extensive instrumentation of the test vessel is realized. The temperatures of the vessel wall inner surface and outer surface are measured at 5 latitudes and 4 locations at each latitude. Heat flux distribution through the vessel wall can be calculated based on these temperatures. Additionally, 80 thermocouples are positioned within the vessel to measure the temperature distribution in the melt pool and in the crust.

The debris melting process after melt relocation was investigated in two tests with different fractions of relocated liquid melt in LIVE-3D facility [Gaus-Liu et al, 2011]. In the L8A test, 70 vol. % of liquid melt and in the L8B test 50 vol.% of liquid melt were poured in a preheated debris bed. Both, the liquid melt and the debris particles are simulated with 20% NaNO3-80% NaNO3 mixture. The particles size is in the range of 3.5 to 16 mm, and the porosity is ~0.5. The maximum temperature of the preheated debris bed was slightly below the solidus temperature. The pouring temperature of the liquid melt is 350 °C. The heating power was switched to 21 kW right after melt pouring and maintained till the end of the test. The total mass of the debris and liquid melt was 351 kg, corresponding to 406 mm pool height of a totally molten pool.

The melt temperature distribution in the preheating phase and after melt relocation in L8B test is shown in the Fig. 2. During preheating period, the maximum debris temperature located at the upper-centre region, which indicates also the location of melting initiation in the debris bed. After melt relocation, the most of voids in the debris bed were filled with liquid melt and an essential fraction of liquid melt was solidified in the lower part of the debris bed.
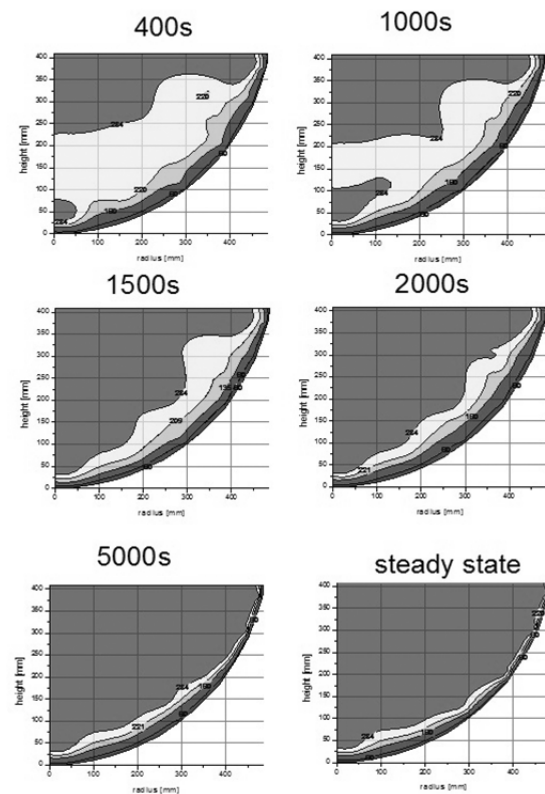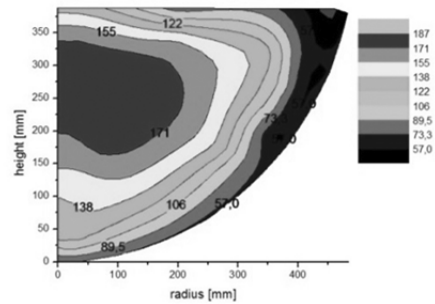
Fig. 2: Melt temperature distribution during L8B test. Top: preheating phase; bottom: after the melt relocation

DISCO experiments

The DISCO experiments [Meyer et al. 2009] are designed to investigate the fluid-dynamic, thermal and chemical processes during melt ejection out of a breach in the lower head of a PWR pressure vessel at pressures below 2 MPa with an iron-alumina melt and steam. In the frame of these investigations the following issues are addressed: final location of corium debris, loads on the reactor pit and the containment in respect to pressure and temperature, and the amount of hydrogen produced and burned. The main components of the facility (Fig. 3) are scaled about

1:18 linearly to a large PWR. The model of the containment pressure vessel has a height of 5.80 m and a total volume of 14 m³. The volumes of the reactor cooling system and the reactor pressure vessel are modeled by a vertical pipe.

Standard test results are: pressure and temperature history in the reactor pressure vessel (RPV), the cavity, the reactor compartments and the containment vessel, post-test melt fractions in all locations with size distribution of the debris, video film in the subcompartments and containment (timing of melt flow and hydrogen burning), and pre- and post-test gas analysis in the cavity and the containment. The gas analysis allows determining the amount of produced, burned and remaining hydrogen.

Possible containment overpressurisation caused by corium jets after the RPV failure is a design-specific issue and is being investigated thoroughly for several plant designs (EPR, French PWR and VVER-1000, Konvoi). Using the DISCO database, the development of direct containment heating (DCH) models for integral codes has made a significant progress though the available model approaches have not yet been applied to a reactor-scale scenario. Based on the scaled experiments, the hazard of overpressurisation was not regarded as an issue for the abovementioned European designs.

In the last series of the experiments, DISCO facility was used to analyze the phenomena, which occur during an ex-vessel fuel concrete interaction (FCI). The test is focused on the premixing phase of the FCI without a trigger used for explosion phase. The objectives of the test were to evaluate the dispersion of water and melt out of the pit, characterize the debris, estimate the oxidation, provide the pressurization and assess the combustion of hydrogen supplied by oxidation.

The experiment was performed with a pit geometry close to a French 900 MWe reactor configuration at a scale of 1:10. The fuel was a melt of iron-alumina with a temperature of 2400 K. The nozzle diameter was set to 0.030 m which corresponds to 0.30 m diameter break in reactor scale. There was no hydrogen initially present in the test and the pressure in containment was set to 1 bar of air and 1 bar of vapor. The water level

in the pit was about 0.54 m, just below the nozzle, at a temperature of 85 °C.
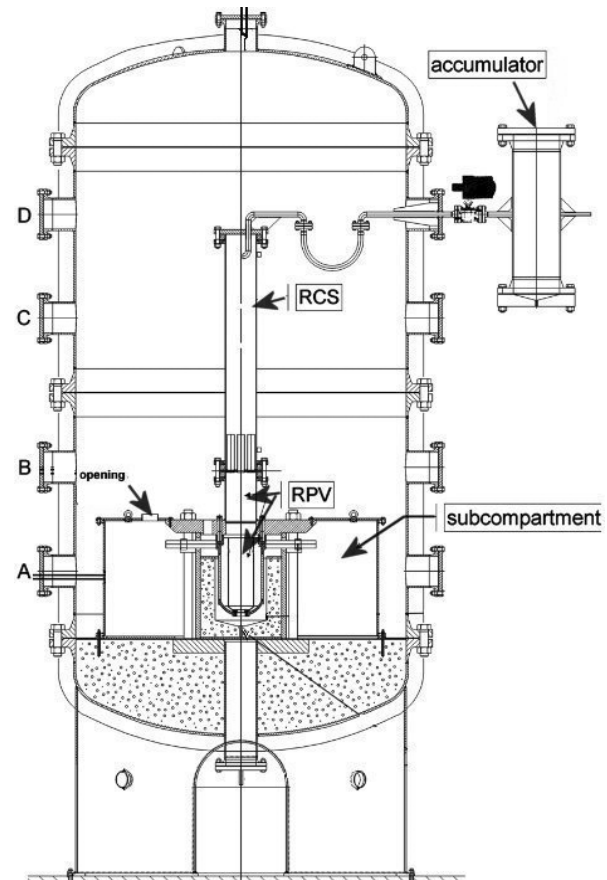
Fig. 3: Scheme of the DISCO facility.

The containment pressure increased by 0.04 MPa to reach about 0.24 MPa. The pressure in the cavity was characterized by several peaks and no spontaneous steam explosion occurred (Fig. 4). The water inside the cavity (initial 125 kg) has been totally ejected. 66% of the initial fuel mass (10.62 kg) remained in the cavity mainly as compact crusts. The fraction of fuel transported out of the pit was about 27 %. The size distribution supplied by sieved analysis indicates tendency to small particles with a median size diameter of 0.4 mm. The amount of hydrogen produced by oxidation was about 3% of total moles of gas. The oxidation rates are important and similar to the previous DCH tests performed in the DISCO facility.
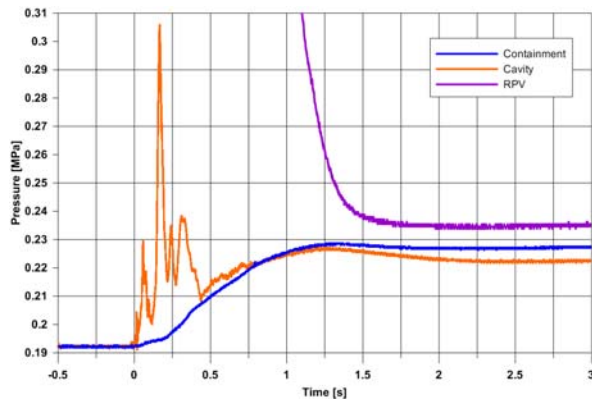
Fig. 4: Pressures in the containment, RPV and in the cavity

MOCKA experiments

The MOCKA facility [Foit et al, 2012] is a new facility which is designed to investigate the corium/concrete interaction in an anticipated core melt accident in LWRs, after the metal melt is layered beneath the oxide melt. The experimental focus is on the cavity formation in the basemat and the risk of a long-term basemat penetration by the metallic part of the melt.

Even though extensive research has been undertaken over several years in the area of core-concrete interaction, several subjects need further investigations. An important issue concerns the distribution of the heat flux to the concrete in the lateral and axial directions during the long-term 2-dimensional concrete erosion by a core melt. The knowledge of this partition is important in the evaluation of the consequences of a severe reactor accident.

In all MOCKA experiments, a cylindrical concrete crucibles with an inner diameter of 25 cm are used. Both, the sidewall and basemat, were instrumented with Type K thermocouple assemblies to deter-mine the concrete erosion as a function of time. A total of 63 thermocouples were used. The initial melt consists of 42 kg Fe together with 4 kg Zr, overlaid by 68 kg oxide melt (initially 56 wt.% Al_2O_3, 44 wt.% CaO). The initial height of the metal melt was about 13 cm. The melt temperature at start of interaction was approximately 2273 K. The initial temperature was estimated from the reaction enthalpy of the used thermite taking into account the temperature measurements from the former BETA tests.

The CaO admixture lowers the solidus temperature and the viscosity of the oxide melt. The resulting solidus temperature of approx. 1633 K is sufficiently low to prevent a formation of an initial crust at the oxide/concrete. The internal heat generation in the oxide phase is simulated by a succession of additions of pure thermite and Zr metal to the melt from the top being the first of a kind heating method realized for high temperature melts worldwide. The heat generated by the exothermal oxidation reactions of the continuously added Zr is deposited in the oxide phase. Due to density-driven phase segregation the metal melt at the bottom of the crucible is fed by the enthalpy of the Fe melt, which is generated in the oxide phase by the thermite reaction of the added thermite. Approximately 80 % of the heating power was deposited in the oxide phase and 20 % in the iron melt. In this way, a prototypic heating of both melt phases was achieved.

The long-term axial erosion by the metallic phase in the MOCKA tests was a factor of 2-3 higher than the lateral ablation. Similar results were obtained in former BETA and COMET-L experiments. In contrast to the findings in BETA and COMET-L experiments, significant lateral concrete erosion by the oxide melt was observed. The more pronounced downward erosion seems to be inherent to the erosion by metal melts. Typical concrete erosion profile in MOCKA tests is shown in Fig. 5. Initial size of the crucible is indicated, the red line shows the initial height (13 cm) of the metal melt. The axially-elongated shape of the erosion profile (typically obtained for cylindrical siliceous concrete crucibles without reinforcement by the erosion by a metal melt). The maximum downward erosion rate as high as 14 mm/min was observed. A lateral concrete erosion of 6.5 cm versus 15 cm of axial ablation by the metal melt was found. The sideward erosion by the oxide extends to 5 cm. The knowledge of relation between the axial and lateral basemat erosion is important in evaluation of the consequences of a severe reactor accident. However, the experiments need careful interpretation for application to the reactor accident, as the analysis of the MCCI at the reactor scale still requires extrapolation beyond the existing experimental database.
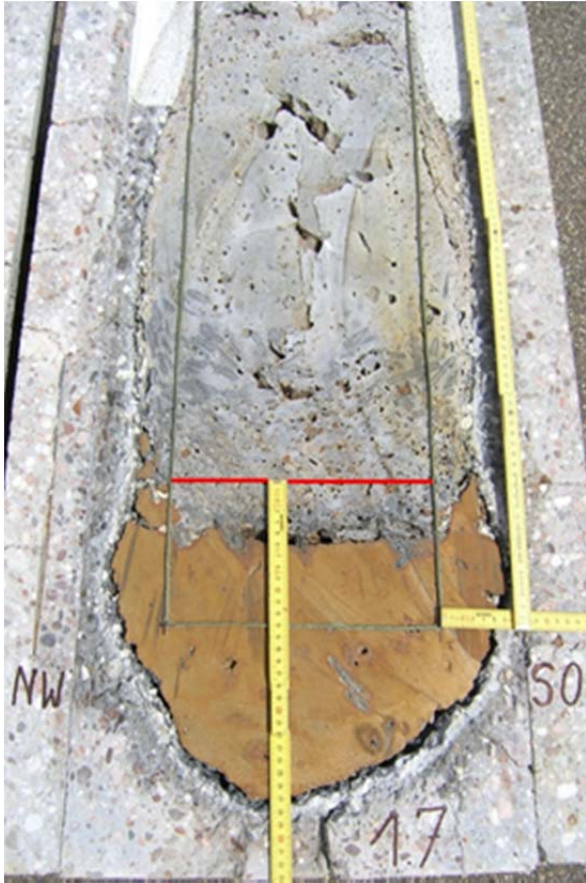
Fig. 5: Cross-section of the MOCKA crucible.

Being one of the still unresolved issues, the two-dimensional concrete ablation caused by oxidic melt as well as by stratified oxide-metal melt in presence of steel reinforcing bars will be studied in the future MOCKA experiments. Moreover, MCCI for other concrete compositions (e.g. lime-stone/common sand, basaltic and serpentinite concretes) will be addressed focusing on 2D convective heat transfer distribution.

COSMOS experiments

The water loop for flow boiling heat transfer experiments at low pressure COSMOS-L (Critical-heat-flux On Smooth and MOdified Surfaces) was constructed and put into operation and comprehensive series of two-phase flow experiments were successfully completed (Fig. 6). The influence of surface structure on critical heat flux for flow boiling of water was investigated for Zircaloy tubes in a vertical annular test section [Haas, et al. 2011]. Only a small influence of modified surface structures on critical heat flux was observed for the pressure of 120 kPa in the present test section geometry (Fig. 7). Though only a small influence of modified surface structure on critical

Fig. 6: COSMOS-L test facility for the investigation of the influence of surface structure on CHF

heat flux (CHF) was observed at low pressure in the COSMOS-L test section, the increase of CHF value is expected to be more pronounced (up to 30%) at higher pressure for certain clad surface structures, like micro channels, porous and oxidized layers. To quantify these phenomena for high pressure and to study the cooling of fuel assemblies of pressurized water reactors, with the objective to increase the safety margin to the start of boiling crisis in prototypic conditions, the high-pressure water loop COSMOS-H is being constructed. (Fig. 8). In this loop the reactor conditions will be reached for one fuel rod bundle. The test section will consist of a rod bundle with internal heating and a comparable mass flow rate. Main parameters of the COSMOS-H facility are given in the Table 1.

The objective is to study safety-relevant components of light-water reactors (e.g. fuel assem-

Table 1. Main parameters of the COSMOS-H facility

	BWR-Mode	PWR- Mode
Parameter	Value	Value
Max. pressure [bar]	70	170
Max. mass flux [kg/m^{2}s]	4.000	4.000
Max. temperature, at testsection inlet [°C]	286	352
Fluid density at testsection inlet [kg/m^3]	0,036 - 0,74	0,12 - 0,57
Fluid Viscosity [µPas]	19-91	24-65
Steam mass fraction at test section inlet	0-0,3	0-0,3
Mass flow, test section [kg/s]	~1,4	~1,4
Max. temperature at test section outlet [°C]	~400	~450
Max. thermal power [MW]	1,8	1,8
Max. heat flux [kg/m^2]	2.500	2.500
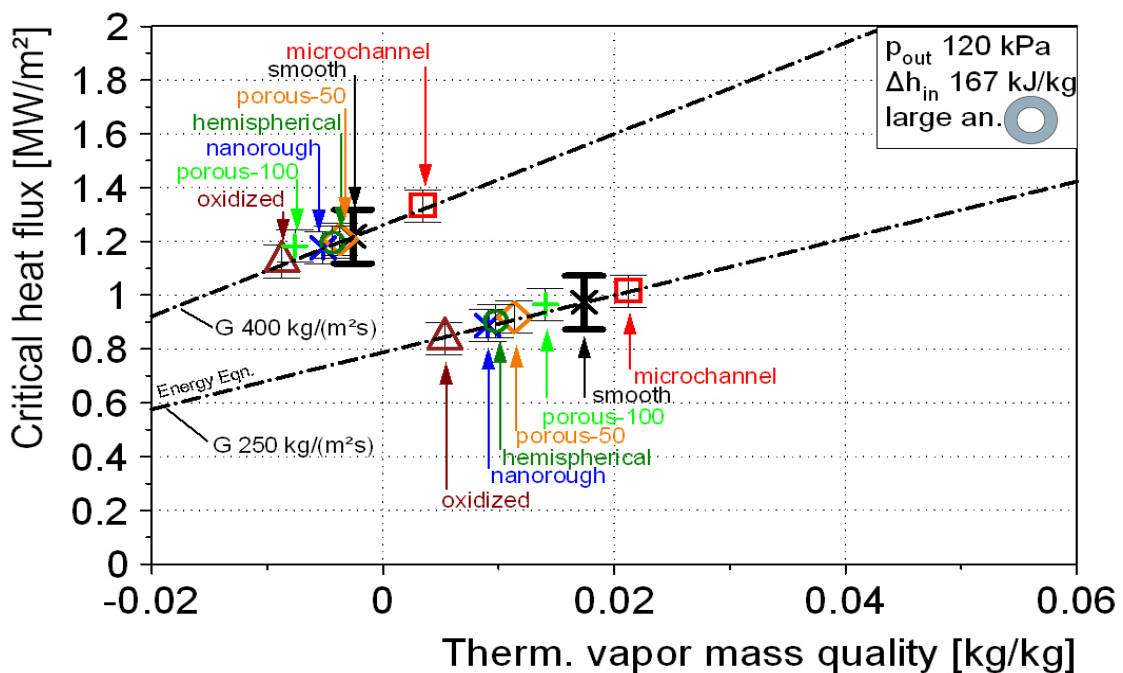
Fig. 7: Comparison of critical heat flux at outlet pressure of 120kPa (1.2bar)

blies) in terms of heat removal, boiling crisis, pressure loss, and the influence of the material used on these parameters, e.g. by multi-dimensional surface modifications. Particular at-tention shall be paid to the behaviour of steam films during dry-out as well as to the influence of surface roughness on boiling heat transfer and the critical heat flux (CHF). New measurement technologies will allow for the determination and validation of physical correlations to be used in the benchmarking of systems codes and the backfitting of CFD codes in the long term. The focus shall be on the use of up to date and innovative measurement techniques (e.g. LDA, PIV, high-speed cameras) of high temporal and spatial resolution and adapt them to applications at very high pressures.
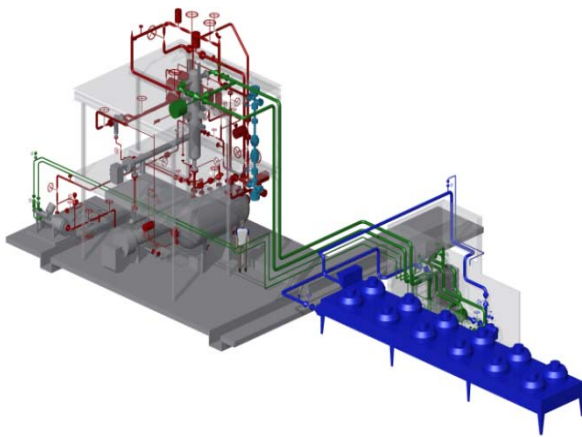
Fig. 8: CAD model of the COSMOS-H facility

WENKA experiments

The WENKA-channel (Water Entrainment channel Karlsruhe) at IKET-UNA serves the investigation of counter-current stratified two-phase flows. These complex flow phenomena are relevant in accident scenarios of pressurized water reactors like the reflux condensation mode after a Loss Of Coolant Accident (LOCA). The objective of the experimental work is the provision of detailed datasets for development and validation of turbulence- and phase-interaction models for new CFD codes. However, the development of turbulence- and phase interaction models for theses flows requires local measurements of various flow parameters with high spatial resolution.

The WENKA channel has a modular construction concept and operates under ambient conditions. Water- and air flow rate can be controlled in a wide range. The current configuration (Fig. 9) allows the observation of different flow regimes, such as supercritical flow, supercritical flow with droplet entrainment, partially reversed flow and fully reversed flow. These flow regimes are including flow phenomena like hydraulic jumps, bubble- and droplet entrainment and propagation of capillary and gravity waves.
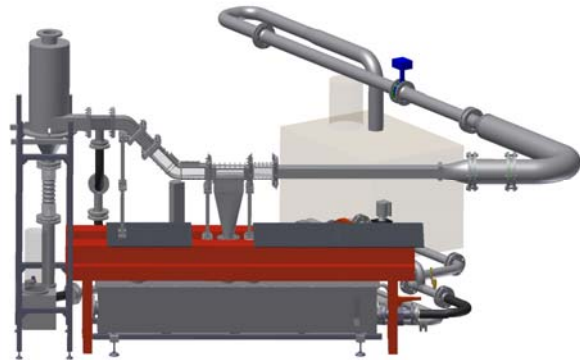
Fig. 9: CAD model of the WENKA facility.

For measurement advanced optical methods were used such as intrusive devices. The velocity and velocity-fluctuation profiles were measured by particle image velocimetry (PIV, Fig. 10). For measurement in water fluorescent tracer particles were used to suppress reflexions at the liquid surface. The velocity profiles are illustrating the flow behavior of the liquid phase in the flow regime "partially reversed flow".

To provide high resolved void fraction data, the OVM-Method (Fig. 11) has been developed. The Method uses sequences of high speed images and image processing methods to calculate a 2D distribution of the volumetric void fraction. After image postprocessing, it calculates the presence probability of two-phase area by averaging over a period of 16 s. Then the void fraction can be calculated by integration of the intensity values. The result image shows the probability that the two-phase area is below the regarded position. This is equal to the probability, that there is air at the current position which is the void fraction.

The validation was done by simultaneous measurement with an electric needle probe and demonstrates a measurement uncertainty of 8.6 %.
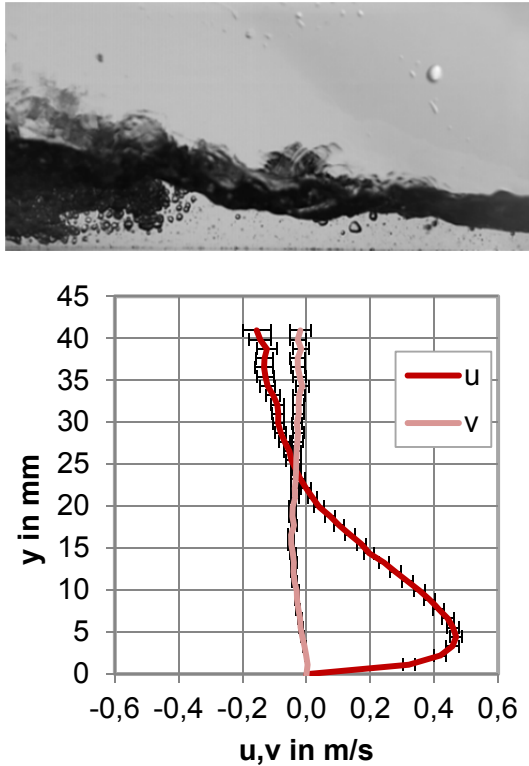
Fig. 10: Water velocity profile

Using these and other instruments, a huge dataset containing data like high speed movies, flow maps, turbulence and velocity data such as droplet mass flow data, has been elaborated within the last three years. The measurement data can be directly compared with the results of CFD-simulations. The new dataset contains 31 different and systematically examined measurement points in five flow regimes.

Expansion of the model basis in MELCOR

The severe accident code MELCOR is used at IKET-UNA to investigate hypothetical core melt accidents in nuclear power plants. Since IKET-UNA is also active in the field of the investigation of core melt accidents in the lower plenum with the LIVE facility, this is the basis for expanding the model basis in MELCOR to improve the prediction of a core melt in the lower plenum.

The objective of the previous work was to reactivate the existing but not any more correctly working coupling interface in the MELCOR code [Szabó et al., 2014]. Currently a program which provides the interface for the integration of additional models is developed and coupled to MELCOR. This allows to externally add new models without modification of the source code.

The program DINAMO (Direct Interface for Adding Models) was developed based on the existing coupling interface in MELCOR 1.8.6. To establish the coupling between MELCOR and DINAMO the communication program MPIEXEC that is provided by Sandia National Laboratories, the developers of MELCOR is required. The first simulations show that the activation of the coupling
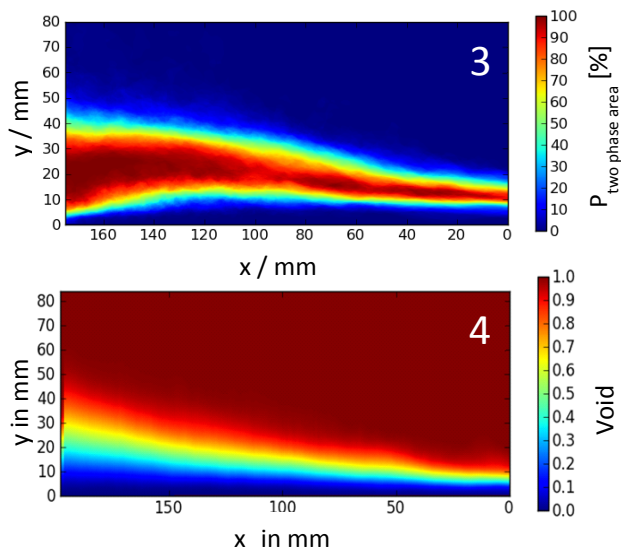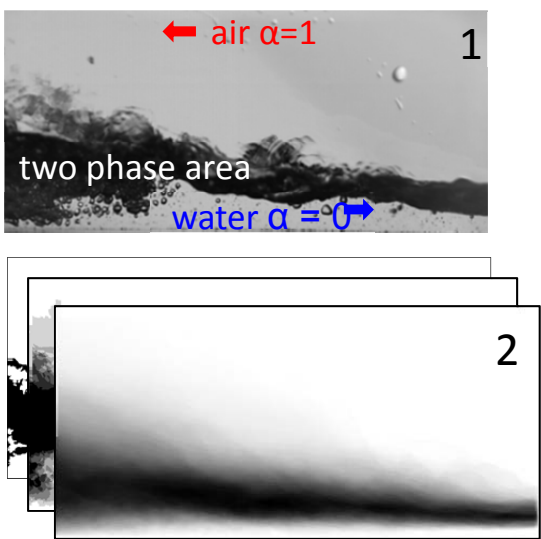
Fig. 11: New 2D phase distribution measurement method

interface significantly influences the results even if the exchanged variables are not considered in the further calculations. Due to the presetting of the coupling timestep by MPIEXEC the timestep-progress in MELCOR is changed compared to the standalone calculations, which causes the occurring deviations. Therefore, a method was developed to synchronize the coupling of MEL-COR and DINAMO. The new coupling timestep is now defined by MELCOR, which ensures that the timestep progress in MELCOR is not changed. Also the link between DINAMO and MELCOR is improved because a data exchange now takes place at every MELCOR-Timestep.

The correct functionality of DINAMO was tested by the integration of the Larson-Miller-Model for creeping. This model was coupled to MELCOR and used to predict the failure of the lower core support plate during a postulated severe accident. Therefore the Larson-Miller-Model had to be adapted to the specific geometric dimensions of the lower core support structure because this information could not be provided by the coupling interface. In order to avoid future adaptions of models to specific circumstances, a method was developed to increase the amount of parameters that can be send to another program by MEL-COR using the coupling interface. As part of this investigation, it was possible to implement the formerly externally coupled Larson-Miller-Model into the MELCOR source code. The comparison showed that, due to the synchronous coupling and the adaption of the model in DINAMO, the results were exactly the same, despite the fact that the internal use of the Larson-Miller-Model significantly reduced the calculation time. However, in order to implement a model to the MEL-COR source code, a deep understanding of the source code is necessary, and only models that possess exactly one output parameter can be implemented using this method due to the restrictions of the Control-Function (CF) package that was used to develop this approach. The effect of the coupled Larson-Miller-Model on the temperature profile of the lower plenum can be seen in Fig. 12.
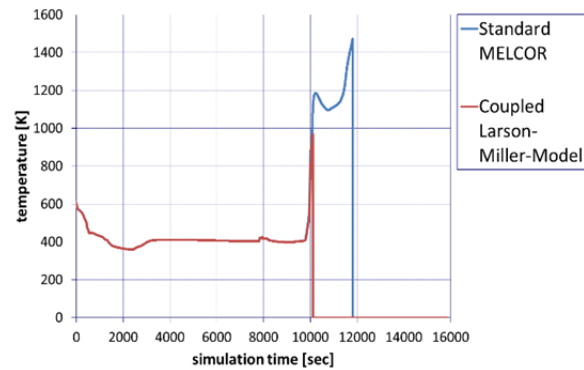
Fig. 12: The effect of the coupled Larson-Miller-Model on the temperature profile of the lower plenum

References

(1) Gaus-Liu, X.; Miassoedov, A.; Cron, T.; Schmidt-Stiefel S. und Wenz, T.; „LIVE-L8B test - Debris melting process", SARNET2-COOL-P06, 2011.

(2) Meyer L.; et al.; "Direct containment heating integral effects tests in geometries of European nuclear power plants," *Nucl. Eng. and Design*, 239, Issue 10, (2009).

(3) Foit J.; et al.; "MOCKA Experiments on Concrete Erosion by a Metal and Oxide Melt," Proc. ERMSAR-2012, Cologne, Germany, March 21-23, 2012.

(4) Haas, C.; Meyer, L.; Schulenberg, T.; "Flow instability and critical heat flux for flow boiling of water in a vertical annulus at low pressure", Proceedings of the ASME/JSME 2011 8th Thermal Engineering Joint Conference AJTEC2011, March 13-17, 2011, Honolulu, Hawaii, USA.

(5) Gabriel, S.; Schulenberg, T. and Laurien, E.; „Velocity and Void Distribution in a Counter-Current Two-Phase Flow", Proc. Int. Conf. Advances on Nuclear Power Plants, ICAPP'12, Chicago, USA, June 24-28, 2012.

(6) Szabó, T.; Kretzschmar, F.; Schulenberg, T.; „Obtaining a more realistic hydrogen distribution in the containment by coupling MELCOR with GASFLOW", *Nuclear Engineering and Design*, 269 (2014), 330-339.

(7) Cranga, M.; Spengler, C.; Atkhen, K.; Fargette, A.; Fischer, M.; Foit, J.; Gencheva, R.; Guyez, E.; Haquet, J.F.; Journeau, C.; Michel, B.; Mun, C.; Piluso, P.; Sevon, T.; Spindler, B.; "Towards an European consensus on possible causes of MCCI ablation anisotropy in an oxidic pool". 6th European Review Meeting on Severe Accident Research (ERMSAR 2013), Avignon, F, October 2-4, 2013, Paper 4.4-IRSN.

(8) Fluhrer, B.; Miassoedov, A.; Gaus-Liu, X.; Cron, T.; Wenz, T.; „Experiments in the LIVE-2D test facility at KIT on melt behavior in RPV lower head". 15th International Topical Meeting on Nuclear Reactor Thermalhydraulics (NURETH 2013), Pisa, I, May 12-17, 2013, NURETH15-513.

(9) Foit, J.J.; Cron, T.; Fluhrer, B.; „Interaction of a metal and oxide melt with reinforced concrete in MOCKA experiments". 15th International Topical Meeting on Nuclear Reactor Thermalhydraulics (NURETH 2013), Pisa, I, May 12-17, 2013, NURETH15-539.

(10) Foit, J.J.; Fischer, M.; Journeau, C.; Langrock, G.; „Experiments on MCCI with oxide and steel". 6th European Review Meeting on Severe Accident Research (ERMSAR 2013), Avignon, F, October 2-4, 2013, Paper 4.2-KIT.

(11) Gabriel, S.; Schulenberg, T.; Laurien, E.; „Experimentelle Untersuchung entgegengerichteter und geschichteter Zweiphasenströmungen". Chancen der Energiewende. Wissenschaftliche Beiträge des KIT zur 1. Jahrestagung des KIT-Zentrums Energie, 19.06.2012. KIT Scientific Reports, KIT-SR 7640 (April 2013) S. 143-148.

(12) Gabriel, S.; Schulenberg, T.; Laurien, E.; „Experimental investigation of droplet separation in a horizontal counter-current stratified air/water flow". 11th Multiphase Flow Conference and Short Course, Dresden, November 26-28, 2013.

(13) Gaus-Liu, X.; Miassoedov, A.; Foit, J.; Cron, T.; Kretzschmar, F.; Palagin, A.; Wenz, T.; Schmidt-Stiefel, S.; „LIVE-L4 and LIVE-L5L experiments on melt pool and crust behavior in lower head of reactor pressure vessel". *Nuclear Technology*, 181 (2013) 216-226.

(14) Gaus-Liu, X.; Miasoedov, A.; "LIVE experimental results of melt pool behaviour in the PWR lower head with insulated upper lid and external cooling". 21th International Conference on Nuclear Engineering (ICONE21), Chengdu, China, July 29 - August 2, 2013, Proc. on DVD Paper ICONE21-15204, New York, N.Y.: ASME, 2013.

(15) Gaus-Liu, X.; Miassoedov, A.; Cron, T.; Fluhrer, B.; "LIVE-3D and LIVE-2D experimental results on melt pool heat transfer with top cooling conditions". 6th European Review Meeting on Severe Accident Research (ERMSAR 2013), Avignon, F, October 2-4, 2013.

(16) Haas, C.; Schulenberg, T.; Wetzel, T.; „Critical heat flux for flow boiling of water at low pressure in vertical internally heated annuli". *International Journal of Heat and Mass Transfer,* 60 (2013) 380-391.

(17) Miassoedov, A.; Cron, T.; Gaus-Liu, X.; Palagin, A.; Schmidt-Stiefel, S.; Wenz, T.; „LIVE experiments on melt behavior in the reactor pressure vessel lower head". *Heat Transfer Engineering*, 34 (2013) 1226-1236.

(18) Miassoedov, A.; Steinbrück, M.; Tromm, W.; „Overview of LWR severe accident research activities at the Karlsruhe Institute of Technology". *Transactions of the American Nuclear Society*, 109 (2013) 928-930.

(19) Miassoedov, A.; Tromm, T.W.; Birchley, J.; Fichot, F.; Fleurot, J.; Ma, W.; Pohlner, G.; Matejovic, P.; "Corium and debris coolability studies performed in the severe accident research network of excellence (SARNET2)". 6th European Review Meeting on Severe Accident Research (ERMSAR 2013), Avignon, F, October 2-4, 2013.

(20) Müller, M.; Szabo, T.; Kretzschmar, F.; „Optimierung eines Reaktorsicherheitsbehälter-modells zur genaueren Strömungssimulation". KIT Scientific Reports, KIT-SR 7653, (Oktober 2013).

(21) Pham, Q.T.; Seiler, J.M.; Combeau, H.; Gaus-Liu, X.; Kretzschmar, F.; Miassoedov, A.; "Modeling of heat transfer and solidification in LIVE L3A experiment". *International Journal of Heat and Mass Transfer* 58 (2013) 691-701.

(22) Spengler, C.; Fargette, A.; Foit, J.; Agethen, K.; Cranga, M.; "Transposition of 2D molten corium-concrete interactions (MCCI) from experiments to reactor". 6th European Review Meeting

on Severe Accident Research (ERMSAR 2013), Avignon, F, October 2-4, 2013, Paper 4.1-GRS.

(23) Sultsky, A.A.; Smirnov, S.A.; Granovsky, V.S.; Khabensky, V.B.; Krushinov, E.V.; Vitol, S.A.; Kotova, S.Yu.; Fischer, M.; Hellmann, S.; Tromm, W.; Miassoedov, A.; Bottomley, D.; Piluso, P.; Barrachin, M.; "Oxidation kinetics of corium pool". *Nuclear Engineering and Design*, 262 (2013) 168-179.

(24) Szabo, T.; "Coupling of MELCOR and GASFLOW for enhanced simulation of hydrogen distribution during accident analysis". 5th Meeting of European MELCOR User Group (EMUG 2013), Stockholm, S, May 2-3, 2013.

(25) Szabo, T.; Benz, S.; Kretzschmar, F.; Jordan, T.; „Coupling of MELCOR and GASFLOW for enhanced simulation of hydrogen distribution during accident analysis". 15th International Topical Meeting on Nuclear Reactor Thermalhydraulics (NURETH 2013), Pisa, I, May 12-17, 2013, NURETH15-327.

(26) Van Dorsselaere, J.P.; Auvinen, A.; Beraha, D.; Chatelard, P.; Kljenak, I.; Journeau, C.; Miassoedov, A.; Paci, S.; Zeyen, R.; "European view on severe accidents research". Jahrestagung Kerntechnik, Berlin, 14.-16. Mai 2013, Berlin : INFORUM GmbH, 2013.

Liquid Metal Technologies for Energy Conversion

Thomas Wetzel, Julio Pacio, Leonid Stoppel, Luca Marocco, Frank Fellmoser, Markus Daubner, Karsten Litfin

Introduction

During 2013, the Karlsruhe Liquid Metal Laboratory (KALLA) has undertaken research activities on several topics related to liquid-metal (LM) technology, with special emphasis on:

- Core thermal-hydraulic experiments for Accelerator Driven Systems

- Direct pyrolysis of methane in a liquid metal bubble column reactor

- LMs as efficient heat transfer fluids for concentrated solar power systems

The scientific investigations on these topics are on different levels of maturity. In the following sections, the main scientific outcomes obtained during 2013 are presented.

Core thermal-hydraulic experiments with LBE

Several advanced concepts for the reduction of nuclear waste by transmutation of long lived fission products are currently under development throughout the world. Some of the most promising designs for transmutation machines, be it fast-reactor or accelerator-driven-systems, rely on heavy liquid metals, such as lead and as lead bismuth eutectic (LBE) as coolants. Their low

Prandtl number, although reflecting their favorable heat transfer capabilities, prevents the application of classical thermal hydraulic models for turbulent heat transfer in core-representative geometries. Furthermore, experimental information for according flows is very limited.

In this context, aiming to achieve a better understanding of these complex flows, an experimental campaign in the frame of the European project THINS has been recently completed at KALLA. The test section for this first-of-its-kind experiment consists of an electrically-heated 19-pin hexagonal rod-bundle with three grid spacers, as shown in Figure 1. Detailed temperature profiles were obtained by means of thermocouples (24 at the rod wall, 14 within the fluid) installed using the walls of the grid spacers as guides.

Extensive tests were performed at typical conditions in terms of operating temperature (200°C - 450°C), power density (up to 1.0 MW m-2) and velocity (up to 2 m s-1) of the LBE. The main results for this comprehensive campaign are shown in Figure 2 for both the spacer pressure drop (left) and the mean heat transfer coefficient (right). In general, the pressure drop results are in good agreement with empirical correlations based on an extensive database of water and air experiments. For the heat transfer, modifications had to be applied to existing correlations, which had so far mainly been calibrated for light metals.
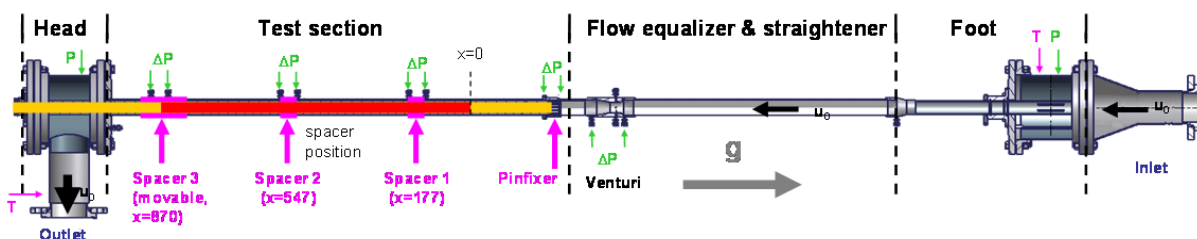
Figure 1: Sketch of the test section in the rod-bundle experiment, details of the grid spacers with 0.25 mm diameter thermocouples
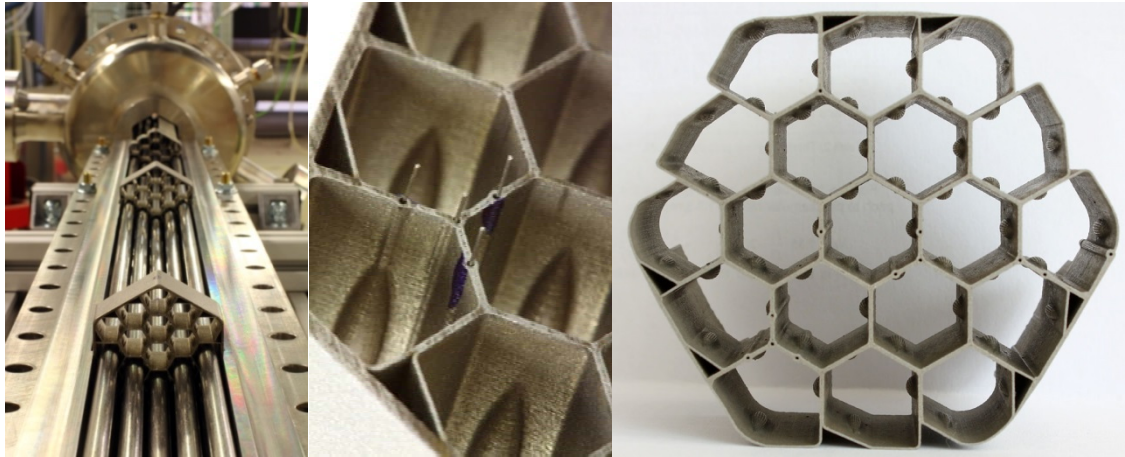
Figure 2: Several views of the test section in the rod-bundle experiment, details of the grid spacers with 0.25 mm diameter thermocouples
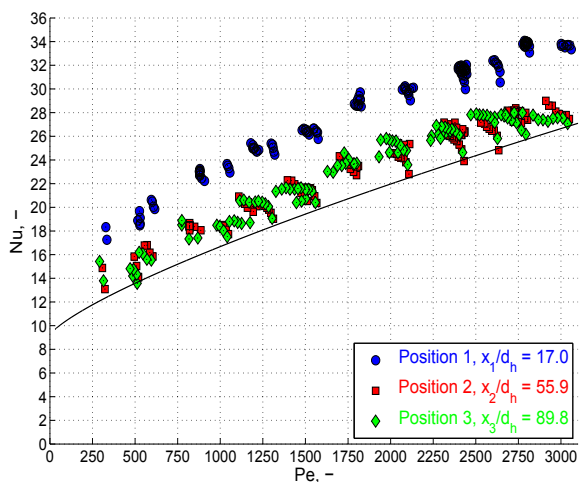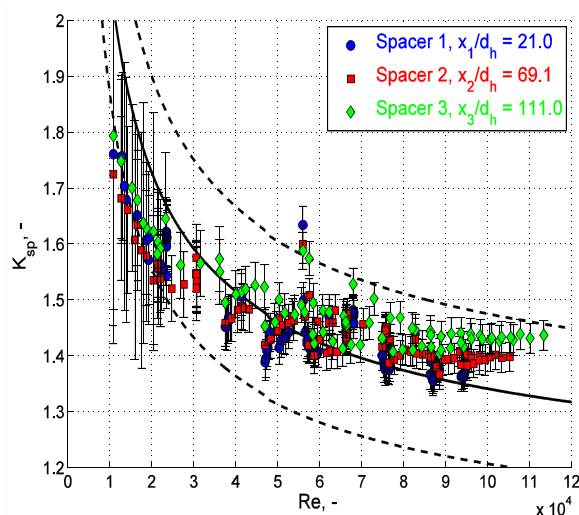
Figure 3: Non-dimensional results of the rod-bundle experiment. Top: pressure drop coefficient at the spacers as a function of the Reynolds number. Bottom: Nusselt number as function of the Péclet number

Further details about these tests and their results can be found in [Pacio et al, 2013 (15)]. In summary, the results from this extensive campaign present a high level of confidence, derived from their good repeatability within the experimental uncertainties. Based on this successful experience, further LBE core thermal-hydraulic tests are envisaged. In the short term, a test section consisting of a 19-pin rod bundle with helical wire spacers is currently under construction for investigation during 2014.

Methane cracking

The new project "Hydrogen from Methane without CO_2 Emissions" starting in December 2012 saw substantial progress during 2013. In this project, KIT cooperates with the Institute for Advanced Sustainability Studies (IASS) in Potsdam. The scientific director of this institute and enabler of this project, Prof. Carlo Rubbia, visited KALLA in spring 2013, see Fig. 4. The main idea behind this project is to use a liquid metal based bubble column, making use of the high temperature capabilities of liquid metal, certain catalytic effects, very high specific surface of the liquid-gas interface, etc. On the other hand, many knowledge gaps concerning influence of process variables, kinetics, corrosion of structural materials, morphology of reaction products – to name just a few – have to be filled. The technical infrastructure for carrying out according research work has been created at KALLA: a new laboratory room has been established, the gas supply

system has been constructed, the technical safety precautions have been determined. The experimental facility HELiS (Hydrogen Experiments in Liquid Sn) with automatic control system and data acquisition has been developed and built. The first experimental reactor is based on a slim vertical tube with a volume of 1.3 l. Remote filling and drainage of the molten metal is possible through an external sump tank. The reactor is equipped with thermocouples to measure temperatures in both the liquid and gaseous phases, pressure transducers, an external electrical heater and thermal insulation. A first experimental campaign has been carried out, validating the desired reactor behaviour based on the recorded temperature, pressure and flow rate data.

Figure 4: Nobel Prize Laureate in physics Carlo Rubbia visited KIT. (Photo: M. Lober)

Concentrated Solar Power (CSP)

It is well agreed within the international CSP community, that next-generation plants require advanced heat transfer fluids for an improved efficiency and cost performance. This specifically transforms into high upper temperature limit (far) beyond 600 °C to improve power cycle efficiency and high heat transfer capability to minimize heat losses at the solar receiver surface, particularly for central receiver systems like the one in Fig. 5. With their attractive thermo-physical properties and long operating experience, liquid metals are prominent candidates for that purpose. KALLA entered into this field in 2012 and has made important progress since. A solar furnace installation is under construction and in the frame of the HELMHOLTZ Alliance LIMTECH, five new scientific positions have been created, two of them in cooperation with German Aerospace Center DLR and Leibniz University Hannover LUH.

During 2013, preliminary evaluations allowed to identify the most relevant scenarios to be studied experimentally in a 10 kW solar furnace setup with receiver, LM cooling loop, intermediate storage, etc. Both fundamental scientific questions like e.g. the liquid metal heat transfer and entropy generation in an asymmetrically-heated cylindrical (receiver) tube, and applied scientific questions like the operation of a liquid metal heat transfer system under highly transient conditions, have been identified and will be further investigated in the upcoming time.

Figure 5: The Ivanpah solar plant in California is the world´s biggest. It has a capacity of almost 400 megawatts (MW) and more than 347,000 mirrors focus on three tall towers, which contain water (http://www.theatlantic.com/infocus/2014/03/the-ivanpah-solar-electric-generating-system/100692/)(1)

Conclusions

In 2013, KALLA has continued its strong involvement in the international scientific community dealing with liquid metal technology. Beside the substantial progress reached in describing basic thermal hydraulics for vertical hexagonal rod bundles for nuclear applications like transmutation machines, first steps in innovative fields of application like chemical processing and concentrating solar power have been made. The common foundation for the successful scientific work in all these areas is the combination of long lasting experience with large scale experimental facilities with a strong theoretical background including numerical simulation.

References

(1) http://www.theatlantic.com/infocus/2014/03/the-ivanpah-solar-electric-generating-system/100692/.

(2) Di Piazza, I.; Tarantino, M.; Martelli, D.; Gaggini, P.; Pacio, J.; Litfin, K.; Marocco, L.; Wetzel, T.; "Fuel bundle experiments. Lecture series on Fluid Mechanics and Chemistry for Safety issues in HLM nuclear reactors", Rhode St Génese, Belgium, November 25-27 2013.

(3) Litfin, K.; Batta, A.; Class, A. G.; Wetzel, T.; "LBE Free Surface Target Experiment". THINS (Thermal-Hydraulics of Innovative Nuclear Systems) - WP 4 Two-phase flow. 3rd Technical Review Meeting, Petten, September 09-10 2013.

(4) Litfin, K.; "MAXSIMA Work Package 3: Core Component Safety". Joint SEARCH and MAXSIMA Technical Review Meeting, Pula , May 2013.

(5) Litfin, K.; "Fuel assembly heat transfer & blockage Experiments at KIT". Joint SEARCH and MAXSIMA Technical Review Meeting , Pula, May 2013.

(6) Litfin, K.; "Some existing Experimental Facilities for Fast Neutron System at KIT", Technical Meeting on Existing and Proposed Experimental Facilities for fast neutron systems, Vienna, 10-12 June 2013.

(7) Pacio J.; Wetzel, T.; "Assessment of liquid metal technology status and research paths for their use as efficient heat transfer fluids in solar central receiver systems". *Solar Energy*, 2013, 93, 11-22, 10.1016/j.solener.2013.03.025.

(8) Pacio, J.; Singer, C.; Wetzel, T.; Uhlig, R.; "Thermodynamic evaluation of liquid metals as heat transfer fluids in concentrated solar power *plants", Applied Thermal Engineering* , 2013, 60, 295–302.

(9) Pacio, J.; Fritsch, A.; Singer, C.; Uhlig, R.; "Liquid metals as efficient coolants for high-intensity point-focus receivers: implications to the design and performance of next-generation CSP systems". SolarPACES (Solar Power and Chemical Energy Systems) 2013 International Conference, Las Vegas, NV, USA, September 17-20, 2013.

(10) Pacio, J.; Wetzel, T.; "Experimental activities on heavy-liquid-metal thermo-hydraulics". Thorium Energy Conference ThEC2013, Geneve, Switzerland, October 27-31 2013.

(11) Pacio, J. and Wetzel, T.; "Liquid metals as heat transfer fluids in high-temperature processes with indirect thermal energy storage", 2nd International Conference on Materials for Energy EnMat II, Karlsruhe, Germany, May 12-16, 2013.

(12) Pacio, J.; "Liquid metals: efficient heat transfer fluids for advanced CSP systems". EUROTHERM Seminar No. 98, Concentrating Solar Energy Systems, Vienna, Austria, July 4-5 2013.

(13) Pacio, J.; Wetzel, T.; "Advanced high-efficiency solar central receiver systems using liquid metals as heat transfer fluids". ASME 7th International Conference on Energy Sustainability, Minneapolis, MN, USA, July 15-17 2013.

(14) Pacio, J.; Litfin, K.; Marocco, L.; Wetzel, T.; "Status of LBE rod bundle experiment at KIT". THINS (Thermal-Hydraulics of Innovative Nuclear Systems) - WP 1 Advanced reactor core thermal-hydraulics. 3rd Technical Review Meeting, Petten, Netherlands, September 09-10 2013.

(15) Pacio, J.; Daubner, M.; Fellmoser, F.; Litfin, K.; Marocco, L.; Taufall, S. and Wetzel, T.; "Mid-term report on experimental rod bundle data". THINS (Thermal-Hydraulics of Innovative Nuclear Systems) - WP 1 Advanced reactor core thermal-hydraulics. Technical Report D1.1.06. October 2013.

(16) Pacio, J.; Daubner, M.; Fellmoser, F.; Litfin, K.; Marocco, L.; Taufall, S.; Wetzel, T.; "Final report on experimental rod bundle data". THINS (Thermal-Hydraulics of Innovative Nuclear Sys-

tems) - WP 1 Advanced reactor core thermal-hydraulics. Technical Report D1.1.14. December 2013.

(17) Pacio, J.; Litfin, K. and Wetzel, Th.; "Fuel assembly heat transfer and blockage experiments". Joint SEARCH and MAXSIMA Technical Review Meeting, Rhode St Génese, Belgium, November 28-29, 2013.

(18) Plevan, M.; "Hydrogen production via thermal decomposition of methane", Breh, W. [Hrsg.], Impulse für die Zukunft der Energie : Wissenschaftliche Beiträge des KIT zur 2. Jahrestagung des KIT-Zentrums Energie Doktorandensymposium, 13.06.2013, KIT Scientific Reports, KIT-SR 7646 (Dezember 2013) S. 9-14.

(19) Plevan, M; Stoppel, L.; Wetzel, T.; Heinzel, A.; Weisenburger, A.; Müller, G.; Fazio, C.; Konys, J.; Schroer, C.; Rubbia, C.; Abánades, A.; Falco, C.; Ghannadzadeh, A.; Stückrad, S.; Salmieri, D.; "Hydrogen Production via Direct Thermal Cracking of Methane: Concept of a Molten Metal Bubble Column Reactor". In: Proc. Of the 5th World Hydrogen Technologies Convention (WHTC2013).

(20) Plevan, M.; Geißler, T.; Herbst, S.; Stoppel, K.; Wetzel, T.; "Experimental Investigation of Bubble Rise Velocities in a Molten Metal Bubble Column Reactor". Proc. of the 11th Multiphase Flow Conference & Short Course.

(21) Taufall, S.; Wetzel, T.; Daubner, M.; „Kühlung thermisch hochbelasteter Oberflächen mittels flüssiger Metalle", Chancen der Energiewende. Wissenschaftliche Beiträge des KIT zur 1. Jahrestagung des KIT-Zentrums Energie, 19.06.2012.KIT Scientific Reports, KIT-SR 7640 (April 2013) S. 137-142.

Group: Accident Management Systems

International Conference on Information Systems for Crisis Response and Management

Wolfgang Raskob, Tim Müller, Stella Möhrle, Thomas Münzberg

Abstract

In 2013, the International Conference on Information Systems for Crisis Response and Management (ISCRAM) was organised by KIT-IKET and Fraunhofer IOSB and held from May 12 to 15 in Baden-Baden. The ISCRAM Conference 2013 focused on Holistic Crisis Management, which aims at the interdisciplinary development and design of information systems. Integrated approaches that combine organisational, behavioural, technical, economic, and environmental aspects are used, to enable better crisis planning, response, mitigation, recovery, and training.

About 250 researchers attended the conference and approximately 150 papers have been presented. More than 20 different topics were discussed and important questions such as how to bridge the gap between science and practice were addressed in plenary sessions. The consistently positive feedback confirms the great success of the conference. The organisational efforts were highly appreciated and KIT, Fraunhofer IOSB, and CEDIM strengthened their position in the ISCRAM community.

Introduction

The Information Systems for Crisis Response and Management (ISCRAM) community consists of researchers, academics, practitioners, and policy makers and is not limited to any specific type of natural or man-made disaster. When ISCRAM Conference started in 2004, it was much influenced by but not limited to nuclear emergencies. Most research was dedicated to the question how IT and in particular decision support systems might help in the management of crises.

One of the objectives of the ISCRAM Conferences is "Promoting research and development, ex-change of knowledge and deployment of information systems for crisis management. Both the social, technical and practical aspects of all information and communication systems used or to be used in all phases of management (mitigating) of emergencies, disasters, and crises are treated." (ISCRAM web page) These aspects have been intensively discussed in former ISCRAM conferences focusing on the various aspects of crisis management and information systems.

ISCRAM 2013

The conference was organised by the Karlsruhe Institute of Technology (KIT). Professor Dr.-Ing. Jürgen Beyerer, head of the Institute of Anthropomatics - Vision and Fusion Laboratory (IES), chaired the conference. The Institute for Nuclear and Energy Technologies (IKET) was responsible for the local organisation.

ISCRAM 2013 was held in Baden-Baden from 12 to 15 May 2013, and the 10th anniversary of that series of conferences. The conference attracted about 250 researchers from all over the world and following a double-blind peer review process, 146 papers have been accepted. With a rejection rate for full papers of nearly 50%, the review process clearly demonstrated that only high level contributions were accepted for presentation. The number of papers as well as the number of participants showed the high interest of the community in such a type of conference.

The central conference theme addressed the management of risks and failure of critical infrastructures (CIs) and solutions to minimise their

impact on society, economy, and environment. Further tracks discussed "decision support", "complexity and interoperability", "human factors", and "training and gaming", which were part of ISCRAM Conferences since long. New tracks that emerged over time broach the issue of "Social Media", "Humanitarian Relief Logistics", "Visual Analytics for Crisis Management", and "Critical Infrastructures".

Fig. 1: Participants of the ISCRAM 2013 in Baden-Baden

The ISCRAM Conference always intended to integrate research and application. In this respect, industry was invited to present tools. In addition, a Practitioners' Track and the Panel "Bridging the gap" was part of ISCRAM Conference 2013. This assured that the high academic standards of the conference support also the migration of knowledge to the end user which are either first responder or decision maker.

Role of CEDIM

The KIT has a strong focus on technological development in widespread areas and deals with many aspects of critical infrastructures. These activities are bundled in the Centre for Disaster Management and Risk Reduction Technology (CEDIM). In order to strengthen the competence of ISCRAM as a whole on the one hand and CEDIM on the other, CEDIM supported the organisation of the ISCRAM conference in May 2013.

CEDIM is an interdisciplinary research centre in the field of disaster management founded by the Helmholtz Centre Potsdam - German Research Centre for Geoscience (GFZ), and the KIT. The

main goal of CEDIM is to advance our scientific understanding of natural and man-made hazards and to develop disaster management solutions for the early detection and reduction of the related risks. CEDIM is dedicated to developing technologies and tools in the areas of risk assessment, risk communication and management in a world with increasing population, rapid urbanization and the growing threat associated with climate change.

At the ISCRAM Conference, CEDIM presented a concept of near real-time "Forensic Disaster Analysis" (FDA), which has been implemented as CEDIM's research strategy for the years 2012 to 2014. In this context, "near real-time" refers to the publication of first reports and analysis results to end users from science, practice, and other groups within a time frame of few hours to days after a catastrophic event.

CEDIM organised a track at the ISCRAM Conference 2013 related to the new field of FDA: "Rapid integrated understanding of disasters: holistic disaster assessments in near-real time". Moreover, CEDIM members chaired two further tracks: "Decision Support Methods and Tools for Holistic Emergency Management" and "Efficient Planning and Decision Support for Robust Critical Infrastructure Systems".

Role of KIT-IKET

One of the central topics of the ISCRAM Conference 2013 addressed crisis management for large-scale disasters affecting one or more critical infrastructures (CI). In former ISCRAM conferences, CI was not extensively discussed and existing crucial and still unsolved problems such as the support of the decision maker in a crisis situation, emphasize the need to build an ISCRAM conference around this topic. On the one hand, sophisticated simulation models exist describing individual CI structures and (inter-) dependencies between CIs. On the other hand, the decision making team requires a flexible deployment of databases and simulation capabilities as the area, the scope and the impact of a crisis cannot be foreseen a priori. This leads to the following questions to be addressed:
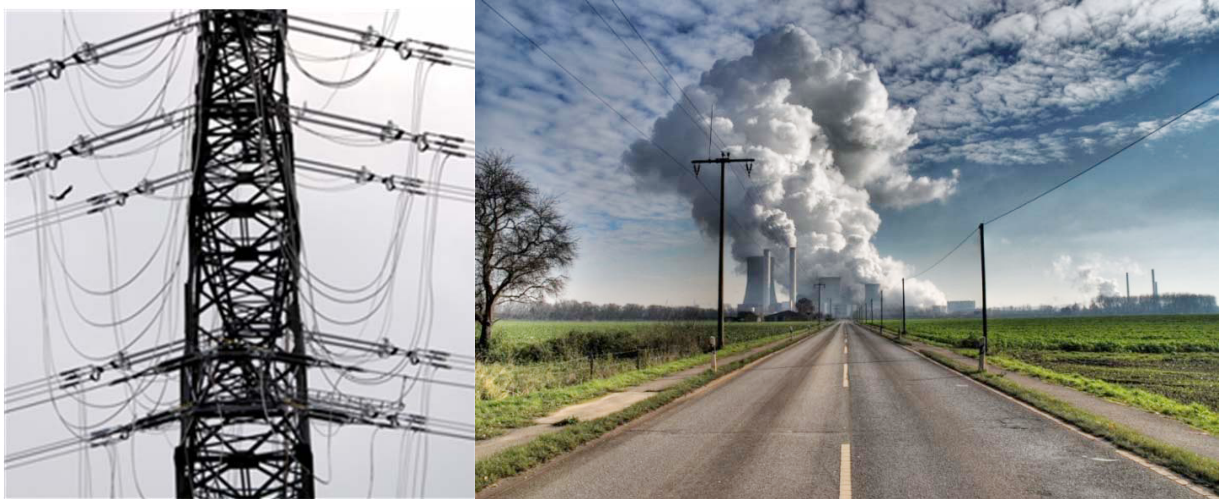
Fig. 2: Critical Infrastructures, partly affected by a crisis event (left hand side)

- To what extent can simulation models be used for decision making?

- What are the needs of decision making when CIs are substantially affected?

- Is there a way to combine complex simulation models with coarser but easier-to-use simulation models taking uncertainty explicitly into account?

- Is there a way to couple simulation models with sensor-based data acquisition to support the assessment of system dynamics?

- Which complexity of simulation and databases is optimal for decision making (with regards to configuration and result interpretation)?

The group "Accident Management Systems" (UNF) of IKET addresses these questions within their new research activity. UNF agreed in 2011 to organize the ISCRAM Conference 2013 in Baden-Baden in order to facilitate this new research line and demonstrate its capabilities. Besides being the local organisers and being part of the scientific program members, the group presented three papers [Möhrle, 2013 and Münzberg, 2013].

Summary

The 10th ISCRAM conference organised by KIT-IKET succeeded in bringing together approximately 250 people from the research and operational community to discuss information systems for crisis response and management and how such tools can help the practical implementation.

For CEDIM and the UNF group of KIT-IKET, this conference provided a sound basis to demonstrate their capabilities in research and served as a platform to become much more visible in this community than before. The collaboration was advantageous for both sides. The ISCRAM community was pushed further and KIT has started playing an important role in the community.

References

(1) CEDIM http://www.cedim.de/english/13.php.

(2) ISCRAM http://www.iscramlive.org/portal/.

(3) Moehrle, S.; "Modeling of countermeasures for large-scale disasters using high-level Petri nets". Comes, T. [Hrsg.], 10th International Conference on Information Systems for Crisis Response and Management (ISCRAM), Baden-Baden, May 12-15, 2013, Conference Proceedings S. 284-289, Karlsruhe: Karlsruhe Inst. of Technology, Campus North, 2013, ISBN 978-3-923704-80-4.

(4) Münzberg, Th.; Mueller, T.; Möhrle, S.; Comes, T. & Schultmann, F. (2013): "An Integrated Multi-Criteria Approach on Vulnerability Analysis in the Context of Load Reduction". Proceedings of the 10th International Conference on Information Systems for Crisis Response and Management (ISCRAM 2013), Baden-Baden 2013. Conference Proceedings S. 312-316, Karlsruhe: Karlsruhe Inst. of Technology, Campus North, 2013, ISBN 978-3-923704-80-4.

(5) Münzberg, Th.; Berbner, U.; Comes, T.; Friedrich, H.; Gross, W.; Pfohl, H.-C. & Schultmann, F.; (2013); "Decision Support for Critical Infrastructure Disruptions: An Integrated Approach to Secure Food Supply", Proceedings of the 10th International Conference on Information Systems for Crisis Response and Management (ISCRAM 2013), Baden-Baden 2013. Conference Proceedings S. 312-316, Karlsruhe: Karlsruhe Inst. of Technology, Campus North, 2013, ISBN 978-3-923704-80-4.

(6) Kunz, M.; Mühr, B.; Kunz-Plapp, T.; Daniell, J.E.; Khazai, B.; Wenzel, F.; Vannieuwenhuyse, M.; Comes, T.; Elmer, F.; Schröter, K.; Fohringer, J.; Münzberg, T.; Lucas, C.; Zschau, J.; "Investigation of superstorm Sandy 2012 in a multidisciplinary approach". *Natural Hazards and Earth System Sciences*, 13 (2013) 2579-2598.

(7) Lin, L.; Brauner, F.; Münzberg, T.; Meng, S.; Moehrle, S.; „Priorization of security measures against terrorist threats to public rail transport systems using a scenario-based multi-criteria method and a knowledge database". 8th Future Security Conference, Berlin, September 17-19, 2013.

(8) Moehrle, S.; "Towards a decision support system for disaster management". European Safety and Reliability Conference (ESREL 2013), Amsterdam, NL, September 29 - October 2, 2013.

(9) Müller, T.O.; „Software architecture of the BOOSTER comprehensive approach to crisis management in case of dirty bomb attacks". Global Conference on Radiation Topics (Con-Rad), München, May 13-16, 2013.

(10) Münzberg, T.; Ludäscher, S.; Bach, C.; „Stromausfall gegen Stromausfälle. Wie Lastreduzierungen Netzzusammenbrüche verhindern können und welches Dilemma daraus für den Bevölkerungsschutz und die Gefahrenabwehrplanung resultiert", *Bevölkerungsschutz* 1 (2013) 36-39.

(11) Münzberg, T.; Käser, B.; Bach, C.; Schultmann, F.; „Beherrschung und Bewältigung von Stromausfällen. Vorbereitung der Kommunalen Gefahrenabwehr". *vfdb - Zeitschrift für Forschung, Technik und Management im Brandschutz* (2013) Nr.4, S. 205-211.

Group: Hydrogen

Some Highlights of the Hydrogen Group

Thomas Jordan

Flame acceleration and DDT in flat semi-open layers with concentration gradients

Experiments with homogeneous and gradient mixtures were carried out in middle and large scale (in the H110 Test Vessel), up to layers of 10m length, 3m width and 0.8m height. Detailed analysis of the filling strategy was performed, to guarantee reproducible gradient mixtures. Additionally, special measurement systems have been developed which allow automated and precise measurement of the local concentration gradients. The effective flame speed was measured for different premixed status of the cloud and different obstacle geometries.

Results

Thus, sigma- and lambda-criterion derived from homogeneous mixtures combusted in closed tubes have been extended to the more realistic conditions, characterized by partial confinement and inhomogeneity of the mixture composition. The extended criterion for the flame acceleration (FA) converges to the "classical" condition with full confinement, where the critical sigma equals 3.75. Similarly the deflagration-to-detonation (DDT) criterion was relaxed, i.e. larger premixed systems are required under vented conditions compared to full enclosure. Instead of 7 times the detonations cell size almost double (factor 13.5) as large premixed clouds are required for a detonation transition. It was shown that a minimum layer height of 0.6m is required to achieve a detonation without further obstruction.

The inhomogeneous mixture showed a surprising behavior. The overall behavior seems to be controlled rather by the maximum concentration instead of by the average concentration. This emphasizes the importance of accounting for the mixing processes and initial distribution of hydrogen in the flammable cloud.
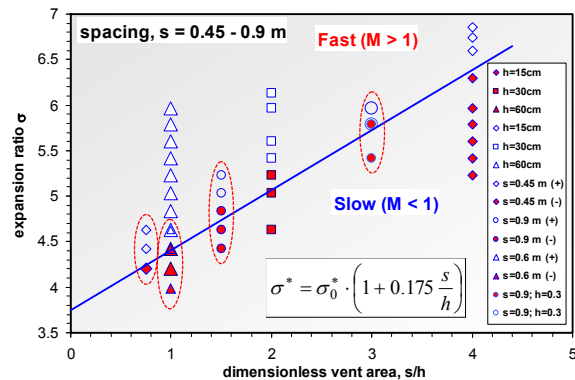
Figure 1: Extended sigma-criterion for flame acceleration including semi-open flat layer configuration

Acknowledgements

Flame Instabilities

The focus of this work is to investigate hydrogen flame behavior in a planar geometry and particularly, how the intrinsic instabilities of hydrogen flame affect its propagation in such geometry. Flame instabilities give rise to the development of a cellular structure on the surface of the flame. The cellular structure results in an increase of flame surface area and hence, promotes higher rate of fuel consumption. This results in flame acceleration (FA), which in turn could lead to the transition from deflagration to detonation (DDT). Combustion of hydrogen – air and hydrogen – oxygen mixtures were performed in between two transparent glass plates at ambient conditions.

The experiments were performed in a glass plate assembly with various configurations with respect to hydrogen (H_2) concentration, gap size between the two plates, ignition positions and openings along the periphery of the glass plate assembly. Two different dimensions of the glass plate assembly were used; 500 mm x 500 mm and 200 mm x 200 mm. H_2 concentration was varied between 7% - 60% for H_2 – air mixture and 13% - 80% for H_2 – O_2 mixtures Three different gap sizes were used: 6 mm, 4 mm and 2 mm. Spark electrodes were used to ignite the combustible mixtures and the position of this ignition source can either be at the top, center or at the bottom of the glass plate assembly. The openings along the periphery of the glass plate assembly were varied as all sides open, two of the sides open or only one side open. All experiments were performed at ambient conditions.
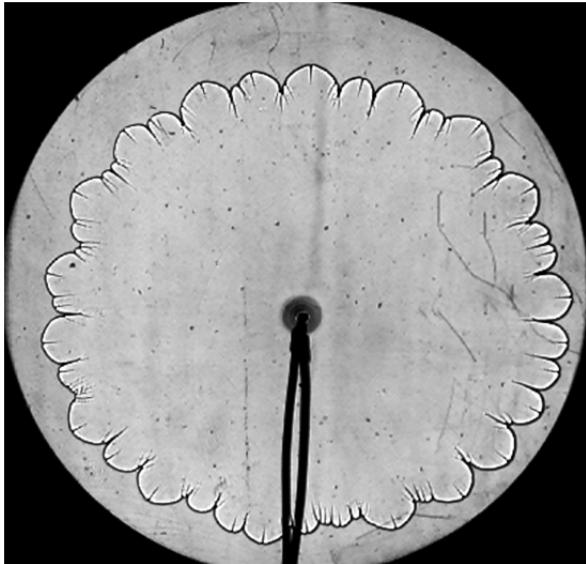
Figure 2: Shadowgraph of wrinkled flame in the planar gap in between two glass plates

Flame propagation within the glass plate assembly was visualized using the shadowgraph method. Shadowgraph enables visualization of the invisible hydrogen combustion by casting shadows of the process. The flame propagation was recorded by a high-speed camera at 27000 fps and 40000 fps.

Results

Shadowgraph images show that for all investigated H_2 mixtures, the flame surface goes through a transition from smooth surface to a cellular structure. For open wall configuration, lean H_2 – air flame surface develops cellular structure in the early stage of the flame propagation and the appearance of such a structure is gradually delayed as concentration of H_2 increases. With increasing gap size, the cellular structure is observed to appear earlier. For H_2 – O_2 mixtures, the cellular structure development shows no significant influence with varying H_2 concentration and gap size. The early appearance of the cellular structure for lean H_2 – air mixture is due to the two main intrinsic instabilities of flame, thermal – diffusive instability and hydrodynamic instability, namely Landau – Darrieus instability. For rich mixtures, the flames are only unstable against the hydrodynamic instability, hence the structure appears later.

The flame velocity dependence on mixture composition and gap size have been determined. Maximum velocity of 4.09 m/s is reached at 40% H_2 concentration in the 6 mm gap configuration for H_2 – air mixture, while for H_2 – O_2 mixture, the maximum velocity reached is 21.93 m/s at 66.6% H_2 in the 2 mm gap configuration. Markstein lengths were determined optically to describe the influence of stretch on the flame and thermal – diffusive instability. Negative Markstein lengths were obtained for lean H_2 – air mixtures (H_2 concentration < 14% in this work) which indicates that the stretch results in acceleration of the curved flame propagation. Positive Markstein lengths were obtained for H_2 – air mixtures containing higher H_2 concentration and for all investigated H_2 – O_2 mixtures, indicating that the stretch causes a deceleration in the propagation of the curved flame.

In the frame of this work, flame acceleration and DDT phenomena were not observed in open wall configuration. Had the scale of the glass plate assembly been larger, DDT would occur in the open wall configuration. Flame acceleration was observed in mixtures with H_2 concentration ranging between 40% and 70%. The early phase of detonation was clearly observed in configurations in which two of the sides were closed for H_2 concentration ranging between 60% and 70%. The main preconditioning events for the occurrence of DDT are the reflection of shock waves from the wall and turbulent boundary layers.

Hybrid Hydrogen/Dust Explosions

The fundamental studies on hydrogen/dust explosion hazards in case of a severe accident scenario in ITER have been continued also in 2013. Although this work is primarily motivated by fusion reactor research, the results are easily transferred to hydride hydrogen storage systems.

Previous studies concerned graphite and tungsten dusts. These studies have shown that pure dusts from both materials could be exploded, however the required ignition energies were relatively high. On the other side when hydrogen as part of the mixture can be easily ignited by a weak ignition source, e.g. an electric spark, the hydrogen combustion is then able to initiate a dust cloud explosion.

A far more reactive behavior of beryllium (Be) used as first wall material in ITER has been anticipated. Due to its toxicity tests with Be dusts are not possible our combustion facilities. So it was decided to identify and test a suitable surrogate material and to do few small scale reference tests in the laboratories of INNL.

Results

Measurements of the explosion properties of the Be-substitute Al dust in mixtures with hydrogen have been performed. The results have shown that flames in hybrid Al/H_2 mixtures in closed geometries can accelerate to fast flame propagation regimes indicating that Be/H_2 hybrid mixtures can be much more dangerous than C or W/H_2 mixtures, resulting even in deflagration/ detonation regimes.

One objective has been to study the scalability of the DUSTEX - a small scale standard spherical device - results and to extend the database of Al/H_2 explosion properties/regimes to medium scale.

Al dust of about 1 micrometer grain size was tested in the DUSTEX experiments. The tests results are:

- Hybrid mixtures of 1 micrometer Al dust/hydrogen/air had been tested for five dust concentrations – 100, 200, 400, 800, and 1200 g/m^3 – each at 8 hydrogen concentrations stepping from 7 to 20 vol. %;

- At each dust concentration a reliable ignition occurred starting from 8 vol. % hydrogen;

- Explosion pressures ranged from 2.9 bar for the leanest mixture (8 vol. % H_2/100 g/m^3 Al dust) to 10.5 bar at 8 vol. % H_2/1200 g/m^3 Al dust;

- Pressure-rise rates ranged from 5 to 2200 bar/s (K_{st} from 1.4 m bar/s to 600 m bar/s);

- The lean H_2/Al dust mixtures reacted in two stages: first hydrogen exploded fast, then Al dust burnt out the remaining oxygen, the latter was usually slower than the former;

- The most 'severe' mixtures were with an Al dust concentration of 800 g/m^3; this value appeared to be the optimum dust concentration for pure dust/air mixtures.

Based on these results the test matrix for mid-scale PROFLAM II facility has been designed. Tests involving mixtures with 100, 400, 800, and 1000 g/m^3 Al-dust, each dust concentration with 8, 10, 12, 14, 16, 18, and possibly 20 vol. % hydrogen were planned.

The PROFLAM test series was started with C_{dust} = 100 g/m^3. In addition to the hybrid test results, also the values measured in pure hydrogen tests in PROFLAM were generated as reference cases. In general, the explosion behavior of these mixtures is quite similar to that observed in DUSTEX with similar mixtures.

The PROFLAM II tests with C_{dust} = 400 g/m^3 were stopped at a hydrogen concentration of 13 vol. %. At this hydrogen concentration the explosion seemed to reach another regime: the pressure rise rate in this case was enormously high – 1160 bar/s – which in K_{st} terms is 770 m bar/s. It has to be emphasized that this is 2.7 times higher than the value limiting the higher explosion Class 3 of 300 m bar/s, while the factor distinguishing Class 3 from Class 2 (200 m bar/s) is 1.5.
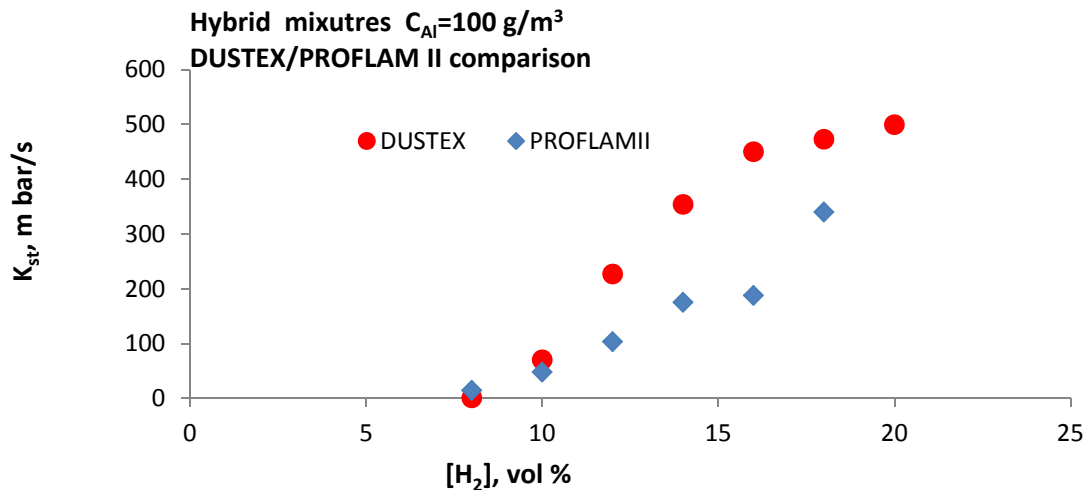
Figure 3: K_{st}-values for the tests in PROFLAM and DUSTEX with hydrogen/Al dust hybrid mixtures at C_{dust} = 100 g/m³.

The data gained in the DUSTEX and PROFLAM facilities was used to validate the computer code DET3D, which is under development at IKET to model pressure loads of severe accident scenarios, e.g. in ITER. Modelling of the performed experiments was started and proceeded in parallel with the tests. Good agreement between experiment and calculations has been observed.

Safe use of hydrogen indoors or in confined space

The IKET's role in the associated EC project HyIndoor is to analyze via CFD simulations and experimental studies vented deflagrations and hydrogen jet releases in partially confined (vented) geometries.

The experiments in the 2013 campaign were devoted to study the effects of vent opening, mixture reactivity, ignition position, blockage ratio, mixture non-uniformity and vent cover on maximum over-pressure inside the test chamber. General results of the experiments are analyzed in terms of maximum combustion pressure and temperature as integral characteristics of combustion process. Dynamics of combustion process was studied using Background Oriented Schlieren (BOS) method. In total, 98 experiments have been done to cover the full set of variables. It was found that general behavior and maximum combustion pressure of vented deflagration depends on internal and external combustion processes.

Main results are the following: Hydrogen concentration has strong effect on vented deflagration regime leading to different maximum overpressure and structure of the pressure signal (single or multiple peaks structure) WP3.2. Two thresholds of gaseous mixture reactivity were found in middle scale KIT experiments. First, there is no visible pressure increase (above the pressure signal noise) for vented deflagration with hydrogen concentration less than 8%. The second threshold is between 10 and 11% hydrogen. When hydrogen concentration is higher than 10%, the single pressure peak structure changes to multiple peak structure with significant increase of maximum overpressure.

With very lean mixtures (<11%H_2) a strong increase of maximum overpressure up to 100 mbar was found only for 10x10 cm² vent area. For vent areas more than 50x50 cm², the overpressure above 100 mbar was achieved only for mixtures with hydrogen concentration above 15%.

A further series of four benchmark experiments was done in order to scale down FM Global experiments and to proof the existing scale correlations of maximum explosion pressure as a function of hydrogen concentration and vent area. It was found a perfect agreement of our data and FM Global experiments for the same hydrogen concentration.

Figure 5: High speed photo of external explosion of hydrogen: unreacted material domain (blue dotted line); combustion zone (red dotted line); time scale is given from ignition moment

Provided that hydrogen inventory remains to be the same, stratification in hydrogen-air mixture (hydrogen concentration gradient) increases the explosion pressure (rate of combustion). This was shown by that the maximum overpressures of stratified mixtures were several times higher that of the mixture with uniform concentration and same total mass.

Acknowledgements

Figure 4: Explosion overpressure as function of hydrogen concentration (top) and vent area (bottom)

The nature of external explosion leading to the multiple pressure peak structure was investigated using pressure measurements and high speed Schlieren photos. It was found that strong external explosion leading to secondary pressure peak occurred before the internal explosion. The reason of strong pressure oscillations was found due to the acoustic oscillations of combustion chamber as Helmholtz resonator.

References

(1) Akkerman, V.; Bychkov, V.; Kuznetsov, M.; Law, C.K.; Valiev, D.; Wu, M.H.; "Fast flame acceleration and deflagration-to-detonation transition in smooth and obstructed tubes, channels and slits". Proceedings of the 8th National Combustion Meeting, Park City, Utah May 19-22, 2013, Vol. 2 S. 970-978, Red Hook, N.Y.: Curran Associates, 2013, ISBN 978-1-62748-842-6.

(2) Benz, S.; Royl, P.; Band, S.; "Analysis of a hypothetical loss of coolant accident in a konvoi type NPP by GASFLOW and COCOSYS". Jahrestagung Kerntechnik, Berlin, 14.-16. Mai 2013, Berlin : INFORUM GmbH, 2013.

(3) Bykov, V.; Kuznetsov, M.; Yanez, J.; „On numerical analysis of hydraulic resistance phenomena in obstructed channels". 14th International Conference on Numerical Combustion, San Antonio, Tex., April 8-10, 2013.

(4) Grune, J.; Sempert, K.; Haberstroh, H.; Kuznetsov, M.; Jordan, T.; „Experimental investigation of hydrogen-air deflagrations and detonations in semi-confined flat layers". *Journal of Loss Prevention in the Process Industries,* 26 (2013) 317-323.

(5) Grune, J.; Sempert, K.; Kuznetsov, M.; Jordan, T.; „Experimental investigation of flame and pressure dynamics after spontaneus ignition in tube geometry". International Conference on Hydrogen Safety (ICHS 2013), Bruxelles, B, September 9-11, 2013, Book of Abstracts S. 35, Paper ID 223, ISBN 978-2-9601366-0-9.

(6) Grune, J.; Sempert, K.; Kuznetsov, M.; Jordan, T.; „Experimental investigation of fast flame propagation in stratified hydrogen-air mixtures in semi-confined flat layers". *Journal of Loss Prevention in the Process Industries,* 26 (2013) 1442-1451.

(7) Jedicke, O.; "H$_2$FC European infrastructure project. Science and development alongside the technological hydrogen chain". 10th Hypothesis Hydrogen and Fuel Cell 2013 Conference, Edinburgh, GB, June 11-12, 2013.

(8) Jedicke, O.; "H$_2$FC European infrastructure. Science and Development alongside the technological hydrogen chain". 7th International Symposium Hydrogen and Energy, Stoos, CH, January 21-25, 2013.

(9) Jedicke, O.; "Support to fuel cells and hydrogen development through research infrastructures". E-MRS 2013 Fall Meeting, Warszawa, PL, September 16-20, 2013.

(10) Jedicke, O.; "H$_2$FC European infrastructure project. Integrating European infrastructure to support science and development of hydrogen- and fuel cell technologies towards European strategy for sustainable competitive and secure energy". Fuel Cell and Hydrogen Joint Undertaking Review Days, Bruxelles, B, November 11-12, 2013.

(11) Jedicke, O.R.; Inge-Dahl, P.; „H$_2$FC European infrastructure; research opportunities to focus on scientific and technical bottlenecks". International Conference on Hydrogen Safety (ICHS 2013), Bruxelles, B, September 9-11, 2013, Book of Abstracts S. 56, Paper ID 240, ISBN 978-2-9601366-0-9.

(12) Jordan, T.; "Hydrogen safety - state of the art". The Hydrogen and Fuel Cell Applications Conferences and Trade Show, Albi, F, September 5-8, 2013.

(13) Kotchourko, A.; Baraldi, D.; Benard, P.; Jordan, T.; Kessler, A.; LaChance, J.; Steen, M.; Tchouvelev, A.; Wen, J.; "State-of-the-art and research priorities in hydrogen safety". International Conference on Hydrogen Safety (ICHS 2013), Bruxelles, B, September 9-11, 2013, Book of Abstracts S. 3, Paper ID 229, ISBN 978-2-9601366-0-9.

(14) Kudriakov, S.; Studer, E.; Kuznetsov, M.; Grune, J.; „Experimental and numerical investigation of H$_2$-air deflagration in the presence of concentration gradients". 21th International Conference on Nuclear Engineering (ICONE21), Chengdu, China, July 29 - August 2, 2013, Paper ICONE21-16910, New York, N.Y.: ASME, 2013.

(15) Kudriakov, S.; Studer, E.; Kuznetsov, M.; Grune, J.; „Hydrogen-air deflagration in the presence of longitudinal concentration gradients". ASME International Mechanical Engineering Congress and Exposition (IMECE2013), San Diego, Calif., November 15-21, 2013, Paper IMECE2013-66619, New York, N.Y. : ASME, 2013.

(16) Kuznetsov, M.; Czerniak, M.; Grune, J.; Jordan, T.; "Experimental investigations of laminar flames for hydrogen-air mixtures at elevated temperatures and reduced pressures". European

Combustion Meeting, Lund, S, June 25-28, 2013, Paper P2-90, ISBN 978-91-637-2151-9.

(17) Kuznetsov, M.; Czerniak, M.; Jordan, T.; Grune, J.; "Effect of temperature on laminar flame velocity for hydrogen-air mixtures at reduced pressures". International Conference on Hydrogen Safety (ICHS 2013), Bruxelles, B, September 9-11, 2013, Paper ID 231, ISBN 978-2-9601366-0-9.

(18) Kuznetsov, M.; Pariset, S.; Friedrich, A.; Stern, G.; Jordan, T.; „Experimental investigation of nonideality and nonadiabatic effects under high pressure releases". International Conference on Hydrogen Safety (ICHS 2013), Bruxelles, B, September 9-11, 2013, Book of Abstracts S. 8, Paper ID 239, ISBN 978-2-9601366-0-9.

(19) Kuznetsov, M.; "Flame acceleration and DDT in linear and circular geometries". International Workshop on Detonation for Propulsion (IWDP 2013), Tainan, Taiwan, July 26-28, 2013.

(20) Kuznetsov, M.; "Flame propagation regimes in a stratified semi-confined layer of hydrogen-air mixtures". European Technical School on Hydrogen and Fuel Cells, Heraklion, GR, September 23-27, 2013.

(21) L'Hostis, B.; Ruban, S.; Bernard-Michel, G.; Kotchourko, A.; Brennan, S.; Dey, R.; Hooker, P.; Baraldi, D.; Venetsanos, A.; Der Kinderen, J.; „European pre-normative research project on inherently safer use of hydrogen and fuel cell indoors: knowledge gaps and priorities". International Conference on Hydrogen Safety (ICHS 2013), Bruxelles, B, September 9-11, 2013, Book of Abstracts S. 51, Paper ID 128, ISBN 978-2-9601366-0-9.

(22) Ranft, M.; Class, A.G.; "Stochastic field modeling of cavitating flows in OpenFOAM". 66th Annual Meeting of the APS Division of Fluid Dynamics, Pittsburgh, Pa., November 24-26, 2013.

(23) Rudy, W.; Kuznetsov, M.; Porowski, R.; Teodorczyk, A.; Grune, J.; Sempert, K.; "Critical conditions of hydrogen-air detonation in partially confined geometry". *Proceedings of the Combustion Institute*, 34 (2013) 1965-1972.

(24) Travis, J.R.; Piccioni Koch, D.; Xiao, J.; Xu, Z.; "Real-gas equations-of-state for the GASFLOW CFD code". *International Journal of Hydrogen Energy*, 38 (2013) 8132-8140.

(25) Valiev, D.M.; Akkerman, V.; Kuznetsov, M.; Eriksson, L.E.; Law, C.K.; Bychkov, V.; "Influence of gas compression on flame acceleration in the early stage of burning in tubes". *Combustion and Flame*, 160 (2013) 97-111.

(26) Xiao, J.; Travis, J.R.; "How critical is turbulence modeling in gas distribution simulations of large-scale complex nuclear reactor containment?" *Annals of Nuclear Energy,* 56 (2013) 227-242.

(27) Xu, Z.; Jordan, T.; "Thermal-hydraulic simulations of guard containment in depressurization accidents of a gas-cooled fast reactor". 21th International Conference on Nuclear Engineering (ICONE21), Chengdu, China, July 29 - August 2, 2013, Paper ICONE21-15955, New York, N.Y.: ASME, 2013.

(28) Yanez, J.; Kuznetsov, M.; Redlinger, R.; „The acoustic-parametric instability for hydrogen-air mixtures". *Combustion and Flame,* 160 (2013) 2009-2016.

(29) Yanez, J.; Kuznetsov, M.; Redlinger, R.; „The acoustic-parametric instability for gaseous mixtures with Lewis number smaller than one". 24th International Colloquium on the Dynamics of Explosions and Reactive Systems (ICDERS 2013), Taipei, Taiwan, July 28 - August 2, 2013, Paper ICDERS_0084.

(30) Yanez, J.; Kuznetsov, M.; Bykov, V.; "Sudden acceleration of flames in open channels driven by hydraulic resistance". 24th International Colloquium on the Dynamics of Explosions and Reactive Systems (ICDERS 2013), Taipei, Taiwan, July 28 - August 2, 2013, Paper ICDERS_0164.

The Coarse-Grid-CFD (CGCFD) Methodology: Simulation of a wire wrapped fuel assembly

Andreas Class

Introduction

The core of a nuclear reactor is a few meters in height and in diameter. It is composed of several hundred fuel assemblies which are again composed of tenth of fuel rods with a diameter of about 10 mm. Therefore the relevant length scales for CFD simulations range from the sub millimeter range, relevant for the fuel rod space up to several meters. Describing such a multi scale approach is challenging and the historical approach was to use integral descriptions. These methods are called sub-channel analyses codes and are based on integral equations that are tuned by experiments (compare fig. 1).
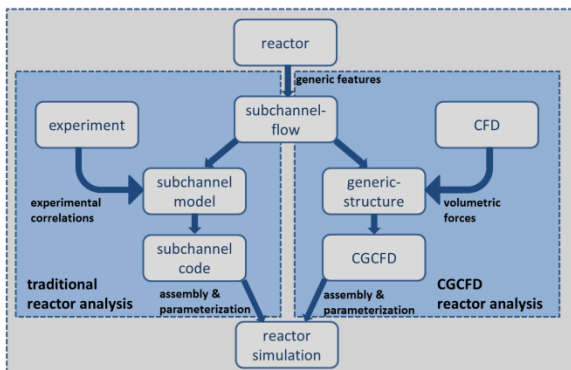
Figure 1: Subchannel analysis and CGCFD approach

With the Coarse-Grid-CFD (CGCFD) [Class, Batta et al, 2011], [Viellieber, Class, 2012], [Roelofs et a, 2012], developed at the AREVA Nuclear Professional School, we present a numerical method which aims at making experiments almost obsolete (compare fig. 1), so that only the used models must generally be verified. The goal of the method development is to perform a 3D CFD simulation of the thermal-hydraulics inside a complete reactor core. The method replaces the experimental or empirical input, used to tune subchannel analysis codes, with CFD data.

Therefore taking advantage of the fast development of commercial CFD software and exploiting the efficiency of subchannel analysis codes. The methodology and strategy of a CGCFD simulation are shown in figure 2.
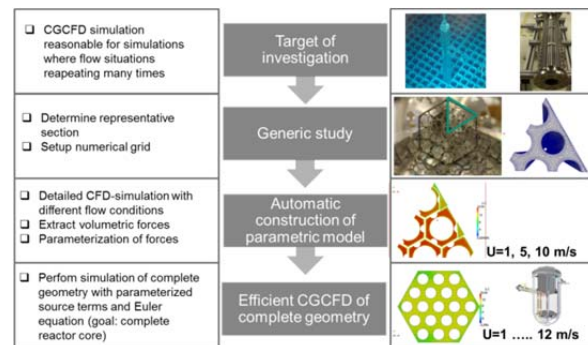
Figure 2: Methodology of the CGCFD for repetitive flow patterns

CGCFD uses the inviscid Euler equations in combination with a coarse mesh of the complete geometry. Hence we are not able to resolve the detailed physics inside the geometry. With respect to the non-resolved physical processes, we extend the Euler equations with volumetric source terms extracted in tabular form from a detailed and well-resolved CFD simulation of one representative segment of the complete geometry. Parameterization of the source terms is accomplished using the ansatz-function established in subchannel analysis.

While the formulation accounts for forces created internally in the fluid, there are other influences, like obstruction and flow guidance through spacer grids, wire wraps etc., that still need to be accounted for when these geometric details are not represented by the coarse mesh. In the 1970ies non-resolved geometrical details were modeled with an Anisotropic Porosity (AP) formulation that was implemented in the COMMIX code [Chien, Domanus, Sha, 1993]. While in this

early code the AP- parameters had to be manually set, the CGCFD automatically determines the parameters from a detailed CFD simulation.

Coarse-Grid-CFD of a wire wrapped Fuel Assembly: Numerical Set UP

During the development of the CGCFD method, we demonstrated the ability of the CGCFD simulations to simulate less complex geometries (compare [Class, Batta, Viellieber 2011]-[Roelofs, Gopala et al, 2012]). Here we present the CGCFD simulation of a wire wrapped fuel assembly. The wires are helically wrapped around the fuel rods (compare figure 3), keeping them at their position and preventing rod vibrations. Wire-wraps are used for small pitch to diameter ratio fuel assemblies instead of spacer grids.

Both, the generation of detailed computational meshes- and the simulation of wire wrapped fuel assemblies in CFD simulations are challenging. This is due to the point contact between the rods and the wires. It is virtually impossible to model the exact geometry due to the point contact between rods and wires. These are modeled as a line contact (compare figure 3). A RANS CFD simulation with a polyhedral mesh is used to extract the volumetric source terms. The mesh was generated with STARCCM+. The boundary conditions and the parameters used to perform the detailed CFD simulation are shown in table 1 and in figure 4.

For the Anisotropic Porosity AP-CGCFD simulation a coarse mesh that consists of merely 19200 cells is representing the computational domain (compare figure 3). This coarse mesh is not body conformal. The AP formulation takes account of the non-resolved wires (compare figure 4). In contrast to the detailed CFD simulation slip boundary conditions are imposed at the rods and walls of the fuel assembly to meet the requirements of an Euler solver.
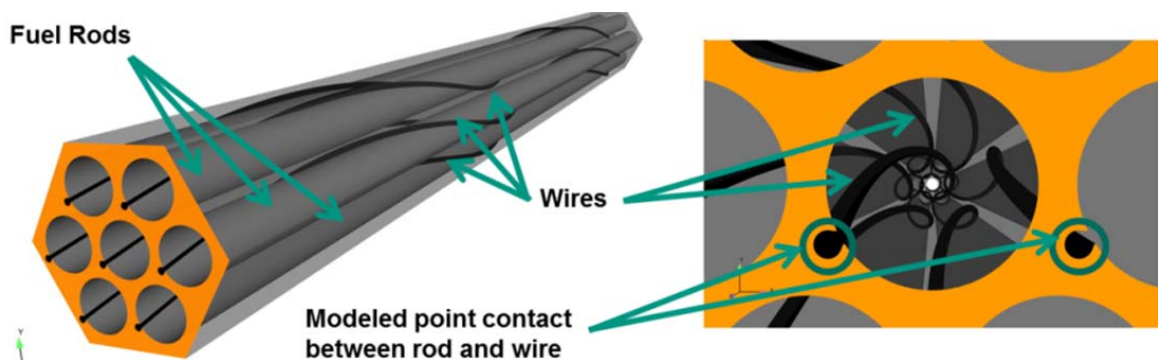
Figure 3: Computational domain of the wire wrapped fuel bundle with modeled point contact between wire and fuel rod.

Tab 1: Numerical settings rod bundle without spacer

Solver	Inflow	Number of cells	Turbulence model	Mesh reduction factor
RANS CFD	0.6 m/s	> 3 million	K-ω	-
CGCFD	0.6 m/s	19200	-	~156
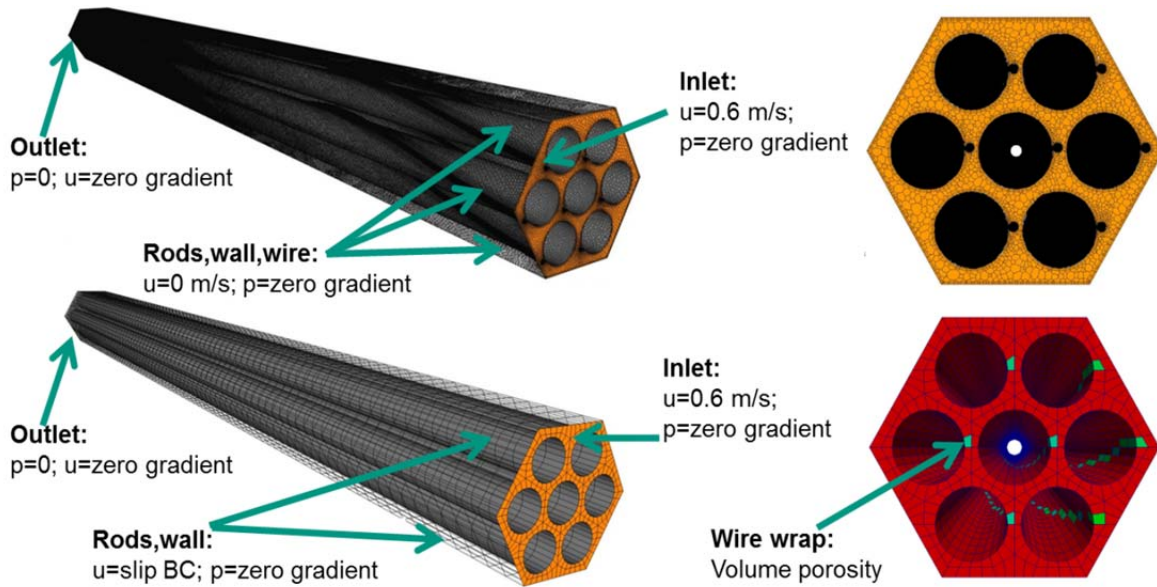
Figure 4: Boundary conditions for detailed RANS CFD and AP-CGCFD simulations

Results ANISOTROPIC COARSE-GRID-CFD (AP-CGCFD) applied to a wire wrapped fuel assembly

Figure 5 and 6 show the results of the detailed RANS CFD simulations compared to the corresponding CGCFD simulations with the AP formulation. The detailed mesh consists of 3 million computational cells and the CFD-simulation employs the K-ω turbulence model. We are aware of the fact that the choice of the polyhedral meshes and the use of a K-ω turbulence model may degrade accuracy. Nevertheless within this investigation we wanted to demonstrate the consistency between both methods. Figure 5 shows the comparison of the velocity profiles of detailed RANS CFD and AP-CGCFD. The AP-CGCFD simulation reproduces the main features of the velocity profile of the detailed CFD simulation.

Clearly the influence of volume porosity and surface permeability can be seen in the velocity plot. We can identify the non-resolved wires in the coarse grid representation by the reduced velocities at the wire positions. Note that the mesh has only two computational cells across subchannels.
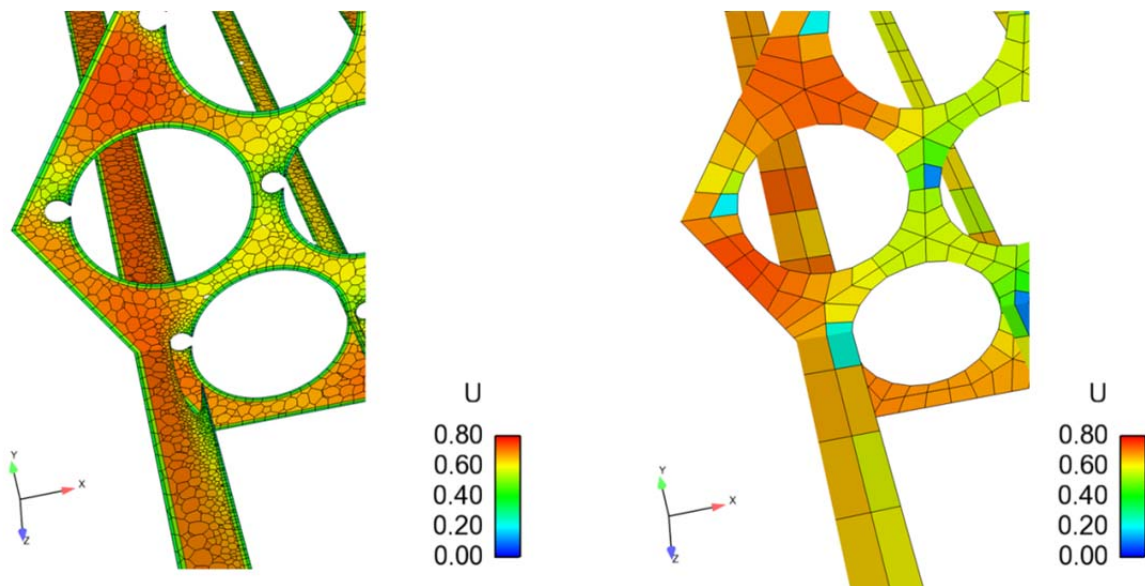
Figure 5: Velocity profile of the detailed RANS CFD and AP-CGCFD simulations

The AP-CGCFD method captures both the qualitative and the quantitative features like the main flow structures and the pressure drop values. Figure 6 shows the comparison of the pressure profile, measured at two positions through the fuel assembly. The black line within figure 6 depicts the detailed RANS K-ω results and the blue lines depict the corresponding coarse grid simulation results. The AP-CGCFD simulation is in nice agreement of the detailed CFD simulation.
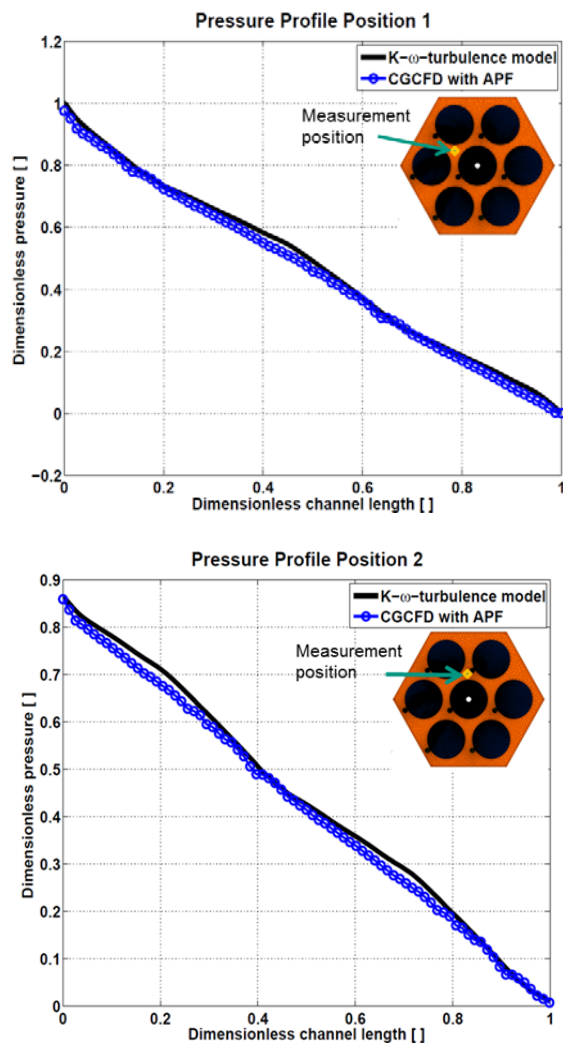
Figure 6: Pressure profile of the detailed RANS CFD and AP-CGCFD simulation at different measurement positions

Conclusion

Within this work we demonstrated the ability of the AP-CGCFD method to deal with complex geometries like wire wrapped spacer grid fuel assemblies. Both qualitative and quantitative values like the pressure profile and velocity struc-

tures could be reproduced from the detailed RANS CFD simulation. Compared to state-of-the-art subchannel analyses, neither parameter tuning is needed, nor empirical or experimental input, to adjust the solvers for a specific geometry. Certainly, this method requires the user making educated decisions on the representative geometry segments and a suitable parameter space for the initial fine CFD simulations needed to extract the volumetric source terms. Since similar flow conditions repeat many times, the costs of the representative CFD simulations needed to extract the volumetric forces are much lower than a full simulation. Thus AP-CGCFD simulations are suitable for simulations of geometries where flow situations are repeating many times.

References

(1) Class, A.G.; Batta, A.; Viellieber, M.; "Coarse-Grid-CFD for Pressure Loss Evaluation in rod bundles" ICAPP Nice, 2011.

(2) Viellieber, M.; Class, A.G.; "Anisotropic Porosity Formulation of the Coarse-Grid-CFD", ICONE20 Annaheim, 2012.

(3) Roelofs, F.; Gopala, V.R.; Chandra, L.; Viellieber, M.; Class, A.; "Simulating fuel assemblies with low resolution CFD approaches", *Nucl. Eng. Des.*, 250,548-559, 2012.

(4) Chien, T.H.; Domanus, H.M. and Sha, W.T.; "COMMIX-PPC: A Three-Dimensional Transient Multicomponent Computer Program for Analyzing Performance of Power Plant Condensers" ARGONNE Nat. Lab., ANL-92/2-Vol. 1, 1993.

(5) Batta, A.; Litfin, K.; Fellmoser, F.; Class, A.G.; Wetzel, T.; "Numerical and experimental hydraulic analysis of the heavy liquid metal free surface of myrrha spallation target experiment". THINS Cluster Workshop, Stockholm, S, February 6-7, 2013.

(6) Batta, A.; Class, A.G.; "Numerical and experimental study of isothermal water flow downstream of split-type spacer grids in rod bundles: OECD/NEA benchmark MATiS-H". Jahrestagung Kerntechnik, Berlin, 14.-16. Mai 2013, Berlin: INFORUM GmbH, 2013.

(7) Batta, A.; Class, A.; "Thermal hydraulic numerical investigation of the heavy liquid metal free surface of MYRRHA spallation target experimental". 2nd International Workshop on Technology and Components of Accelerator-Driven Sys-

tems (TCADS 2013), Nantes, F, May 21-24, 2013.

(8) Batta, A.; Class, A.G.; "CFD study of isothermal water flow in rod bundle with split-type spacer grid". International Conference on Supercomputing in Nuclear Applications and Monte Carlo (SNA & MC 2013), Paris, F, October 27-31, 2013.

(9) Bruzzese, C.; Strein, S.; Class, A.G.; "Simulation and analysis of premixed flames as gasdynamic discontinuities in pseudo-turbulence". European Combustion Meeting, Lund, S, June 25-28, 2013. Paper PP2-70, ISBN 978-91-637-2151-9.

(10) Class, A.G.; Lamm, M.; Niessen, S.; Schulenberg, T.; Jordan, T.; Dumond, J.; „AREVA Nuclear Professional School". Jahrestagung Kerntechnik, Berlin, 14.-16. Mai 2013, Berlin : INFORUM GmbH, 2013.

(11) Class, A.G.; Prill, D.; "Semi-automatic reduced order models from expert-defined transients". 66th Annual Meeting of the APS Division of Fluid Dynamics, Pittsburgh, Pa., November 24-26, 2013.

(12) Dumond, J.; Magagnato, F.; Class, A.; "Stochastic-field cavitation model". *Physics of Fluids*, 25 (2013) S. 073302/1-28.

(13) Grötzbach, G.; "Challenges in low-Prandtl number heat transfer simulation and modelling". *Nuclear Engineering and Design*, 264 (2013), 41-55.

(14) Heinze, D.; Schulenberg, T.; Behnke, L.; „Modeling of steam expansion in a steam injector by means of the classical nucleation theory". 15th International Topical Meeting on Nuclear Reactor Thermalhydraulics (NURETH 2013), Pisa, I, May 12-17, 2013, NURETH15-129.

(15) Litfin, K.; "Some existing experimental facilities for fast neutron systems at KIT". IAEA Technical Meeting on Existing and Proposed Experimental Facilities for Fast Neutron Systems, Wien, June 10-12, 2013.

(16) Litfin, K.; Marocco, L.; Pacio, J.; Wetzel, T.; KALLA Team; „Status of LBE rod bundle experiment at KIT". THINS 3rd Technical Review Meeting, Petten, NL, September 9-10, 2013.

(17) Prill, D.; Class, A.G.; "Predictions by the proper orthogonal decomposition reduced order methodology regarding non-linear BWR stability". Jahrestagung Kerntechnik, Berlin, 14.-16. Mai 2013, Berlin: INFORUM GmbH, 2013.

(18) Prill, D.P.; Class, A.G.; "Verification of non-linear proper orthogonal decomposition reduced order modeling for BWR fuel assemblies". 21th International Conference on Nuclear Engineering (ICONE21), Chengdu, China, July 29 - August 2, 2013, Paper ICONE21-16434, New York, N.Y.: ASME, 2013.

(19) Prill, D.P.; Class, A.G.; "Non-linear proper orthogonal decomposition reduced order modeling: Bifurcation study of a natural convection circuit". 84th Annual Meeting of the International Association of Applied Mathematics and Mechanics (GAMM 2013), Novi Sad, SRB, March 18-22, 2013, *Proceedings in Applied Mathematics and Mechanics*, 13 (2013) 285-286.

(20) Prill, D.P.; "A non-linear reduced order methodology applicable to boiling water reactor stability analysis". Dissertation, Karlsruher Institut für Technologie 2013.

(21) Raque, M.; Schulenberg, T.; "Optimization of the SCWR fuel qualification test for fast depressurization transients". 6th Internat. Symp. on Supercritical Water-Cooled Reactors (ISSCWR-6), Shenzhen, China, March 3-7, 2013, Paper ISSCWR6-13106.

(22) Raque, M.; Frybort, O.; Vojacek, A.; Schulenberg, T.; „Passive residual heat removal system for the SCWR fuel qualification test facility". 15th International Topical Meeting on Nuclear Reactor Thermalhydraulics (NURETH 2013), Pisa, I, May 12-17, 2013, NURETH15-112.

(23) Raque, M.; Herbell, H.; Schulenberg, T.; „Validation of the system code APROS for fast transients". 21th International Conference on Nuclear Engineering (ICONE21), Chengdu, China, July 29 - August 2, 2013, Paper ICONE21-16746, New York, N.Y.: ASME, 2013.

(24) Raque, M.; Schulenberg, T.; "Validation of the system code APROS for fast transients". Workshop on Codes and Experimental Methods to Analyze SCWRs, Budapest, H, September 6, 2013.

(25) Schulenberg, T.; Vojacek, A.; Zeiger, T.; Raque, M.; „Risk and safety analyses of an SCWR fuel quantification test loop". 6th Internat. Symp. on Supercritical Water-Cooled Reactors (ISSCWR-6), Shenzhen, China, March 3-7, 2013, Paper ISSCWR6-13014.

(26) Schulenberg, T.; "Material requirements of the high performance light water reactor". *Journal of Supercritical Fluids*, 77(2013)127-133.

(27) Schulenberg, T.; Matsui, H.; Leung, L.; Sedov, A.; "Supercritical water cooled reactors". GIF Symposium Proceedings, San Diego, Calif., November 14-15, 2012, 2012 Annual Report, Paris: OECD/NEA, 2013 S.63-75, NEA No.7141.

(28) Schulenberg, T.; Raque, M.; Arheidt, K.; „Prediction of heat transfer during depressurization from supercritical pressure". 15th International Topical Meeting on Nuclear Reactor Thermal-

hydraulics (NURETH 2013), Pisa, I, May 12-17, 2013, NURETH15-139.

(29) Schulenberg, T.; "Generation IV nuclear reactors". Stock, R. [Hrsg.], Encyclopedia of Nuclear Physics and its Applications, Weinheim: Wiley-VCH, 2013 S. 663-688, ISBN 978-3-527-40742-2.

(30) Schulenberg, T.; Visser, D.C.; „Thermal-hydraulics and safety concepts of supercritical water cooled reactors". *Nuclear Engineering and Design*, 264 (2013), 231-237.

(31) Schulenberg, T.; "Research expectations for advanced nuclear systems". 8th European Conference on Euratom Research and Training in Reactor Systems (FISA 2013), Vilnius, LT, October 14-17, 2013.

(32) Stokmaier, M.J.; Class, A.G.; Schulenberg, T.; „A hard optimisation test function with symbolic solution visualisation for fast interpretation by the human eye". IEEE Congress on Evolutionary Computation, Cancun, MEX, June 20-23, 2013, S. 2251-2258, Piscataway, N.J.: IEEE, 2013, ISBN 978-1-4799-0454-8.

(33) Viellieber, M.; Dietrich, P.; Class, A.; "Investigation of a wire wrapped fuel assembly with the anisotropic Coarse-Grid-CFD (AP-CGCFD)". Jahrestagung Kerntechnik, Berlin, 14.-16. Mai 2013, Berlin: INFORUM GmbH, 2013.

(34) Viellieber, M.; Dietrich, P.; Class, A.G.; "Coarse-Grid-CFD for a wire wrapped fuel assembly". *Proceedings in Applied Mathematics and Mechancis*, 13 (2013) 317-318.

(35) Zeiger, T.; Raque, M.; Schulenberg, T.; "Consequences of pressure tube fragments in case of rupture during an SCWR fuel assembly test". 6th Internat. Symp. on Supercritical Water-Cooled Reactors (ISSCWR-6), Shenzhen, China, March 3-7, 2013 Paper ISSCWR6-13016.

(36) Zeiger, T.; Raque, M.; Schulenberg, T.; "Study of the consequences of a pressure tube failure for an SCWR in-pile fuel assembly test". 15th International Topical Meeting on Nuclear Reactor Thermalhydraulics (NURETH 2013), Pisa, I, May 12-17, 2013, NURETH15-207.

(37) Zeiger, T.; Schulenberg, T.; "Validation of fragment penetration analysis with ANSYS". Workshop on Codes and Experimental Methods to Analyze SCWRs, Budapest, H, September 6, 2013.

Group: Energy and Process Engineering

Geothermal Power Plant Engineering

Christian Vetter, Hans-Joachim Wiemer, Dietmar Kuhn

Introduction

The working group Energy- and Process-Engineering focusses on the field of energy conversion from low temperature geothermal heat. The experimental group consists of academic and technical staff with expertise in mechanical engineering, process engineering, physics and chemistry. Within the sequence of geothermal projects, the work contributes the late part of such projects.

Starting with the research field in geochemistry, current research projects deal with supersaturation, kinetics of scaling and measures to avoid or control precipitation. Together with experiments to determine physical properties on-site and in-situ, the chemical composition delivers the inlet conditions of the brine into the technical system above surface.

In the second step, research on suitable and tailor-made heat exchangers are addressed. Especially for electricity production, maximising temperature and heat transfer rises significantly the productivity of geothermal power plants.

The thermodynamic simulation of low enthalpy heat applying Organic-Rankine-Cycles is addressed in the third key aspect of the group. Here numerical codes as Dymola / TIL or IpsePro are used to simulate steam cycles. For optimization and variations the in-house code GESI has been developed. The numerical simulations will be completed in future by the large scale test-facility MoNiKa. The facility is currently under construction and will allow for reliable experiments on the thermodynamic conversion cycle. It will convert heat from an oil fired heating system at 150°C to electricity. The cycle is designed as a supercritical propane cycle due to the higher net power output at low temperature compared to conventional ORC-concepts. Various thermodynamic simulations on supercritical cycles show a significant higher net power output for supercritical systems. The following study will quantitatively present the study performed at IKET in this field.

Thermodynamic comparison of sub- and supercritical Organic Rankine Cycles

In this study, the potential of sub- and supercritical low-temperature processes using CO_2 and ten other refrigerants as candidate working fluids was investigated. Power plant processes were modeled and simulated using an in-house program, GeSi (Geothermal Simulation). The program optimizes the thermodynamic process according to steam parameters. The required thermodynamic data for the substances are taken from REFPROP 8.0 of the National Institute of Standards and Technology [Nist]. The GeSi program was validated using IpsePro (Version 4.0, SimTech Simulation Technology) for isopentane as a reference fluid. The aim of this investigation was performance optimization based on live steam parameters; the processes are simulated over a wide range of live steam pressures and temperatures. Dependencies between reinjection temperature of the geothermal fluid, supplied heat, thermal efficiency and the net power of the process are discussed in detail.

Results obtained here are also compared with isopentane (reference fluid), a common working fluid in existing geothermal power plants. Important cycle parameters, such as condensing temperature, minimal temperature difference (MTD) or *pinch point*, and use of an internal heat exchanger, were varied to investigate their influence on the overall net power output. Cycles employing other working fluids at geothermal fluid temperatures of 130 – 170°C were also investigated to show a correlation between the critical temperature of suitable working fluids,

geothermal fluid temperature and the maximum achievable net power output.

Organic-Rankine-Cycle

The Clausius-Rankine cycle, using water as a working fluid, is state-of-the-art in coal, gas and nuclear power plants. Water, however, is not a suitable working fluid for converting low temperature heat, due to high evaporation temperature at ambient pressure; therefore, ORC organic fluids with lower vaporization temperatures are used.

Figure 1 shows the ORC using propane as a working fluid in the T-s diagram, as well as process flow. The working fluid is compressed in the feed pump, heated up and evaporated in the heat exchanger before it is expanded in the turbine. In the last step, which closes the cycle, the remaining heat is removed in the condenser. Changes in state of an ideal process are as follows:

- 1 - 2: isentropic compression, supply of work to the cycle

- 2 - 3: isobaric supply of heat (heat exchanger)

- 3 - 4: isentropic expansion, submission of work out of the cycle

- 4 - 1: isobaric removal of heat (condenser).
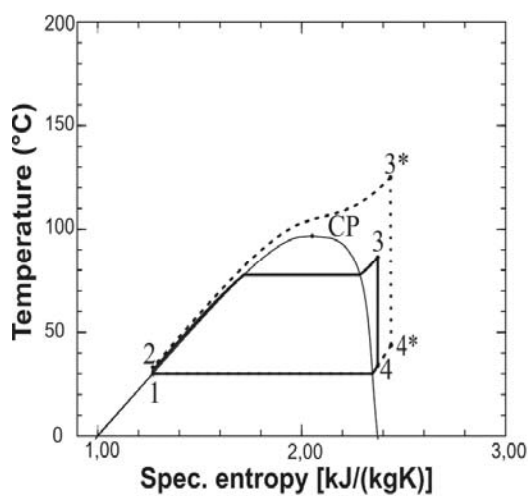
Depending on the pressure at which the heat is supplied, the process is either subcritical, with the fluid evaporating as it passes through the two-phase region (bold line, Fig. 1), or supercritical (dotted line, Fig. 1). Location of the critical point (CP) depends on the fluid.

From the enthalpy differences between the individual state points, the specific energy contribution of each component can be calculated:

Work supplied in the feed pump:	w_{pump}	$= h_2 - h_1$
Heat supplied in the heat exchanger:	q_{in}	$= h_3 - h_2$
Specific work of the turbine:	$w_{turbine}$	$= h_3 - h_4$
Heat removed in the condenser:	q_{out}	$= h_4 - h_1$

By this, the thermal efficiency of the cycle can be calculated:

$$\eta_{th} = \frac{|q_{in}| - |q_{out}|}{|q_{in}|} = \frac{|w_{turbine}| - |w_{pump}|}{|q_{in}|}$$

$$= \frac{(h_3 - h_4) - (h_2 - h_1)}{h_3 - h_2} \tag{1}$$
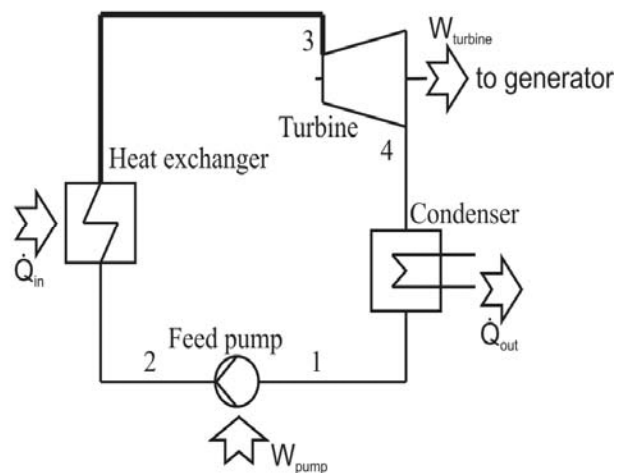
Figure 1: Sub- and supercritical ORC in a T-s-diagram (left side, fluid data from [NIST]) and process flow diagram (right side)

The previously described process is an ideal case, which in reality is affected by losses. Pressure losses in the pipes, heat exchanger and condenser cannot be avoided. In addition, there are losses during compression in the pump and expansion in the turbine. These losses result in an increase in entropy during compression and expansion. This can be described with the isentropic pump and turbine efficiency:

$$\eta_{pump} = \frac{h_{2s} - h_1}{h_2 - h_1} \qquad (2)$$

$$\eta_{turbine} = \frac{h_3 - h_4}{h_3 - h_{4s}} \qquad (3)$$

Geothermal fluid provides the heat source for the process. The heat is extracted in the heat exchanger. This is a sensible heat source, since the temperature of the hot water during the heat dissipation changes. This is why the so-called triangle process as a comparison process is used instead of the Carnot cycle process. The efficiency of this process can be calculated from the upper and lower process temperature (T_{max} and T_{min}), in the same way as the Carnot efficiency [DiPippo, 2007]:

$$\eta_C = 1 - \frac{T_{min}}{T_{max}} \qquad (4)$$

$$\eta_{th,triangle} = \frac{T_{max} - T_{min}}{T_{max} + T_{min}} \qquad (5)$$

Assuming a condensing temperature of T_{min}=303 K and an upper cycle temperature of T_{max}=423 K, the Carnot efficiency is around 28%, whereas the triangle process efficiency is around 16.5%. This efficiency is a realistic upper limit for processes with geothermal heat sources. In order to increase efficiency, an approximation of the real process to achieve this triangular shape should be attempted [Heberle, Brüggemann, 2010]. The efficiency of the heat exchanger plays an important role, discussed in section 2.3 separately.

Working Fluid

Selection of the working fluid depends on its thermo-physical properties. After [Maizza V., Maizza, A., 1996], the working fluid should *inter alia* meet the following criteria:

- Low critical pressure and temperature (compared to water)

- Low specific volume

- High thermal conductivity

- Non corrosive, toxic or flammable and stable

In addition, low ozone depletion potential (ODP) and a low greenhouse warming potential (GWP) are important requirements for the suitability of the working fluid.

Figure 2 shows the wet steam areas of different organic media in the T-s diagram. The two-phase region of water is also included for comparison. Depending on the gradient of the vapor line, a distinction is made between dry (retrograde) and wet fluids. Water as a wet fluid has a negative dew line slope, but many organic media are retrograde – they have a dew line with at least a partial positive slope (*e.g.* isopentane, Fig. 2).

In wet media, the vapor must be superheated, in order to prevent formation of droplets in the turbine after expansion. Since expansion of retrograde fluids in the two-phase region is not possible, superheating is not required. On the contrary, the steam cannot expand to condensing temperature because of superheating during expansion; therefore, a larger part of the supplied heat cannot be used. As a consequence, in cycles with retrograde fluids, an additional internal heat exchanger can be used. In the recuperator, a part of the waste heat is used to preheat the fluid.

A high enthalpy gradient in the turbine is obtained through expansion, until the condensing temperature is reached; this leads directly to a proportional high gross power output. After [Förster, Schmidt, 2006], in wet working fluids a higher average temperature of heat supply and lower average temperature of heat dissipation can be realized, which leads to a higher efficiency. Consequently, the curve progression of the dew line is a relevant criterion for the choice of the working fluid.
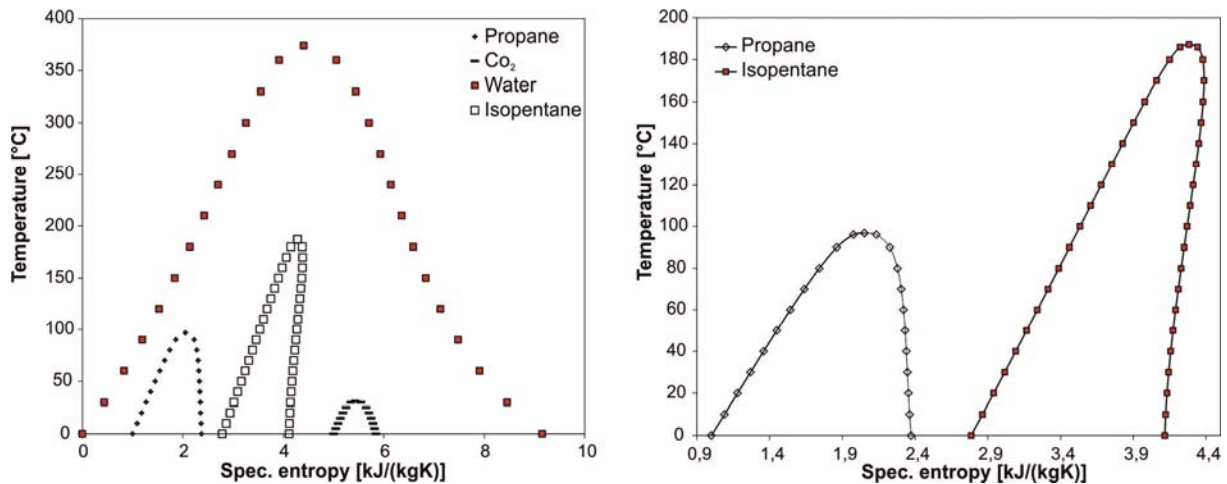
Figure 2: Two-phase regions of some organic fluids and water, fluid data from [NIST, 2010]

Heat Exchanger

Heat input can be calculated using an energy balance equation over the heat exchanger:

$$\dot{Q}_{geo} = \dot{m}_{geo} \cdot c_{p,geo} \cdot (T_{geo,in} - T_{geo,out})$$
$$= \dot{m}_{ORC} \cdot (h_3 - h_2) = \dot{Q}_{in,ORC} \qquad (6)$$

The left side of the formula is the heat removed from the geothermal fluid. This can be calculated from the temperature difference of the geothermal fluid between entry and exit from the heat exchanger, and the mean specific isobaric heat capacity c_p of the geothermal fluid. This heat leads to increased enthalpy and, therefore, to evaporation of the organic fluid on the secondary side.

In this study, the use of a counter current heat exchanger is assumed. The finite heat exchange area leads to temperature differences between the two fluids at all points of the heat exchanger. An important design parameter for the heat exchanger is a MTD between the two fluids. The point where this MTD occurs, the *Pinch Point*, depends on two factors: (1) the pressure and temperature of the organic fluid exiting the heat exchanger, and (2) the temperature of the geothermal fluid at the entry point. A good adaption of the geothermal and organic fluid temperature profiles is important for approaching the triangle process (Sect. 2.1). In consequence, it is necessary to iteratively evaluate the lowest possible temperature of the geothermal fluid at the heat exchanger's exit. This is achieved by the program shown in Figure 3.

The starting value for the iteration is the temperature of the organic fluid at the entry point of the heat exchanger plus the MTD. To check compliance with the minimal temperature difference at all points in the heat exchanger, the program calculates the temperature profiles of the geothermal and organic fluids, depending on the heat exchanged. If MTD falls below the allowed value, as is shown on the right side in Figure 3, the program aborts the calculation and starts with a higher geothermal fluid exit temperature. This is performed until the MTD is maintained at all points. By establishing the temperatures at this stage, the missing parameters of the cycle can be calculated. For the present study, a MTD of 20K is assumed.

Specific net power output

In order to compare different working fluids, this paper focusses on the specific net power output of the thermodynamic cycle. This is the relevant variable for geothermal application and waste heat utilization. If the energy is extracted from a closed loop (*i.e.* CHP systems) or from a valuable energy source, one has to compare the efficiency of the processes. Furthermore, the net power output – considering the electricity demands of the cycle pump and condenser – is taken into account to evaluate the thermodynamic systems. The electricity demand of the geothermal production pump is not considered in the
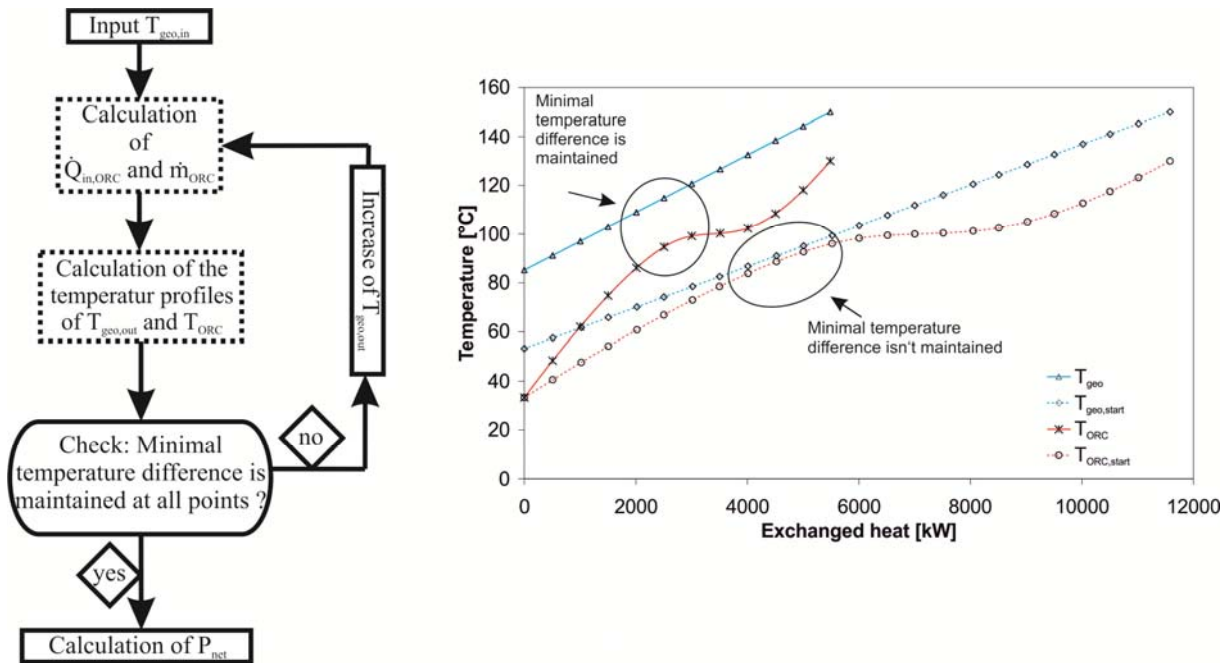
Figure 3: Iteration schema and calculated temperature profiles during iteration

calculations because of its site-specific aspects. Economic aspects can also play an important role in gross power output; this is not addressed in the present work.

The net power output of the cycle is the product of thermal efficiency and the heat supplied to the organic fluid:

$$P_{net,out} = \eta_{th} \cdot \dot{Q}_{in,ORC} \qquad (7)$$

As is seen in this formula, the net power output is dependent on two factors that affect each other. The heat input to the cycle is not a fixed value, but, like thermal efficiency, depends on live steam parameters and cycle design. This is because of the sensitive heat source and the varying exit temperature of the geothermal fluid.

In order to objectively compare various cycle designs with different workings fluids, a new index number is used. This is the specific net power output – the net power output that can be achieved with 1kg/s geothermal fluid mass flow rate under given conditions:

$$p_{net,spec} = \frac{P_{net,out}}{\dot{m}_{geo}} \quad \left[kWs/kg \right] \qquad (8)$$

Simulation and results

Propane and CO_2 as working fluid

Table 1 shows default settings for the simulations of the ORCs with propane and CO_2 as the working fluids.

Table 1: Boundary conditions and parameter settings for the model simulations

ORC-process parameters	
Condensing temperature	30 °C
Pump efficiency	0,8
Turbine efficiency	0,8
Minimal temperature difference in the heat exchanger	20 K
Heat exchanger pressure loss	0,02 MPa
Geothermal fluid parameters	
Mass flow	20 kg/s
Pressure	2,5 MPa
Temperature at heat exchanger inlet	150 °C
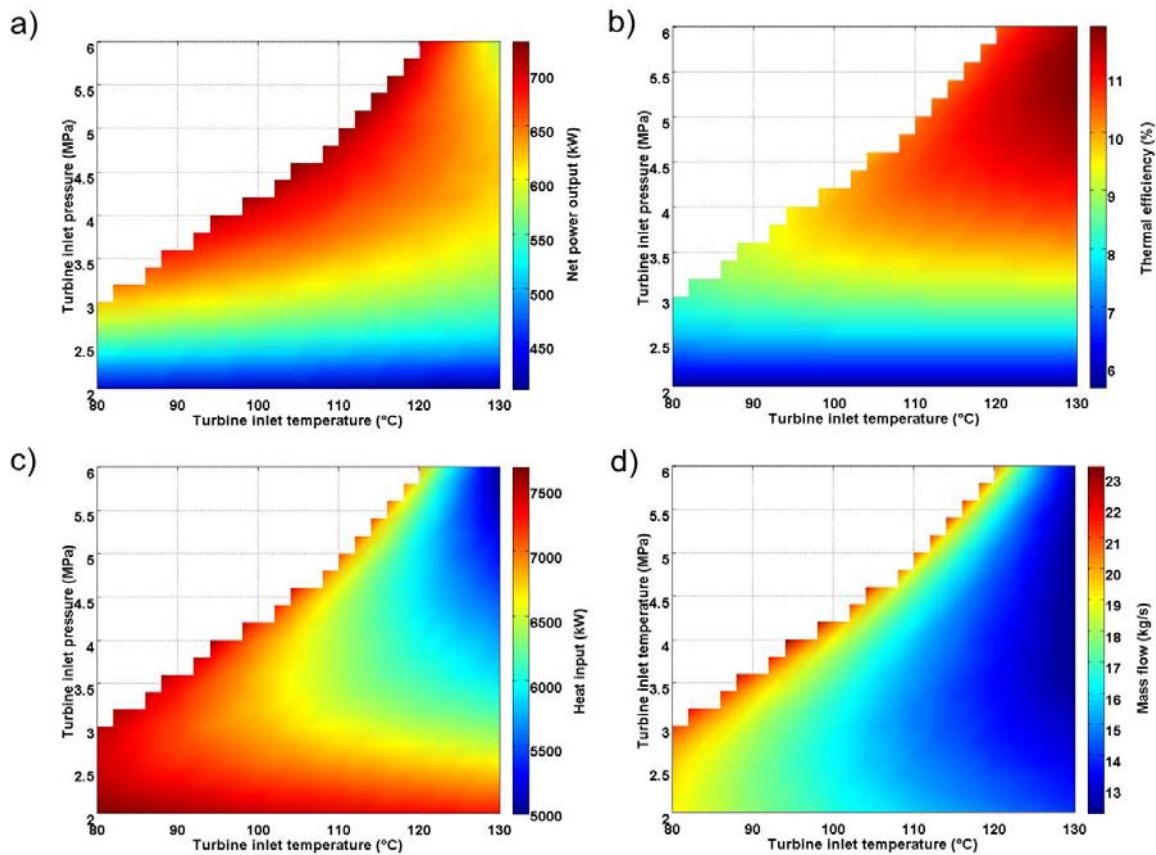
Figure 4: Net power output (a), thermal efficiency (b), heat input (c) and mass flow of the ORC (d) over turbine inlet pressure and turbine inlet temperature, using propane as the working fluid

Additional pressure losses, such as in the pipes, or mechanical losses in the machines were not included in the model parameters and calculations. The geothermal fluid temperature is a standard value for state-of-the-art deep geothermal sites in Europe, but plays also a role for bottoming cycles of direct-use systems overseas.

By varying the live steam parameters (pressure and temperature), the maximum possible net power output was evaluated. The progression of net power output curves is derived from the efficiency and heat supplied to the ORC-process, which depends on the geothermal fluid reinjection temperature. The geothermal fluid reinjection temperature depends on the location of the pinch point in the heat exchanger, which in turn depends on the chosen live steam conditions. It is only limited by the condensing temperature and the MTD of the heat exchanger.

Figure 4 shows the results of simulations using propane as working fluid. The connections between net power, thermal efficiency, supplied heat and propane mass flow in the ORC process

are illustrated. Values are plotted as a function of steam pressure (MPa) and temperature (Celsius). The color value reflects actual quantities.

In Figure 4, white areas represent steam conditions. These cannot be set, since they would lead to an overly wide expansion into the two-phase region (10% relative moisture is set as upper limit) or incomplete evaporation. Net power and supplied heat are given in kW, thermal efficiency in percent and mass flow of the ORC fluid in kg/s. Maximum thermal efficiency lies in the region of the highest pressures and temperatures, whereas maximum net power output can be found at expansion into or near to the two-phase region. Heat input decreases with increasing live steam temperature. This results in a corresponding course of ORC mass flow, which leads to a lower net power output at higher live steam temperatures. A process with optimized thermal efficiency is, therefore, not optimized for net power output performance, since heat input from the geothermal fluid must also be considered.
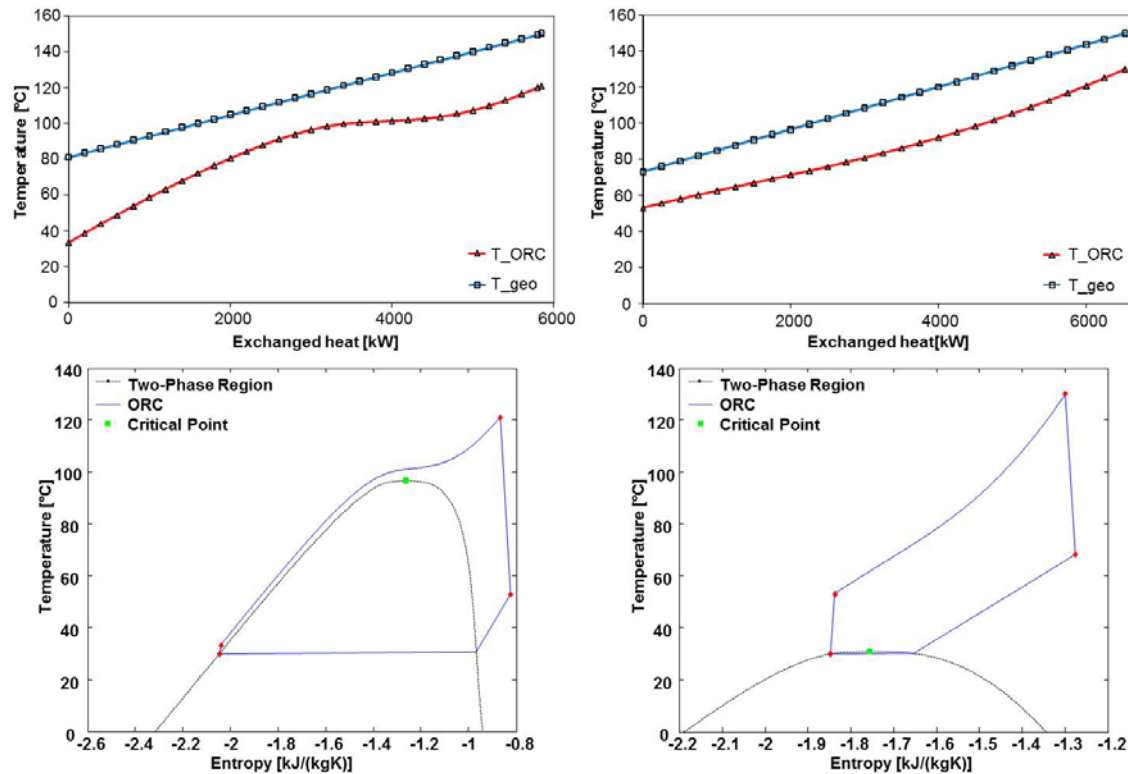
Figure 5: Temperature profiles in the heat exchanger of propane (left), CO_2 (right) and the geothermal fluid; corresponding processes in the T-s diagram

Simulations using CO_2 as the working fluid (Fig. 6) show slightly different behavior. The CO_2 isobars in the heat transfer diagram show different characteristics than the propane isobars for two reasons: the parameters are well above supercritical pressure at which the heat is supplied, and the condensing temperature is near critical. The temperature curve of propane showed a marked S-curve. In contrast, CO_2 has a bent curve with an initially lower, but later on increasing gradient (Fig. 5). As a result, the pinch point for CO_2 is located either at the entrance or at the outlet of the heat exchanger. The temperature of the working medium as it enters the heat exchanger depends on steam pressure and, consequently, determines the minimum possible reinjection temperature of the geothermal fluid.

The highest net output can be achieved with a supercritical ORC process using propane as working fluid. At a live steam pressure of 4.6 MPa and temperature of 104°C, net power output is 735 kW; this complies with a specific net power output of 36,79 kWs/kg and thermal efficiency of 10,1%. The reinjection temperature of the geothermal fluid is 63.2°C. The highest net power output of processes using CO_2 as a working fluid

is substantially lower (specific net power output = 25.6 kWs/kg) because of high pressures and, therefore, reduced thermal efficiencies (~ 8%). Net power output could be increased ~30 % using a supercritical process and propane as the working fluid, compared to a conventional, subcritical process with an isopentane working fluid and similar input values.

Influence of condensing temperature, minimal temperature difference (MTD) in the heat exchanger and application of an internal heat exchanger

Process condensing temperature varies significantly, depending on the climate at the location of the geothermal well and opportunities for cooling. Yearly average ambient temperature is a first reference point for site-specific optimization. Likewise, MTD and auxiliary power for cooling influence the optimal design point. These criteria are location- and system-dependent. In this paper, a range of condensing temperatures based on a geothermal fluid temperature of 150°C was used. Calculations for propane were performed using condensing temperatures of 20 – 35°C, and for CO_2 15 – 30°C. When CO_2 is used as a
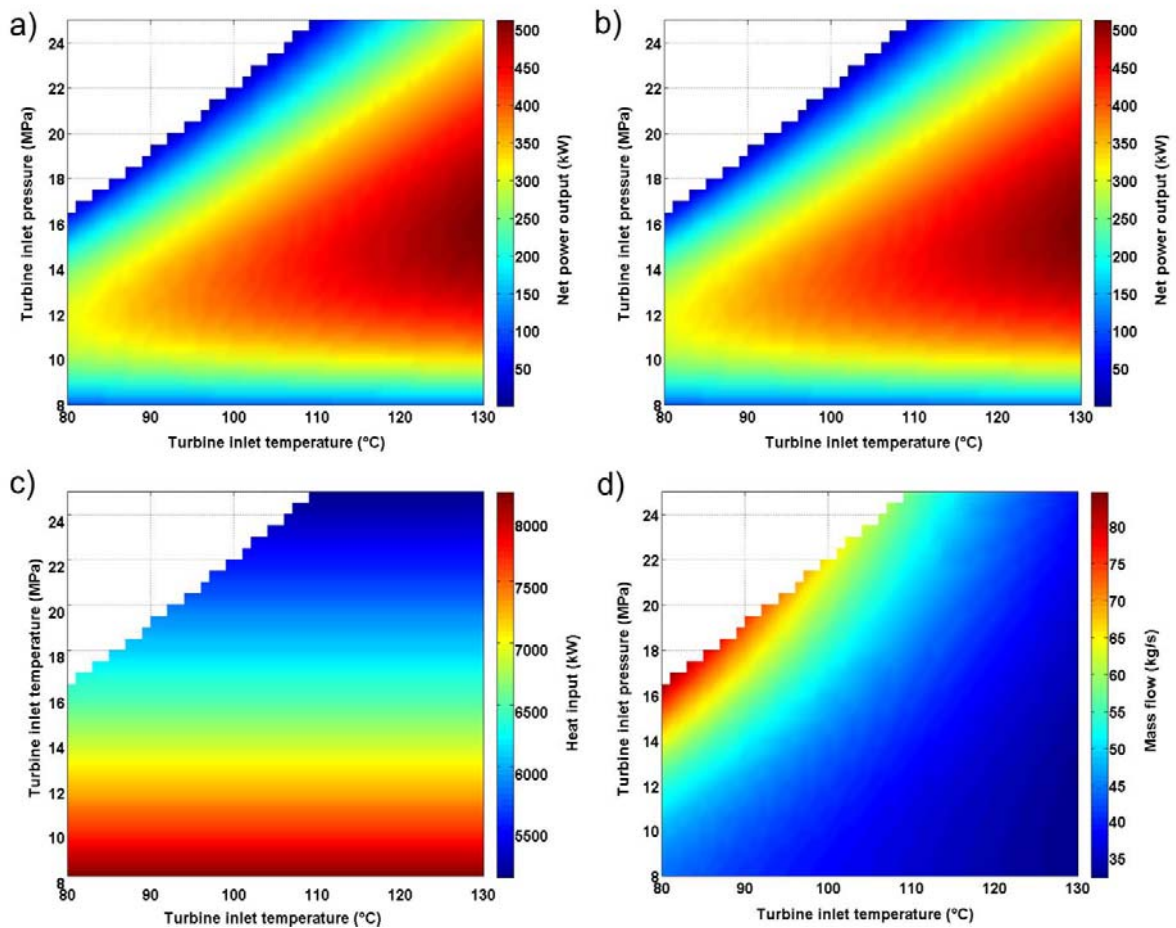
Figure 6: Net power output (a), thermal efficiency (b), heat input (c) and mass flow of the ORC (d) over live steam pressure and temperature, using CO_2 as the working fluid

working fluid, condensing temperatures higher than 30°C are not possible, since the critical condensing temperature is 30.98°C.

The inlet temperature of the ORC medium at the heat exchanger entry decreases at lower condensing temperatures. Consequently, geothermal fluid temperature at the outlet is reduced and more heat is supplied to the process. In combination with a higher thermal efficiency, this significantly increases cycle performance. At a condensing temperature of 15°C with CO_2 as the working fluid, net power output increases 50%, compared to a condensing temperature of 30°C. The process using CO_2 as a working fluid showed a higher sensitivity to condensing temperature variations than with propane, owing to the minor distance to the critical point of CO_2.

By defining the steam parameters and condensing temperature, the cycle is clearly defined. The temperature difference of the heat exchanger has no influence on thermal efficiency; however, heat supplied to the process is influenced by this

parameter, which in turn influences mass flow of the ORC. Processes with propane showed a linear correlation between changes in MTD and net power output. A temperature difference of 20 K reduced net power by 29%, compared to a temperature difference of 5 K.

The CO_2 process showed the highest net power output for the maximum possible steam temperatures. This can be attributed to the temperature curve characteristics of the geothermal fluid using CO_2 in the heat exchanger, with the pinch point positioned near the heat exchanger exit.

A variation of MTD between 20 – 5K, with a constant turbine inlet temperature of 130°C, led to an 18% increase in maximum net power output.

Varying MTD and iteratively optimizing live steam parameters led to a corresponding net power output up to 22% higher for MTD. This indicates that optimizing the heat exchanger requires subsequent optimization of the thermodynamic cycle in order to obtain maximum net power output. In

contrast, scaling or two-phase phenomena affect heat transfer in the heat exchanger, which in turn influences the optimal live steam parameters.

In processes employing retrograde fluids, the use of an internal heat exchanger is state-of-the-art. This application of new technology requires testing and optimizing new working fluids, such as propane and CO_2. However, this study shows that an internal heat exchanger cannot be used at the calculated power maxima. In the case of CO_2, the difference in temperature between the inlet into the heat exchanger and the turbine exhaust temperature was too low. Propane as the working fluid expanded into the two-phase region to the condensing temperature, which is lower than the inlet temperature of the fluid in the heat exchanger. In processes with other steam parameters, the use of an internal heat exchanger led to a net power output increase of up to 20%, compared to the same process without a recuperator. For supercritical propane and CO_2, the calculated maximum power output could not be increased by recuperation.

Comparison with additional working fluids

Based on our prior investigations using a geothermal fluid temperature of 150°C with propane and CO_2 as working fluids, the calculations were extended to the fluids listed in Table 2. Critical fluid pressures and temperatures, thermal efficiency and specific net power output of the most efficient process parameters are listed.

Fluids marked with an asterix (*) show the maximum net power output at supercritical parameters. With the exception of CO_2, all supercritical processes clearly resulted in a higher specific net power output than isopentane, although the thermal efficiency did not deviate significantly from subcritical processes. The values in Table 2 show that a performance increase of up to 41% is possible, depending on the working fluid and associated transition from sub- to supercritical processes, and at a geothermal fluid temperature of 150°C.

The same calculations were also performed at geothermal fluid temperatures of 130°C, 150°C and 170°C for all working fluids (Table 3). The values of the specific net power output marked with a star (*) are achieved at supercritical turbine inlet conditions.

Figure 7 shows specific net power output of the investigated fluids at each of the different geothermal fluid temperatures in relation to the ratio of the critical temperature of the geothermal fluid. Each point depicts the maximum achievable specific net power output of a given fluid. The curves in Figure 7 are polynomial. Under the chosen boundary conditions (Table 1), the highest net power output was achieved employing working fluids with a critical temperature of ~0.8 – 0.9 times the geothermal fluid temperature. Figure 7 also shows that for all simulated geothermal fluid temperatures, subcritical processes have lower maximum net power output gains than supercritical ones. Consequently, depending on the location-specific geothermal fluid temperature, when selecting a fluid critical temperature should be taken into account. This temperature should be lower than that of the geothermal fluid, so that supercritical processes with high performance can be realized. On the other hand, fluids with an overly large discrepancy between the critical and geothermal fluid temperatures show reduced performance, as was observed with CO_2. The highest net power outputs were obtained with the R115 working fluid, at a geothermal fluid temperature of 130°C, R227ea at 150°C and carbonyl sulfide at 170°C. As other fluids yield similar values, environmental impact (ODP, GWP) and safety issues should be taken into account when identifying the optimal working fluid.

Table 2: Investigated fluids with critical parameters, thermal efficiency and specific net power output for processes; geothermal fluid inlet temperature = 150°C (*supercritical cycle)

Fluid	Critical pressure [MPa]	Critical temperature [°C]	Thermal efficiency [%]	Specific net power output [kWs/kg]
R744(CO$_2$)*	7.38	30.98	7.97	25.60
R41 *	5.90	44.13	9.73	34.54
R218 *	2.64	71.87	8.81	34.73
R143a *	3.76	72.71	10.17	37.35
R32 *	5.78	78.11	11.27	36.00
R115 *	3.13	79.95	9.60	37.52
R290 (Propane) *	4.25	96.74	10.05	36.79
R134a *	4.06	101.06	10.46	37.48
R227ea *	2.93	101.75	10.28	39.84
Carbonyl sulfide	6.37	105.62	10.62	29.63
R245fa	3.65	154.01	10.24	29.25
R601a (Isopentane)	3.38	187.20	10.11	28.23
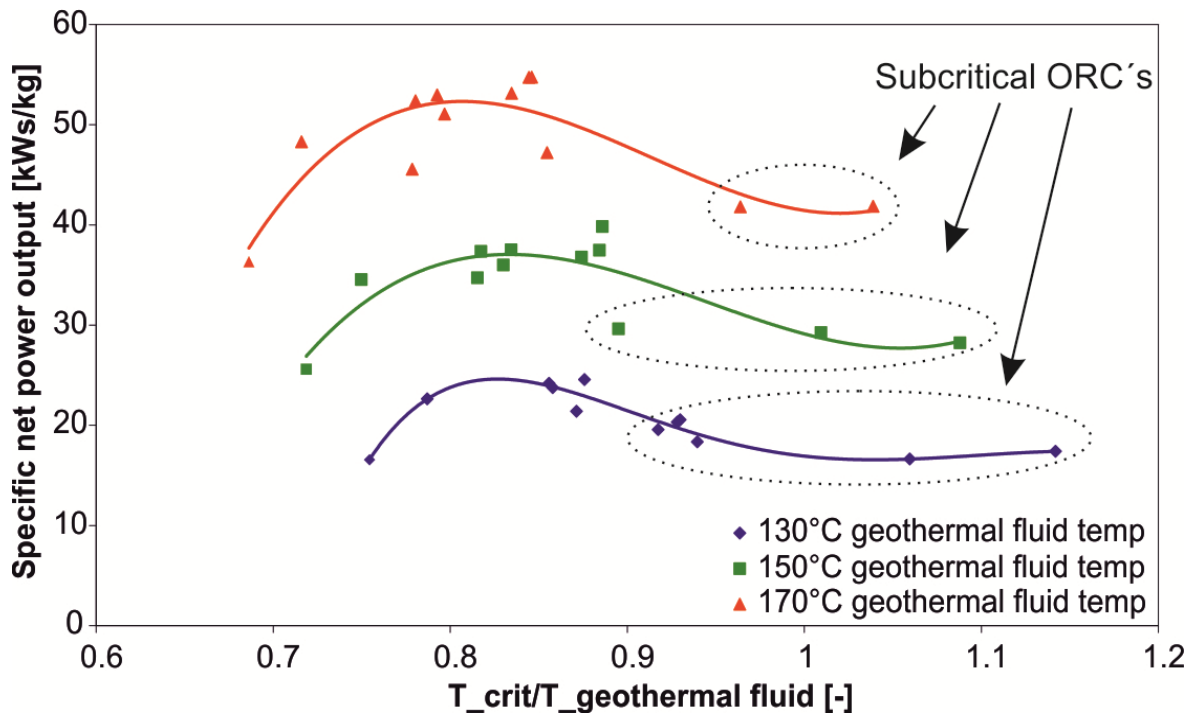
Figure 7: Specific net power output of ORCs with various fluids in dependency of the ratio between critical temperature of the fluid to the geothermal fluid temperature for three different geothermal fluid temperatures. The points represent optimal working points for different fluids.

Table 3: Net power output and live steam parameters at geothermal fluid temperatures of 130, 150 and 170°C for different fluids (*supercritical cycle)

Fluid	$T_{Th.in}$ [°C]	Specific net power output [kWs/kg]	Live steam temp T_3 [°C]	Live steam pressure p_3 [MPa]	Net power increase vs. Isopentane [%]
R744 (CO_2)	130	16.56*	110	14	-4.82
	150	25.60*	130	15.6	-9.31
	170	36.34*	150	18	-13.18
R41	130	22.65*	110	10	30.15
	150	34.54*	130	12	22.36
	170	48.29*	150	14	15.37
R218	130	24.21*	100	4.2	39.10
	150	34.73*	122	5.8	23.01
	170	45.56*	142	7.4	8.84
R143a	130	23.77*	96	5.2	36.60
	150	37.35*	120	6.4	32.31
	170	52.39*	142	8.4	25.16
R32	130	21.41*	110	5.8	23.01
	150	36.00*	130	7.4	27.51
	170	52.99*	150	9.0	26.60
R115	130	24.58*	96	4.0	41.25
	150	37.52*	118	5.6	32.92
	170	51.07*	140	7.2	22.03
R290 (Propane)	130	19.58	82	3.2	12.54
	150	36.79*	104	4.6	30.30
	170	53.14*	130	6.4	26.97
R134a	130	20.33	78	2.5	16.83
	150	37.48*	107	4.4	32.75
	170	54.73*	133	6.6	30.77
R227ea	130	20.55	80	1.8	18.11
	150	39.84*	114	3.6	41.11
	170	54.75*	138	5.6	30.82
Carbonyl sulfite	130	18.36	110	3.4	5.49
	150	29.63	130	4.2	4.97
	170	47.21*	130	7.0	12.80
R245fa	130	16.64	74	0.7	-4.38
	150	29.25	86	0.9	3.6
	170	41.80	97	1.2	-0.14
R601a (Isopentane)	130	17.40	75	0.4	-
	150	28.23	84	0.5	-
	170	41.85	92	0.6	-
Water	150	21.59	130	0.05	-23.52

Conclusions

In the present study, organic Rankine cycles for power generation using low temperature/low enthalpy geothermal wells (geothermal fluid temperature = 150°C) were simulated. Cycles with propane and CO_2 as working fluids were investigated and compared to state of the art cycles with Isopentane. In addition to the effects of thermal efficiency and net power output at given boundary conditions, the influence of the condensing temperature and MTD in the heat exchanger was investigated. A further step included comparing various working fluids at geothermal fluid temperatures of 130°C, 150°C and 170°C.

Organic Rankine cycles using propane as working fluid achieved a specific net power output of 36.8 kWs/kg and a thermal efficiency of 10.1% at supercritical steam parameters. Cycles with CO_2 as working fluid gained only 25.6 kWs/kg and a thermal efficiency of 8.0%. Compared to subcritical processes with Isopentane, an approximately 30% increase of net power output was achieved with propane as working fluid. In contrast, CO_2 did not seem to be a suitable working fluid under the conditions of this study. Cycles with propane also have the advantage that no internal heat exchanger is needed and also not possible. Parameter variations of the condensing temperature and MTD in the heat exchanger showed that both parameters significantly influence the maximum achievable net power output. Design of the geothermal power plant should be carried out with special focus on the optimal adjustment of these components.

Simulations using other organic media showed a relationship between net output of the fluid's critical temperature and geothermal fluid temperature. Maximum power occurred at different geothermal fluid temperatures using fluids that had a critical temperature ~ 0.8 times the respective geothermal fluid temperature. This suggests that the local geothermal fluid temperature and associated optimum critical temperature should be a criterion for the selection of the working fluid, depending on the location of the power plant.

Nomenclature

c_p	specific isobaric heat capacity
h	specific enthalpy
$\dot{m}$	mass flow
P	power
$\dot{Q}$	heat flow
q	specific heat
T	temperature
s	specific entropy
w	specific work
η	efficiency

Indices

C	Carnot
geo	geothermal fluid
in	in
max	maximum
min	minimum
ORC	Organic Rankine Cycle
out	out
pump	pump
s	isentropic
spec	specific
th	thermal
triangle	triangle
turbine	turbine

References

(1) Holm, A.; Blodgett, L.; Jennejohn, D.; Gawell, K.; "Geothermal Energy: International Market Update", in: Geothermal Energy Association, 2010.

(2) DiPippo, R.; "Geothermal Power Plants: Principles, Applications, Case Studies and Environmental Impact", Butterworth-Heinemann, Oxford, UK, 2008.

(3) Saleh, B.; Koglbauer, G.; Wendland, M.; Fischer, J.; "Working fluids for low-temperature organic Rankine cycles", *Energy*, 32 (2007) 1210 - 1221.

(4) Lakew, A.A.; Bolland, O.; "Working fluids for low-temperature heat source", *Applied Thermal Engineering*, 30 (2010) 1262 - 1268.

(5) Heberle, F.; Brüggemann, D.; "Exergy based fluid selection for a geothermal Organic Rankine Cycle for combined heat and power generation", *Applied Thermal Engineering*, 30 (2010) 1326 - 1332.

(6) Schuster, A.; Karellas, S.; Aumann, R.; "Efficiency optimization potential in supercritical Organic Rankine Cycles", *Energy*, 35 (2010) 1033 - 1039.

(7) NIST, "NIST Standard Reference Database 23: Reference Fluid Thermodynamic and Transport Properties-REFPROP", National Institute of Standards and Technology, Gaithersburg, Colorado, USA, 2010.

(8) DiPippo, R.; "Ideal thermal efficiency for geothermal binary plants", *Geothermics*, 36 (2007) 276 - 285.

(9) Maizza, V.; Maizza, A.; "Working Fluids In Non-Steady Flows For Waste Energy Recovery Systems", *Applied Thermal Engineering*, Vol. 16 (1996) 579-590.

(10) Förster, H.; Schmidt, K.-P.; „Kreis-prozesse für die maximale Nutzung von Wärmeangeboten im Temperaturbereich von 80 bis 250 °C in Industrie, Geothermie und Solarwirtschaft", *VDI-Berichte*, Nr. 1924 (2006) 289-303.

(11) Canic, T.; Baur, S.; Adelhelm, C.; "Salzaus-fällungen aus Geothermalwasser - je mehr Bewegung, desto schneller". bbr - *Sonderheft Geothermie* (2013) S. 98-102.

(12) Canic, T.; Baur, S.; Bergfeldt, T.; „Einfluss-parameter auf die Barytausfüllungen aus Ge-othermalwasser". Geothermiekongress 2013, Essen, 12.-14. November 2013.

(13) Herfurth, S.; "Parameter study on basic engineering of geothermal power plants". 4th European Geothermal PhD Day, Szeged, H, May 5-7, 2013.

(14) Kessler, T.; Bockhorn, H.; Schneider, C.; Class, A.G.; Kuhn, D.; „Laser induced ignition of methane free jets". European Combustion Meeting, Lund, S, June 25-28, 2013, Paper P5-16, ISBN 978-91-637-2151-9.

(15) Kuhn, D.; Herfurth, S.; Bockhorn, H.; Steinbrück, J.; Genova, B.; Reichert, D.; Rossbach, M.; Walz, L.; Schröder, E.; Thomauske, K.; „Research activities on geothermal and biomass utilisation at Karlsruhe Institute of Technology". International Conference for Academic Institutions (ICAI 2013), Gujarat, IND, January 9-13, 2013.

(16) Kuhn, D.; „Geothermale Stromerzeugung - Stand und zukünftige Entwicklung". 10. Biberacher Geothermietag, Biberach, 10. Oktober 2013.

(17) Pfeifer, C.; Kuhn, D.; Class, A.G.; „Influence of injection pressure on droplet atomization and auto-ignition of dimethyl ether (DME) at elevated pressure". *Fuel* 104 (2013) 116-127.

(18) Vetter, C.; Wiemer, H.-J.; Kuhn, D.; „Comparison of sub- and supercritical Organic Rankine Cycles for power generation from low-temperature/low-enthalpy geothermal wells, considering specific net power output and efficiency". *Applied Thermal Engineering*, 51 (2013) 871-879.

(19) Vetter, C.; "Supercritical organic rankine cycle for optimized power generation from low enthalpy geothermal heat". 4th European Geothermal PhD Day, Szeged, H,May 5-7, 2013.

(20) Wiemer, H.J.; Herfurth, S.; "Optimierte Stromproduktion bei Niederentalphie-Lagerstätten mit überkritischen ORC-Kraftwerken". Thermodynamik-Kolloquium, Technische Universität Hamburg-Harburg, 7.-9. Oktober 2013.

(21) Wiemer, H.J.; Schulenberg, T.; „Einsatz eines GuD-Kraftwerksimulators in der universitären Ausbildung". 45. Kraftwerks-technisches Kolloquium, Dresden, 15.-16. Oktober 2013.

The annual report of the Institute for Nuclear and Energy Technologies of KIT summarizes its research activities in 2013 and provides some highlights of each working group of the institute. Among them are thermal-hydraulic analyses for nuclear fusion reactors, accident analyses for light water reactors, and research on innovative energy technologies like liquid metal technologies for energy conversion, hydrogen technologies and geothermal power plants. Moreover, the institute has been engaged in education and training in energy technologies, which is illustrated by an example of training in nuclear engineering.